Introduction to X-Ray Photoelectron Spectroscopy

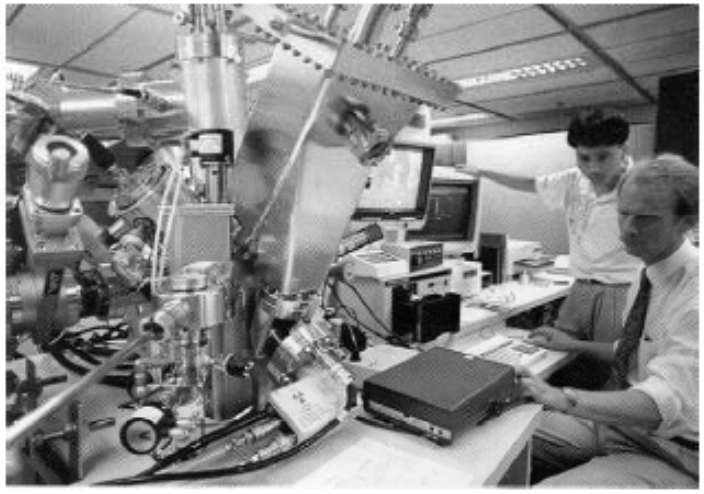

- **Definition:-**

  X-Ray Photoelectron Spectroscopy (XPS)

  or

  Electron Spectroscopy for Chemical Analysis (ESCA)

  - is an electron spectroscopic technique for determining the elemental and chemical composition of materials' **SURFACE**

- **Advantages:-**
- **High information content**
- **Flexibility in addressing a wide variety of samples**
- **Sound theoretical basis**

Introduction to X-Ray Photoelectron Spectroscopy

The principles of XPS measurement:

- Surface to be analyzed is placed in a vacuum environment.
- The surface is irradiated with photons (X-ray photons in XPS) and following events take place:
  - An X-ray photon interacts with an inner-shell electron of an atom
  - Energy of the X-ray photon is transferred to the electron.
  - the electron received enough energy to leave the atom and escape from the surface of the sample.
  - A photoelectron with certain kinetic energy is created.
- The incident x-ray energy is known as $h\nu$. (h is Plank's constant and ν the X-ray frequency)
- The kinetic energy (E_k) of the photoelectron is measurable then the binding energy (E_b) of the electron can be calculated as by: $E_b = h\nu - E_k$
- Each element has a unique binding energy, which can be used to identify the elemental composition of the sample.

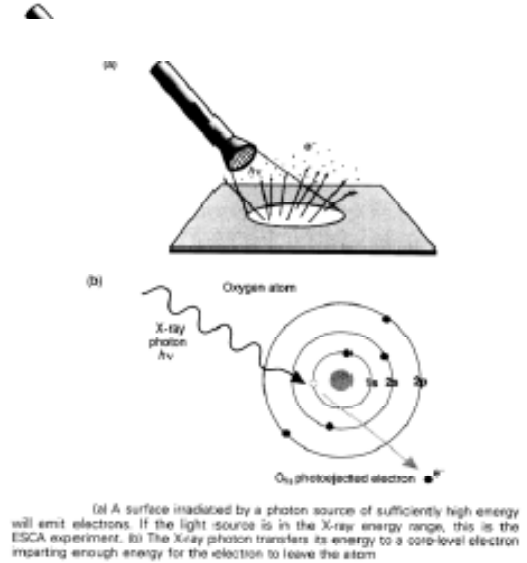

(a) A surface irradiated by a photon source of sufficiently high energy will emit electrons. If the light source is in the X-ray energy range, this is the ESCA experiment. (b) The X-ray photon transfers its energy to a core-level electron imparting enough energy for the electron to leave the atom

- The photoelectrons are separated according to their kinetic energy.
- The number of the photoelectrons with different energy is counted.
- The energy of the photoelectrons is related to the atomic and molecular environment from which they originated.
- The number of electrons emitted is related to the concentration of the emitting atom in the sample

Introduction to X-Ray Photoelectron Spectroscopy

Information derived from a XPS experiment

In the outermost 10 nm of a surface, ESCA can provide:

- Identification of all elements (except H and He) present at concentrations >0.1 atomic %
- Semiquantitative determination of the approximate elemental surface composition (error $< \pm 10\%$)
- Information about the molecular environment (oxidation state, bonding atoms, etc.)
- Information about aromatic or unsaturated structures from shakeup ($\pi^* \rightarrow \pi$) transitions
- Identification of organic groups using derivatization reactions
- Non-destructive elemental depth profiles 10 nm into the sample and surface heterogeneity assessment using (1) angular-dependent ESCA studies and (2) photoelectrons with differing escape depths
- Destructive elemental depth profiles several hundred nanometers into the sample using ion etching (for inorganics)
- Lateral variations in surface composition (spatial resolution of 8–150 μm, depending upon the instrument)
- 'Fingerprinting' of materials using valence band spectra and identification of bonding orbitals
- Studies on hydrated (frozen) surfaces

Introduction to X-Ray Photoelectron Spectroscopy

❖ What information is learned from XPS (ESCA)?

A. Elemental Identification

All elements except hydrogen are detectable with a detection limit of 0.1 atom% or less.

B. Chemical State Identification

Binding energy, peak shape and Auger parameter measurements are used to determine surface chemistry.

C. Quantification

Peak areas of heights are converted to atomic concentrations with the use of elemental sensitivity factors.

D. Depth Profiles

Sputter depth of angle-dependent profiles are used to examine a sample as a function of depth.

E. Maps

The sample may be moved to generate maps or line scans based upon either elemental or chemical information.

Introduction to X-Ray Photoelectron Spectroscopy

Irradiation of a solid by X-ray can also result in emission of Auger electrons.

The energy of Auger electrons is independent of irradiation energy.

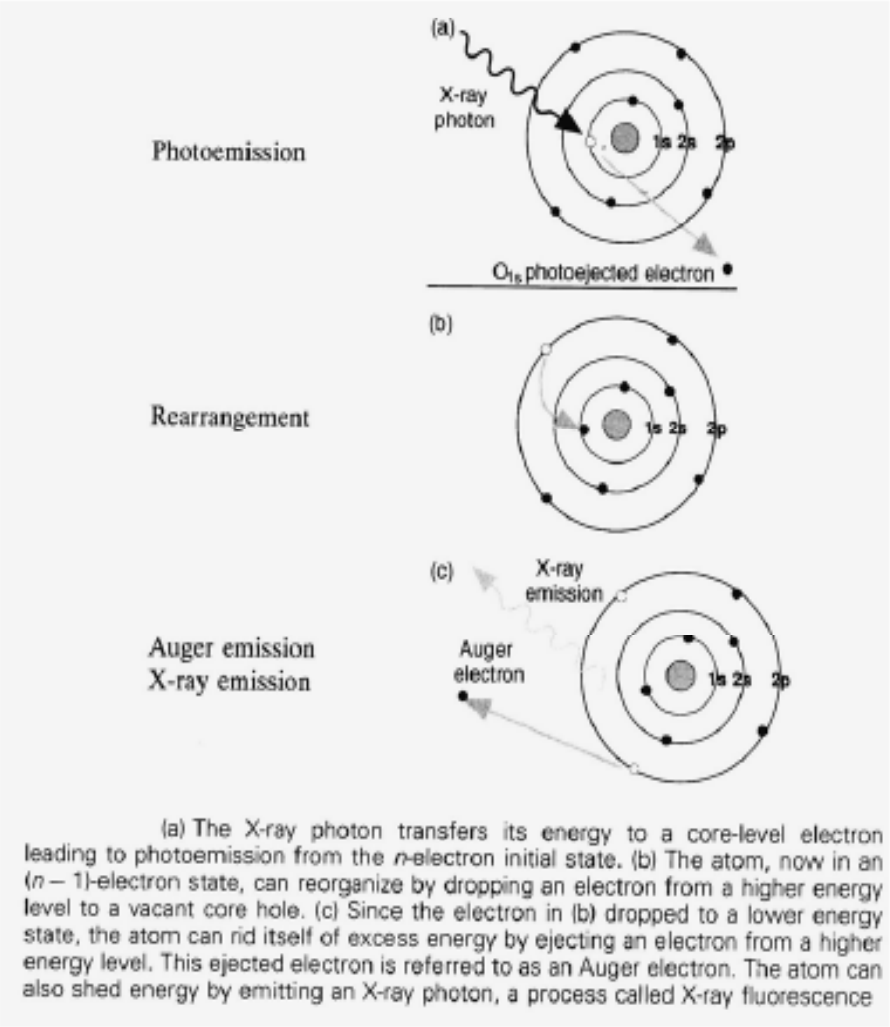

(a) The X-ray photon transfers its energy to a core-level electron leading to photoemission from the *n*-electron initial state. (b) The atom, now in an $(n-1)$-electron state, can reorganize by dropping an electron from a higher energy level to a vacant core hole. (c) Since the electron in (b) dropped to a lower energy state, the atom can rid itself of excess energy by ejecting an electron from a higher energy level. This ejected electron is referred to as an Auger electron. The atom can also shed energy by emitting an X-ray photon, a process called X-ray fluorescence

Introduction to X-Ray Photoelectron Spectroscopy

❖Examples of XPS

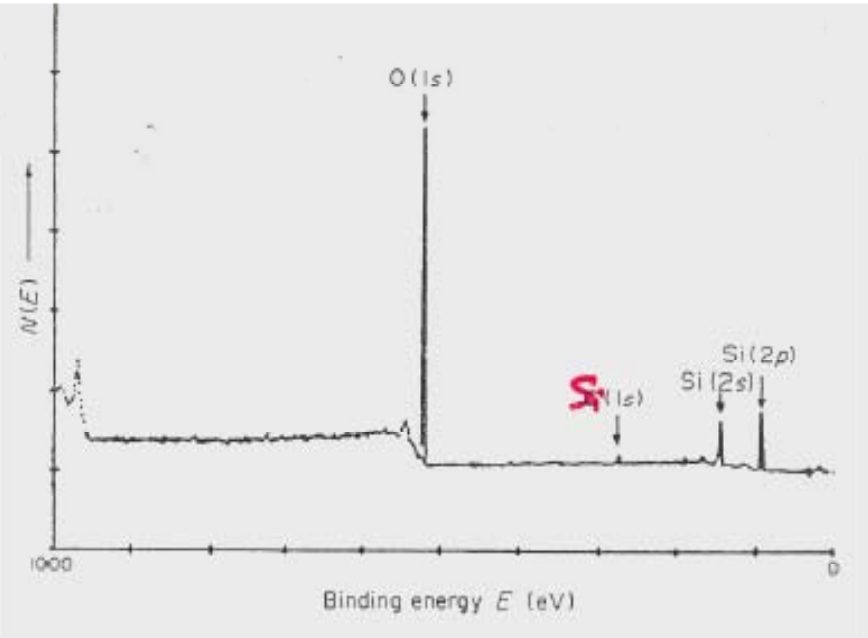

XPS survey spectrum of clean quartz

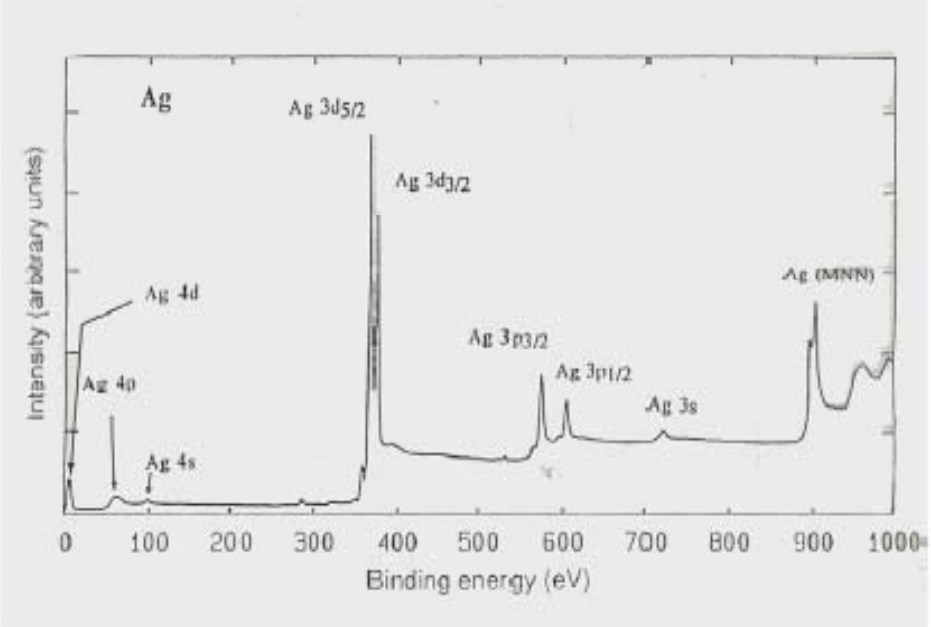

Survey spectrum for silver showing different core levels

Introduction to X-Ray Photoelectron Spectroscopy

❖ Chemical Shift Information

- One of the most valuable features of XPS is its ability to distinguish different chemical bonding configurations as well as different elements.
- The bonding energies of electrons in an atom are affected by the atom's chemical environment.
- The extend of the effect from the chemical environment is termed as Chemical Shift.
- For example, the positions of the three peaks reflect the effects of -O and =O and, the ration of C-C bonds to C-O and C=O bonds can be calculated from the relative areas of the peaks.

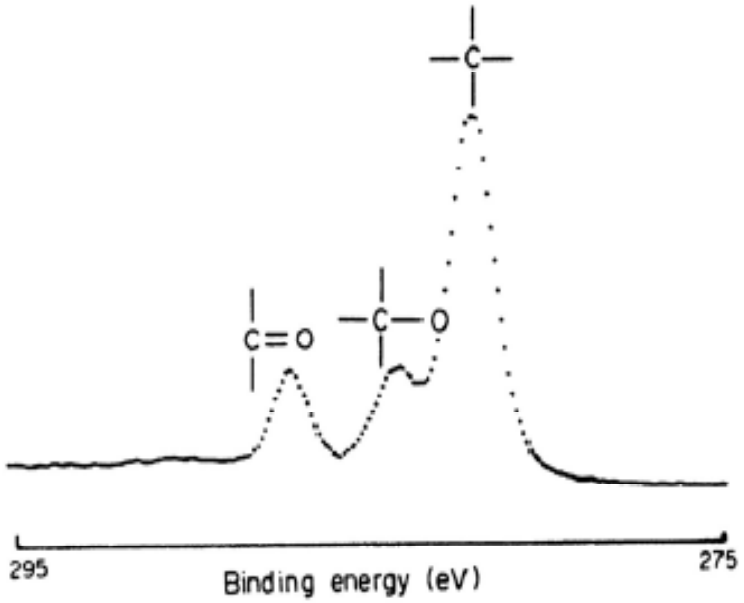

Introduction to X-Ray Photoelectron Spectroscopy

Binding Energies of 30 Elements

Element	Binding energies (eV)						
	$1S_{1/2}$	$2S_{1/2}$	$2P_{1/2}$	$2P_{3/2}$	$3S_{1/2}$	$3P_{1/2}$	$3P_{3/2}$
H	14						
He	25						
Li	55						
Be	111						
B	188			5			
C	284			7			
N	399			9			
O	532	24		7			
F	686	31		9			
Ne	867	45		18			
Na	1072	63		31			
Mg	1305	89		52			
Al		118	74	73			
Si		149	100	99	8		3
P		189	136	135	16		10
S		229	165	164	16		8
Cl		270	202	200	18		7
A		320	247	245	25		12
K		377	297	294	34		18
Ca		438	350	347	44		26
Sc		500	407	402	54		32
Ti		564	461	455	59		34
V		628	520	513	66		38
Cr		695	584	575	74		43
Mn		769	652	641	84		49
Fe		846	723	710	95		56
Co		926	794	779	101		60
Ni		1008	872	855	112		68
Cu		1096	951	931	120		74
Zn		1194	1044	1021	137		87

Table 3.2. Typical C_{1s} binding energies for organic samples*

Functional group		Binding energy (eV)
hydrocarbon	C–H,C–C	285.0
amine	C–N	286.0
alcohol, ether	C–O–H, C–O–C	286.5
Cl bound to carbon	C–Cl	286.5
F bound to carbon	C–F	287.8
carbonyl	C=O	288.0
amide	N–C=O	288.2
acid, ester	O–C=O	289.0
urea	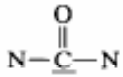	289.0
carbamate	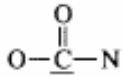	289.6
carbonate	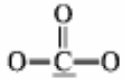	290.3
2F bound to carbon	$-CH_2CF_2-$	290.6
carbon in PTFE	$-CF_2CF_2-$	292.0
3F bound to carbon	$-CF_3$	293–294

*The observed binding energies will depend on the specific environment where the functional groups are located. Most ranges are ±0.2 eV, but some (e.g., fluorocarbon samples) can be larger

Introduction to X-Ray Photoelectron Spectroscopy

Binding Energies of 30 Elements

Element	Binding energies (eV)						
	$1S_{1/2}$	$2S_{1/2}$	$2P_{1/2}$	$2P_{3/2}$	$3S_{1/2}$	$3P_{1/2}$	$3P_{3/2}$
H	14						
He	25						
Li	55						
Be	111						
B	188			5			
C	284			7			
N	399			9			
O	532	24		7			
F	686	31		9			
Ne	867	45		18			
Na	1072	63		31			
Mg	1305	89		52			
Al		118	74	73			
Si		149	100	99	8		3
P		189	136	135	16		10
S		229	165	164	16		8
Cl		270	202	200	18		7
A		320	247	245	25		12
K		377	297	294	34		18
Ca		438	350	347	44		26
Sc		500	407	402	54		32
Ti		564	461	455	59		34
V		628	520	513	66		38
Cr		695	584	575	74		43
Mn		769	652	641	84		49
Fe		846	723	710	95		56
Co		926	794	779	101		60
Ni		1008	872	855	112		68
Cu		1096	951	931	120		74
Zn		1194	1044	1021	137		87

Table 3.3. Typical O_{1s} binding energies for organic samples*

Functional group		Binding energy (eV)
carbonyl	C=O, O–C=O	532.2
alcohol, ether	C–O–H, C–O–C	532.8
ester	C–O–C=O	533.7

*The observed binding energies will depend on the specific environment where the functional groups are located. Most ranges are ± 0.2 eV.

Introduction to X-Ray Photoelectron Spectroscopy

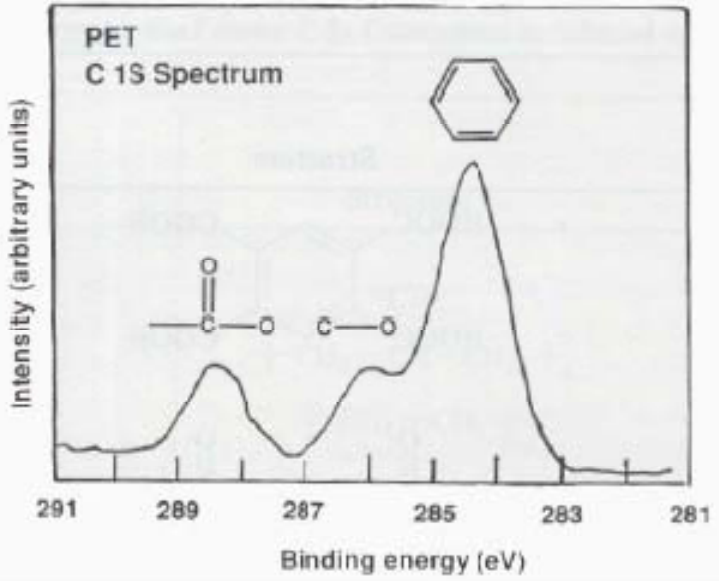

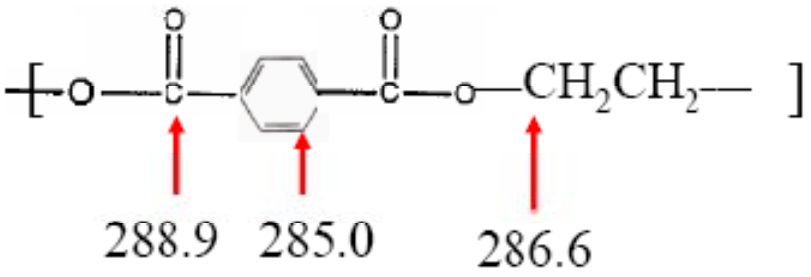

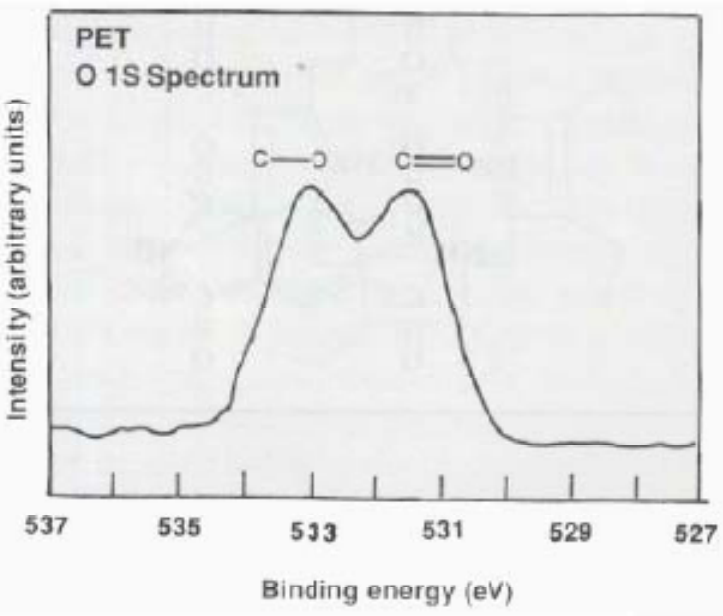

C 1s and O 1s spectra of poly(ethylene terephthalate).

Introduction to X-Ray Photoelectron Spectroscopy

Binding Energies of the C 1s Core Level in Various Polymers

Polymer	Structure[a]
Polyethylene	$+CH_2-CH_2-CH_2-CH_2+_n$ 285.0
Poly(vinyl fluoride)	$+CFH-CFH+_n$ 288.4
Poly(vinylene fluoride)	$+CFH-CH_2-CFH-CH_2+_n$ 288.0, 285.9
Poly(vinylidene fluoride)	$+CH_2-CF_2-CH_2-CF_2+_n$ 286.3, 290.8
Polytrifluoroethylene	$+CF_2-CFH-CF_2-CFH+_n$ 291.6, 289.3
Polytetrafluoroethylene	$+CF_2-CF_2-CF_2-CF_2+_n$ 292.2
Polyhexafluoropropylene	293.7, 291.8, 289.8
Poly(vinyl chloride)	$+CH_2-CHCl-CH_2-CHCl+_n$ 285.0, 286.3

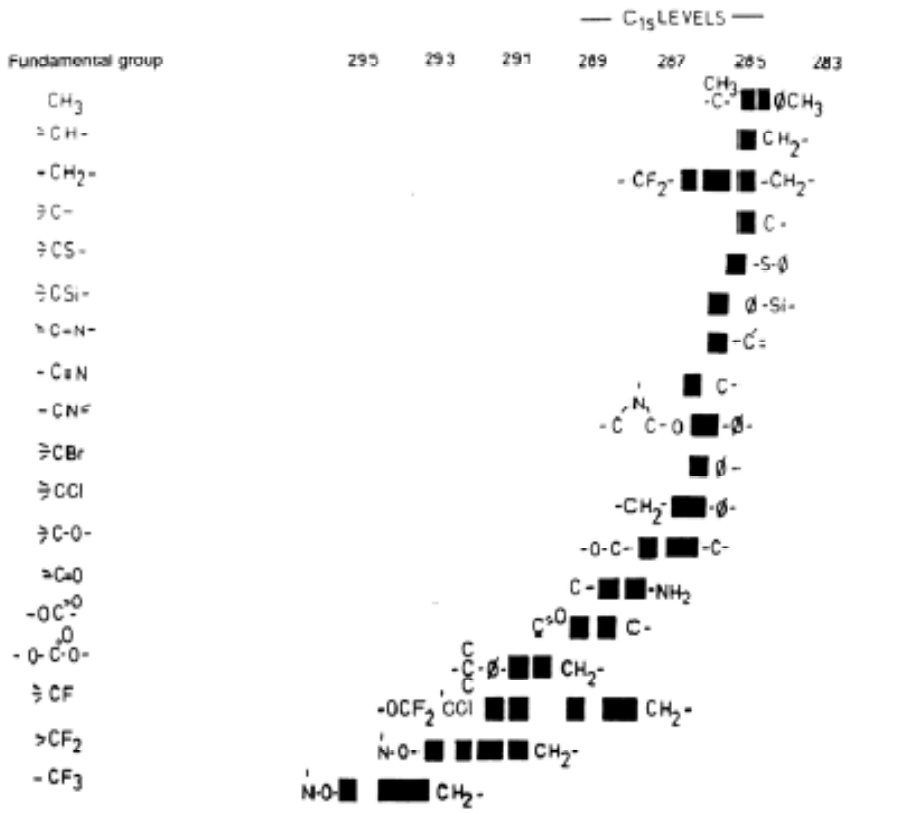

Experimental chemical shifts for C 1s and O 1s core levels in various functional groups

Introduction to X-Ray Photoelectron Spectroscopy

❖ Instrumentation

- Electron Spectrometer
  for example:
  hemispherical analyzer
  - a $1/r^2$ electric field between two concentric spherical surfaces
  - the radius of the electrons are proportional to their energy
  - the electrons with different energi dispersed spatially
- Detector/Signal-processing Systen for example: channeltron

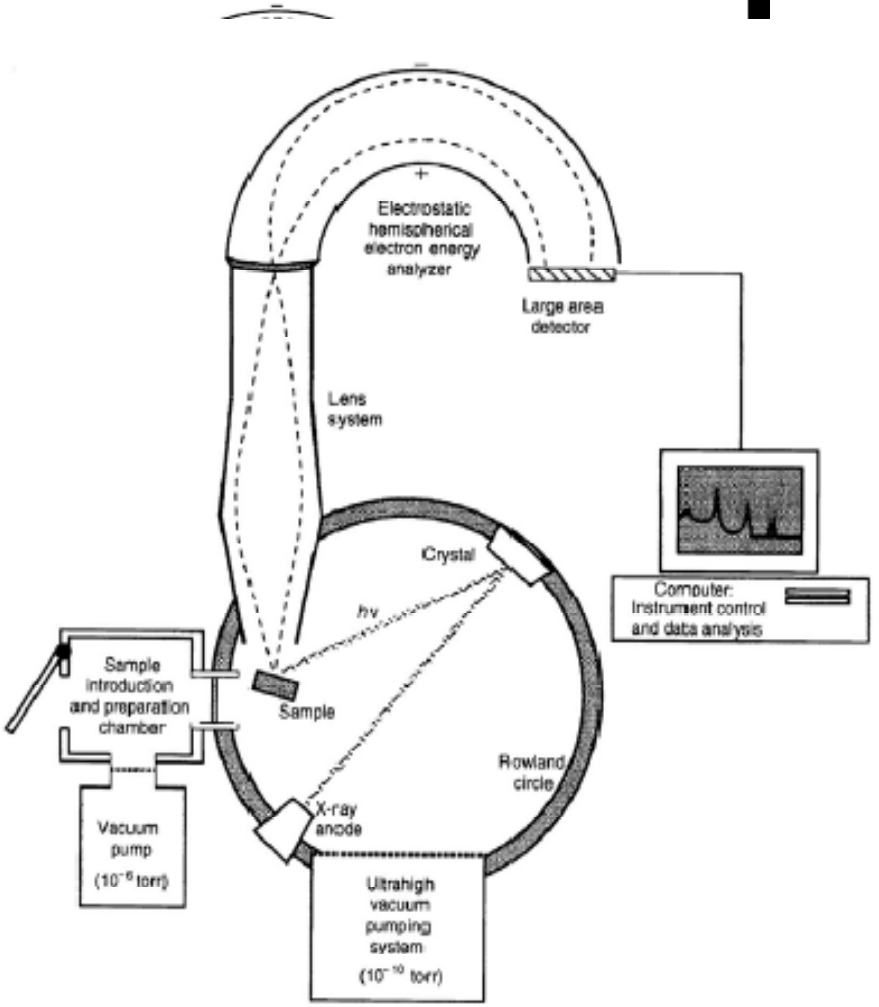

A schematic diagram of an ESCA spectrometer. The key components of a state-of-the-art spectrometer (X-ray anode, monochromator crystal, collection lens, hemispherical analyzer, and large area detector) are shown

Introduction to X-Ray Photoelectron Spectroscopy

❖ Instrumentation

- X-Ray Source with known energy for example: aluminum($K\alpha$, 1486 eV) or magnesium ($K\alpha$, 1253 eV)

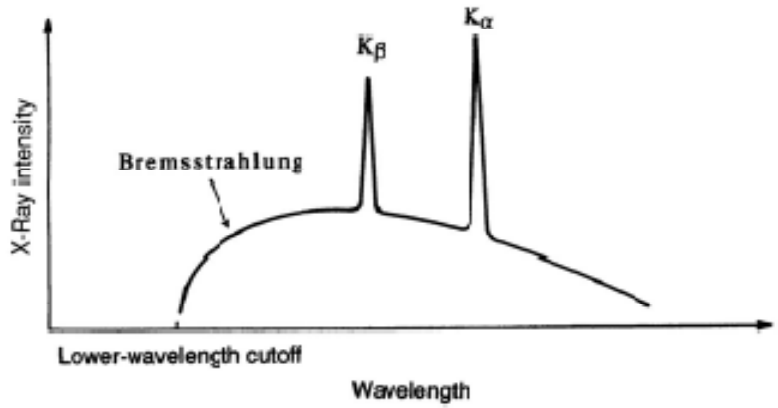

Schematic diagram showing the energy distribution of nonmonochromatic X-ray with the strong characteristic K_α and K_β lines and the bremsstrahlung radiation.

Anode Materials Used for XPS

X-ray	Photoelectrons (eV)	Line width (eV)
Mg K_α	1253.6	0.7
Al K_α	1486.6	0.8
Si K_α	1739.4	1.0
Zr L_α	2042.4	1.6
Au M_α	2122.9	2.2
Mo L_α	2293.2	1.9
Ag L_α	2984.2	2.6
Ti K_α	4510.9	2.0
Cr K_α	5417	2.1
Cu K_α	8048	2.5

Introduction to X-Ray Photoelectron Spectroscopy

Vacuum Requirements

1. Base pressure 10^{-10} torr(10^{-8} Pa)
   a. To minimize contamination of active sample surfaces
   b. To provide an unobstructed path for the photoelectrons into the analyzer
   c. To extend the life of X-ray and electron optics in the vacuum system.
2. Clean vacuum pumps
3. Bakeable vacuum chamber and components
4. The lifetime of a clean surface vs. system pressure

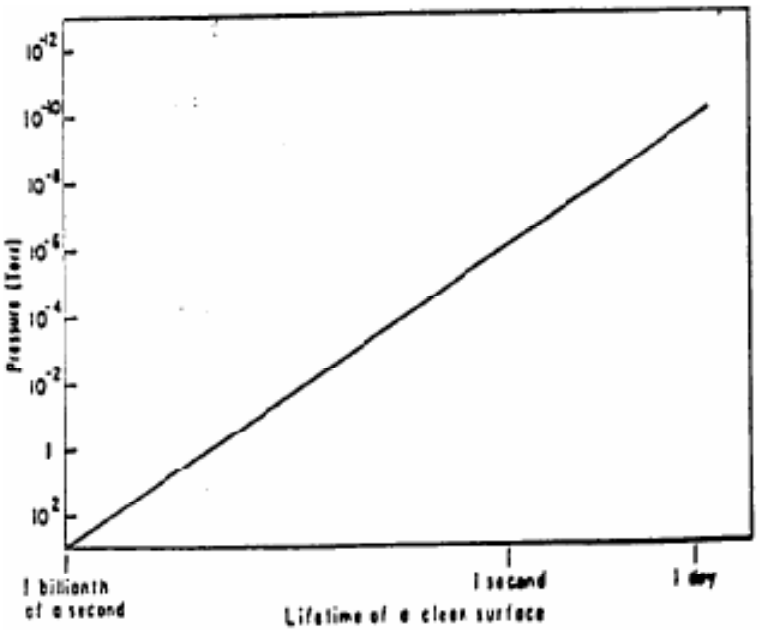

Introduction to X-Ray Photoelectron Spectroscopy

C. Sample Handling Requirements

1. Rapid sample introduction with minimal effect on main chamber pressure
2. Necessary degrees of freedom to move the sample as required (I.e. X,Y,Z and Tilt)
3. Automation of the sample stage.
4. Accessories for heating, cooling, etc.

D. X-ray Source Requirements

1. High X-ray flux at sample
2. Narrow X-ray line width
3. Multiple-anode capability
4. Ability to move the X-ray source (X-Y) and retract it (Z)
5. Long anode and filament lifetime

Introduction to X-Ray Photoelectron Spectroscopy

E. Analyzer Requirements

1. Precision energy measurement across a wide energy range
2. High-energy resolution capability
3. Ability to define the analysis area and, if possible, to change it
4. High dynamic range and low noise detector

Introduction to X-Ray Photoelectron Spectroscopy

♦ Sample Preparation & Surface Damage in XPS

1. Any Sample that is vacuum stable can be analyzed by XPS

2. Sample containing volatile components can be cooled to low temp. to avoid devolatilization

3. Normally, Solid materials, such as metals ceramics & polymer, are fairly stable under X-ray irradiation and damage caused by X-ray is minimal during a typical XPS experiment

4. Films, plaques or powders can be mounted on a sample holder with a double-sided sticky tape of low volatility first and then examined as bulk samples.

Introduction to X-Ray Photoelectron Spectroscopy

5. Certain Polymer & Biological samples would undergo some chemical changes under prolonged X-ray exposures in an XPS experiment. Examples are: PTFE, PVC, PVA, especially., when the materials are in thin films.

6. To minimize the damage, the exposure time should be as short as possible, and the samples are cooled to low temperatures.

7. The causes for the XPS induced damage include: (1) secondary electrons generated at X-ray source & impinging on the polymer or biological sample surface

Introduction to X-Ray Photoelectron Spectroscopy

Understanding and Analysis of XPS Spectra

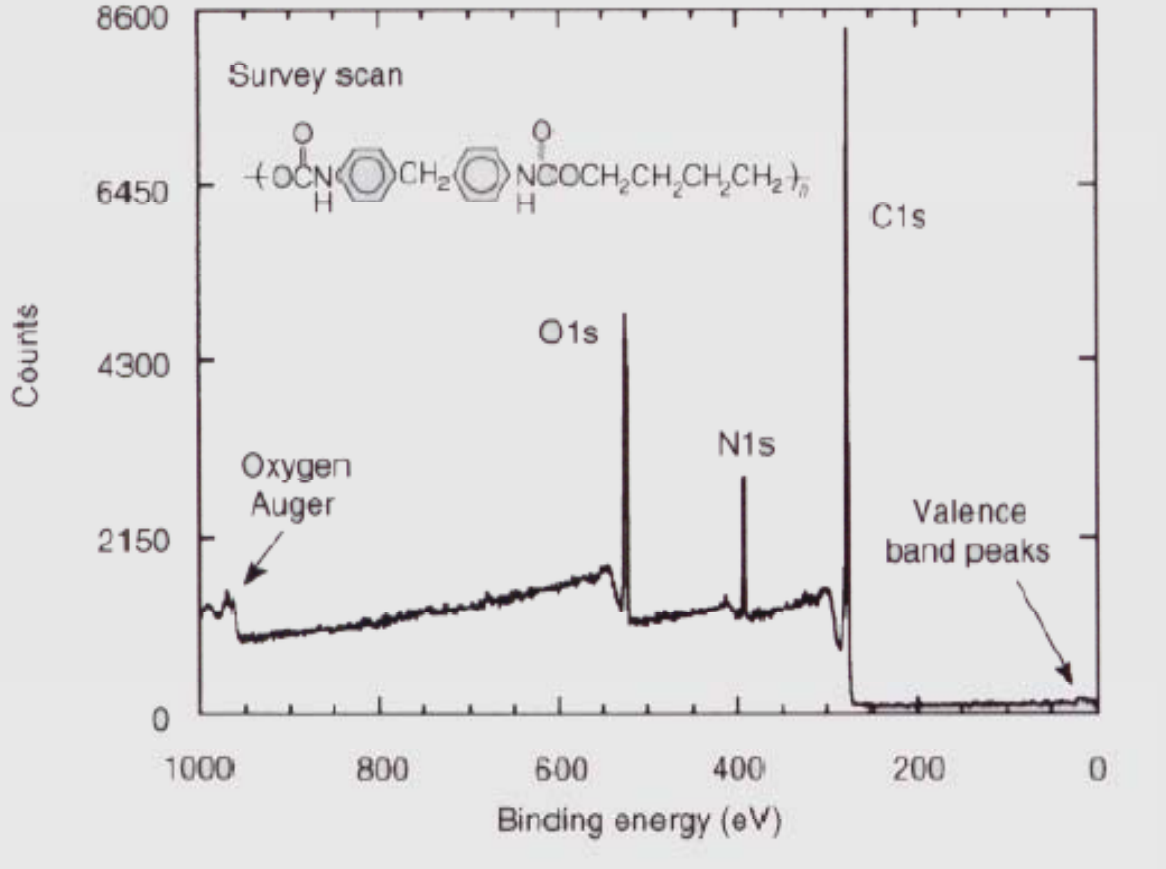

Figure 3.9. The ESCA survey scan of a hard-segment polyurethane

Introduction to X-Ray Photoelectron Spectroscopy

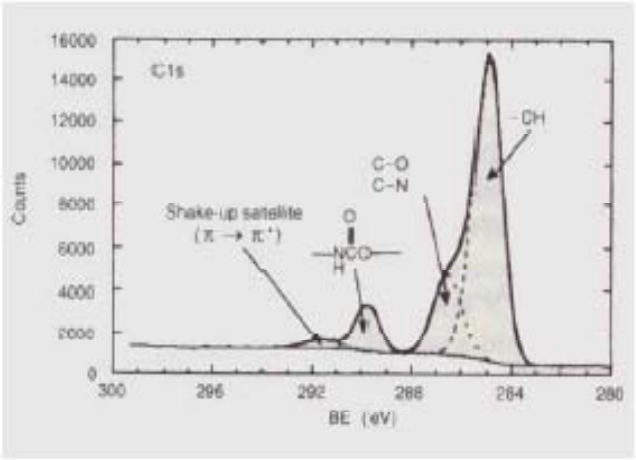

(a) The C_{1s} spectrum (resolved into component peaks) for the hard-segment polyurethane;

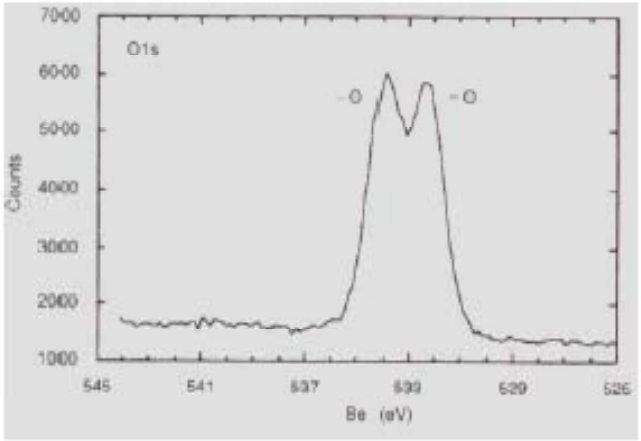

(b) the O_{1s} spectrum for the hard-segment polyurethane

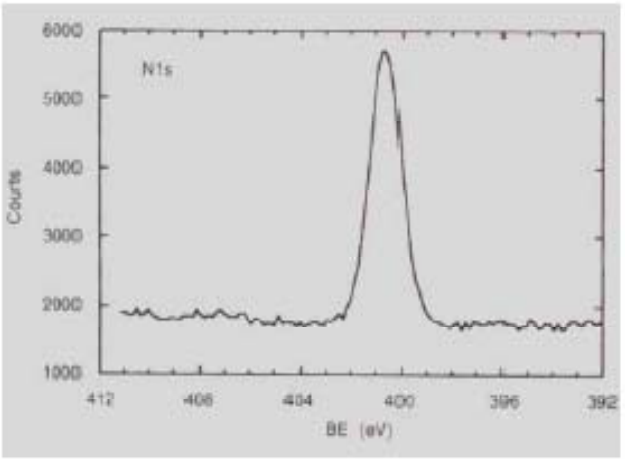

(c) the N_{1s} spectrum for the hard-segment polyurethane

Introduction to X-Ray Photoelectron Spectroscopy

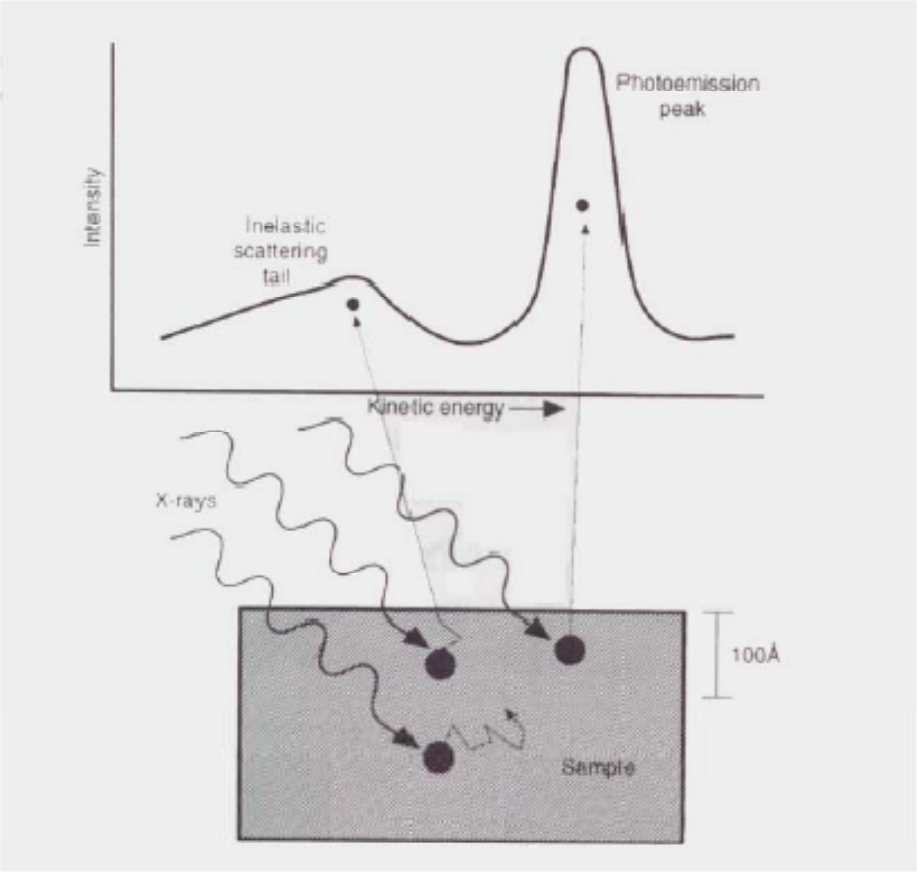

X-rays will penetrate deeply into a sample, and stimulate electron emission throughout the specimen. Only those electrons emitted from the surface zone that have suffered no energy loss will contribute to the photoemission peak. Electrons emitted from the surface zone that have lost some energy due to inelastic interactions will contribute to the scattering background.

Introduction to X-Ray Photoelectron Spectroscopy

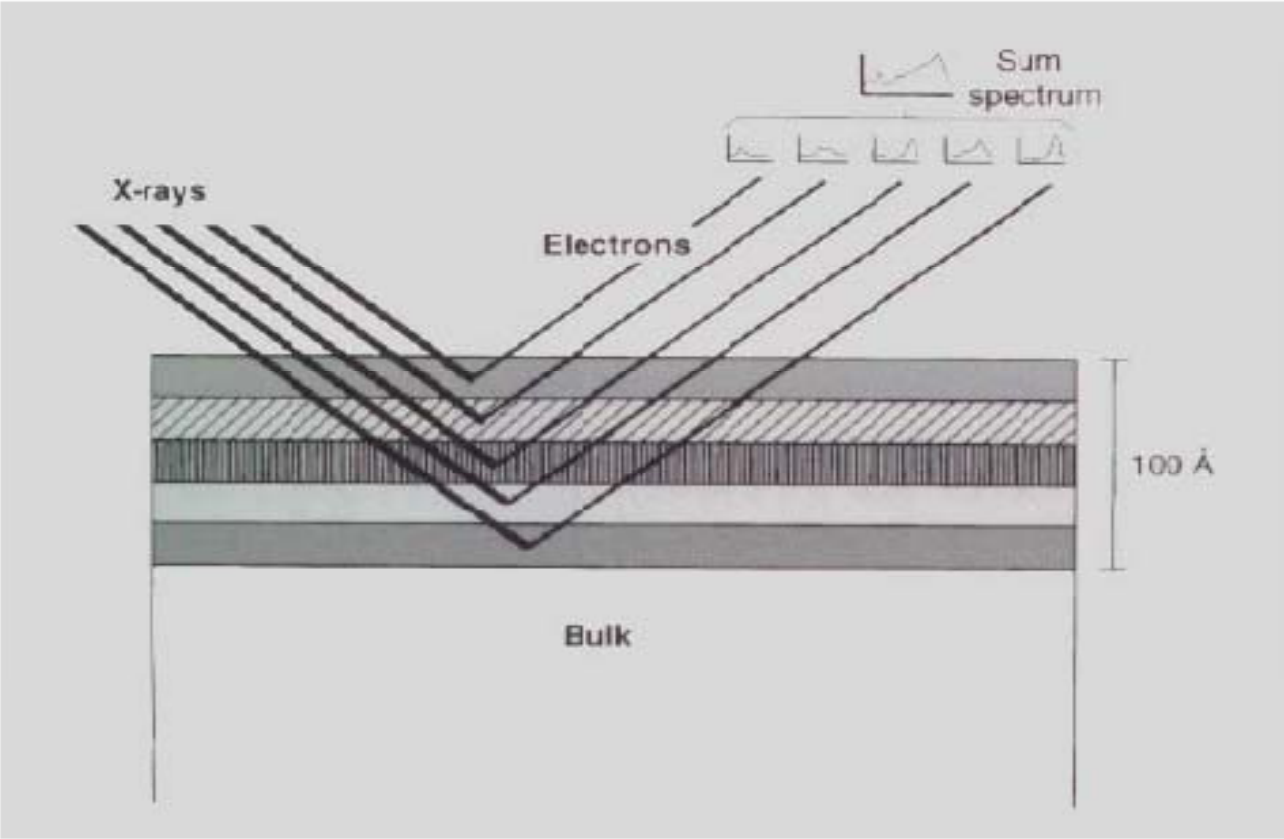

ESCA spectra are convolutions of the information from each depth within the sampling depth.

Introduction to X-Ray Photoelectron Spectroscopy

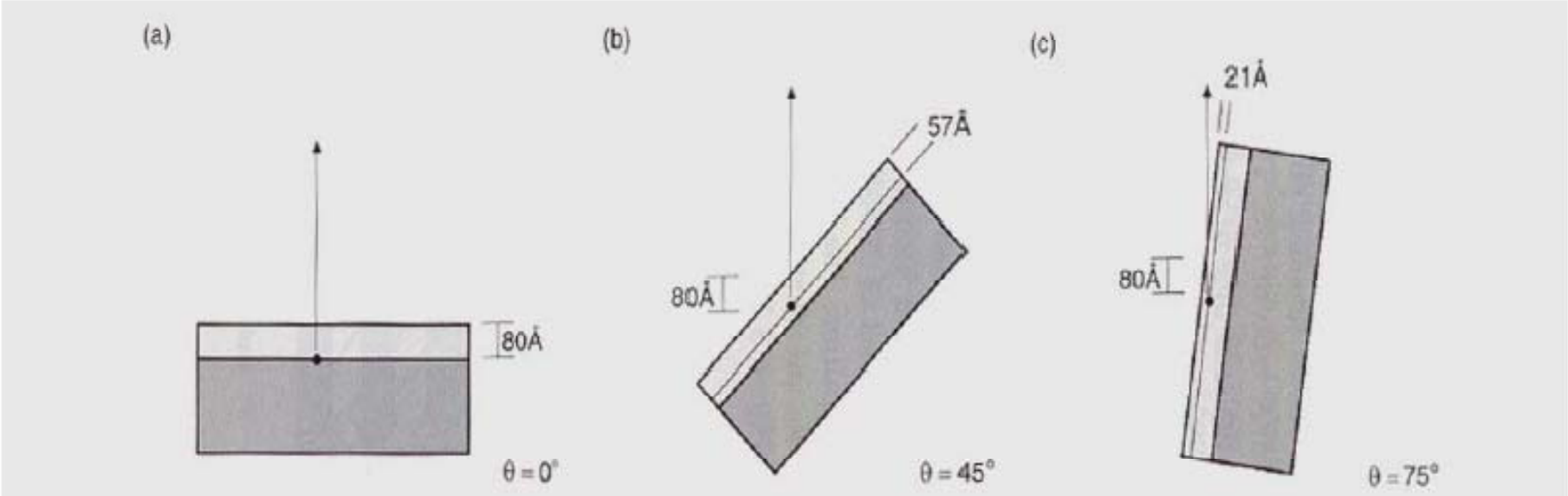

Figure 3.17. As the sample is rotated, maintaining the X-ray source and detector in fixed positions, the effective sampling depth decreases by a factor of cos θ. The sample angle, θ, is defined relative to the normal to the surface

Introduction to X-Ray Photoelectron Spectroscopy

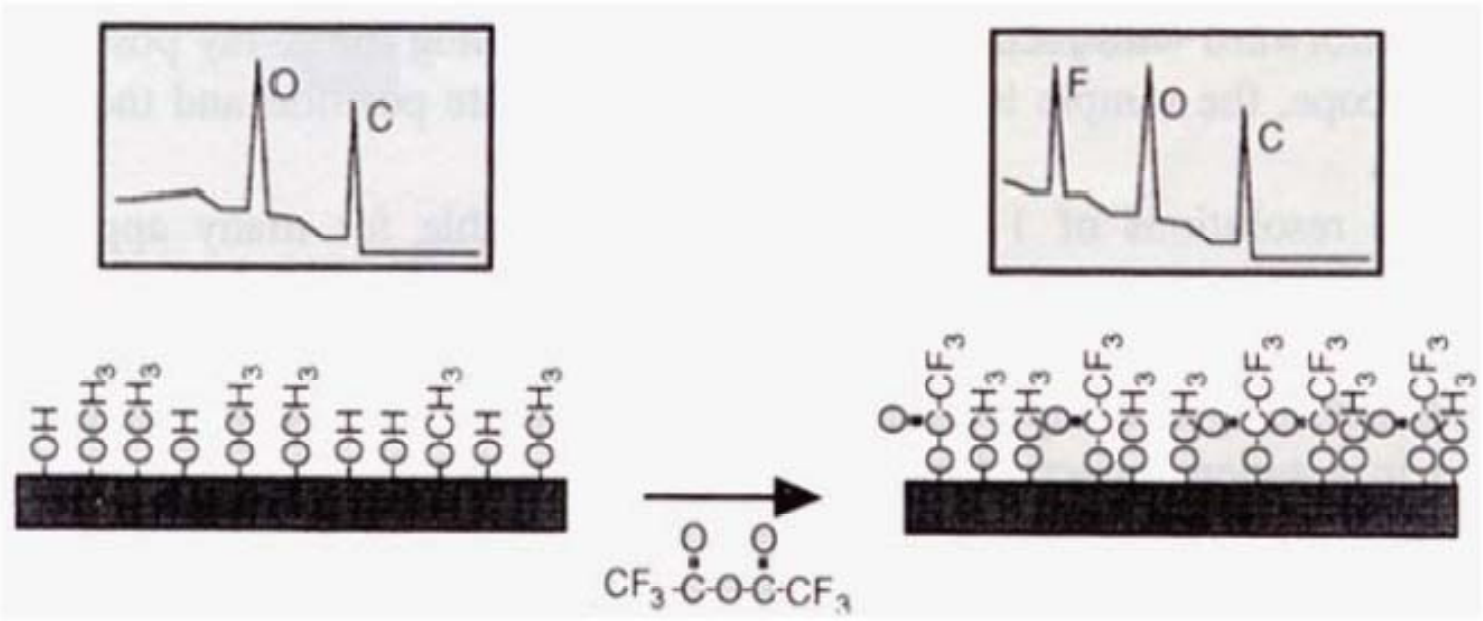

Hydroxy groups and ethers on a surface cannot be distinguished based upon ESCA chemical shifts. If the surface is reacted with trifluoroacetic anhydride, only hydroxyl groups will pick up F. The size of the F peak in the ESCA spectrum will be proportional to the number of reacted hydroxyl groups

Introduction to X-Ray Photoelectron Spectroscopy

❖ *Case study of XPS*

(1). Compositional Analysis of Surfaces:

Case I: Analysis of surface treatment of a piston.

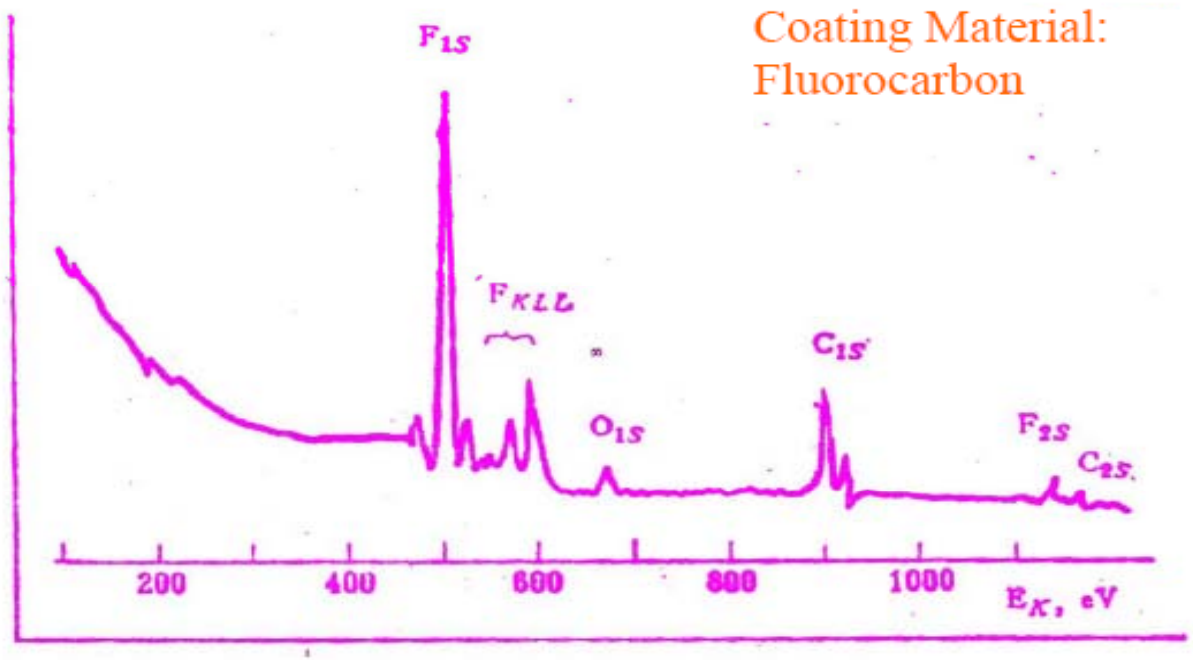

Coating Material:
Fluorocarbon

Introduction to X-Ray Photoelectron Spectroscopy

Case II: Surface Elemental Analysis

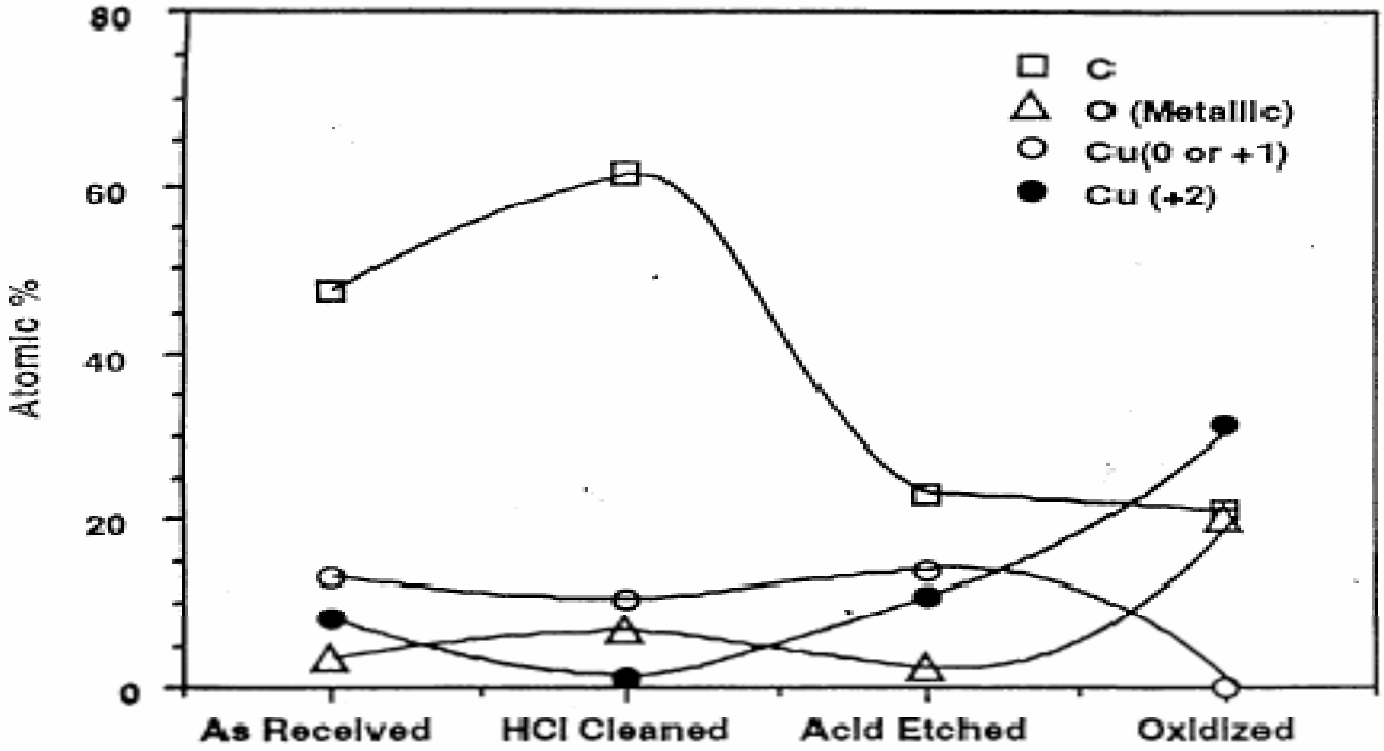

Figure 2.10 **Surface elemental analysis by XPS of Cu lead frames.**

Introduction to X-Ray Photoelectron Spectroscopy

(2) Thin Film Thickness Determination

For a homogeneous over-layer on a substrate, the intensity of the over-layer and the substrate can be calculated :

$$I_0 = I_0^{\infty}[1-\exp(\frac{-d}{\lambda_a^{s}\cos\theta})] \qquad I_s = I_s^{\infty}[\exp(\frac{-d}{\lambda_a^{s}\cos\theta})]$$

where :

I_0^{∞} & I_s^{∞} are intensities for the overlayer of infinite thickness and the clean substrate

d: the thickness of the overlayer

λ_a^{o} & λ_a^{s} are the attenuation lengths for photoelectrons, which are generated in the over-layer and the substrate, traversing the overlayer.

θ : the angle between the direction of emitted photoelectrons to the analyzer and the surface normal.

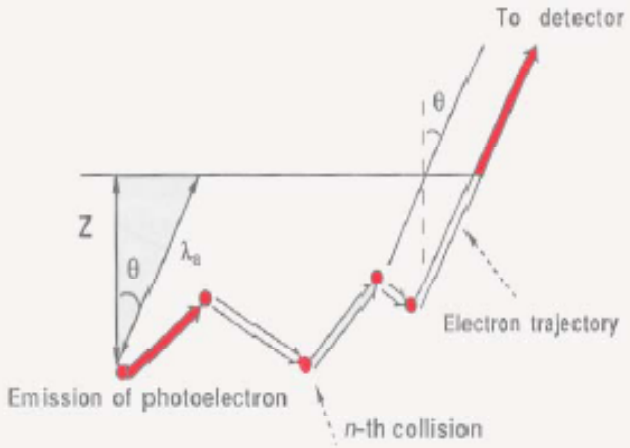

Fig. 3.3 Schematic diagram showing the actual electron trajectory and the attenuation length.

Introduction to X-Ray Photoelectron Spectroscopy

Therefore: measurement of I at different θ we can plot

$\ln(I_0/I_0^{\infty}-1)$ Vs $1/\cos\theta$

With $-d/\lambda_a^0$ or $-d/\lambda_a^s$ as slop

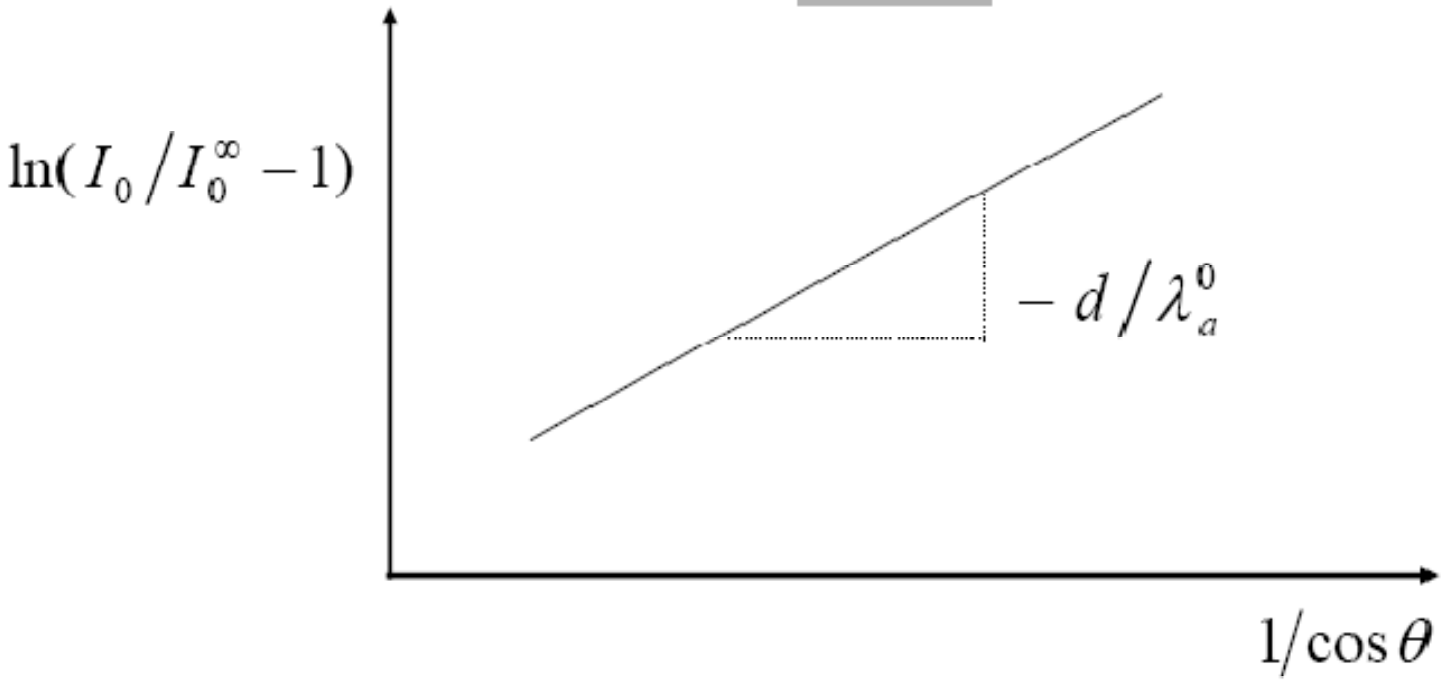

d : the thickness

Introduction to X-Ray Photoelectron Spectroscopy

(3) Adhesion Mechanisms Determination:

--------failure modes & bonding mechanisms

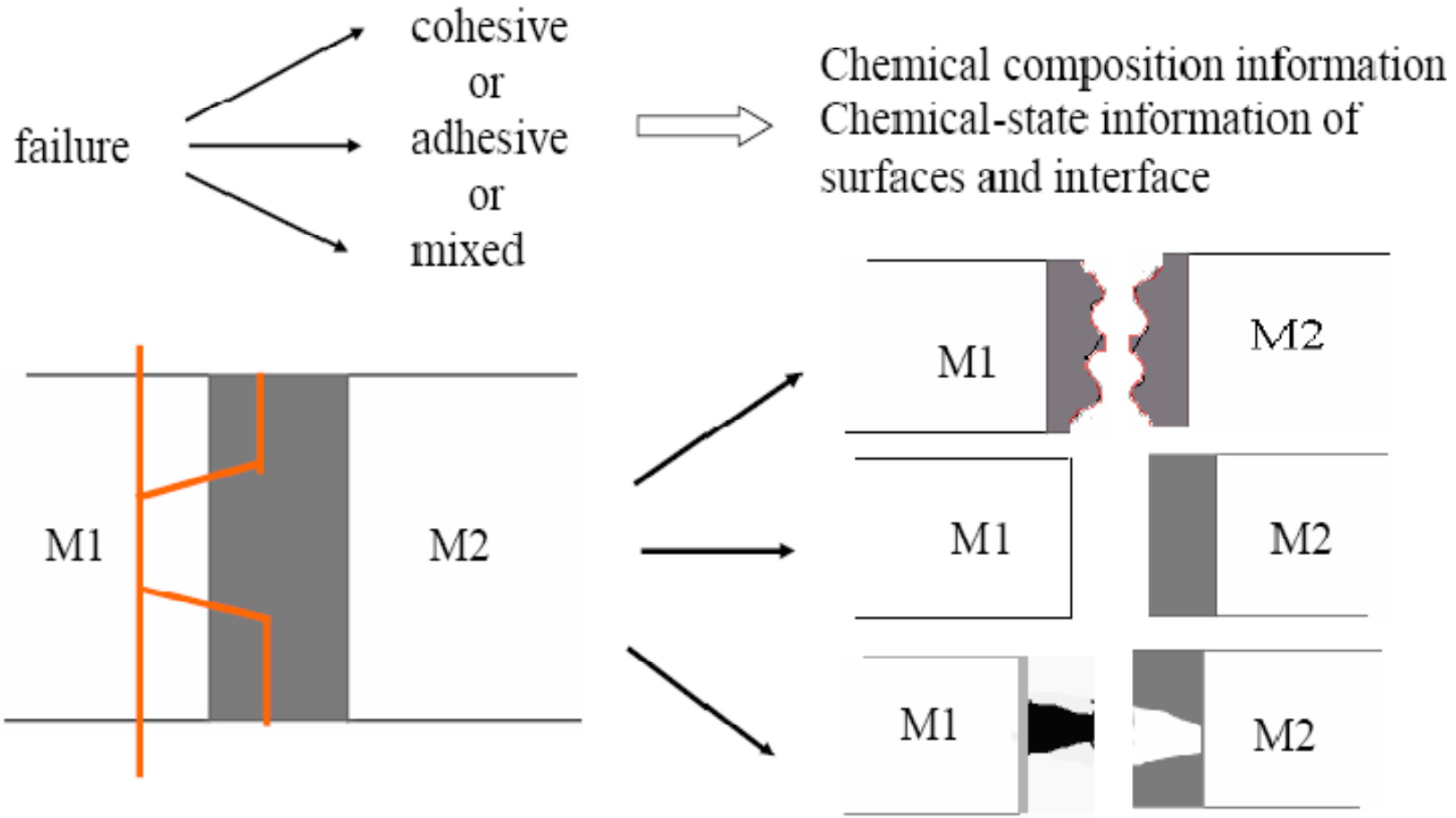

Introduction to X-Ray Photoelectron Spectroscopy

(4) Determination of chemical-structure changes after surface treatment

example: carbon fiber surface treatment with plasma for composites manufacture

(5) Effect of polymer processing on the micro-structure of final parts

(6) Fracture toughness of a whisker reinforced ceramic composite

K_{1c} ⟷ Whisker Surface chemistry

(7) Corrosion of Glass & metal alloys

---------- Na^{+} ---------- O^{2-}

---------- H^{+} ---------- Cl^{1-}

(8) Diffusion in Alloys --------- brittleness of Metal Alloys

(9) Chemical mapping in thin films ---------- Wear & lubrication

(10) Wear Analysis

Introduction to X-Ray Photoelectron Spectroscopy

- ESCA (also known as X-ray photoelectron spectroscopy, XPS) is based on the photoelectron effect. A high energy X-ray photon can ionize an atom, producing an ejected free electron with kinetic energy KE:
- KE = hv - BE
- hv **=photon energy (e.g., for Al Kα =1486.6 eV)**

  BE=energy necessary to remove a specific electron from an atom. BE ~ orbital energy

Introduction to X-Ray Photoelectron Spectroscopy

Basics of Light, EM Spectrum, and X-rays

- Light can take on many forms. Radio waves, microwaves, infrared, visible, ultraviolet, X-ray and gamma radiation are all different forms of light.
- The energy of the photon tells what kind of light it is. Radio waves are composed of low energy photons. Optical photons--the only photons perceived by the human eye--are a million times more energetic than the typical radio photon. The energies of X-ray photons range from hundreds to thousands of times higher than that of optical photons.
- Very low temperatures (hundreds of degrees below zero Celsius) produce low energy radio and microwave photons, whereas cool bodies like ours (about 30 degrees Celsius) produce infrared radiation. Very high temperatures (millions of degrees Celsius) produce X-rays.

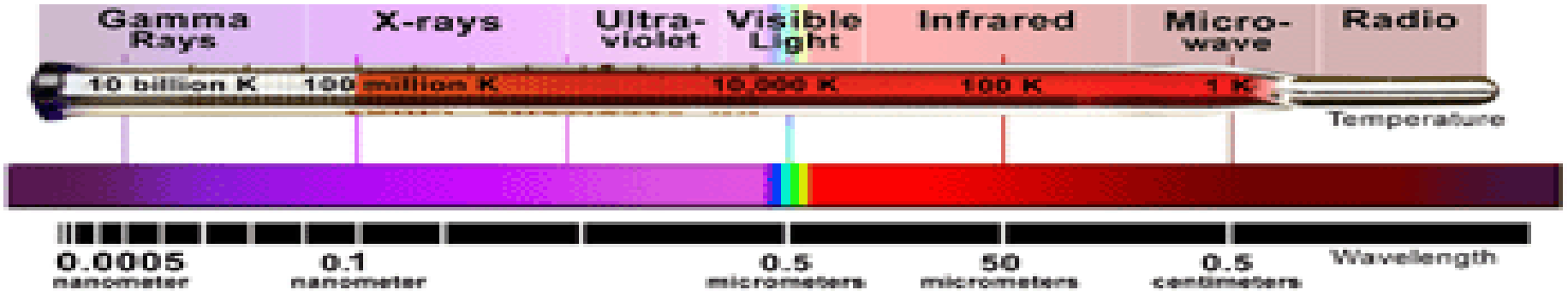

Introduction to X-Ray Photoelectron Spectroscopy

- **All energies expressed in electron volts (eV);**
- **1 eV=1.6x10^{-19} J**
- **In ESCA, you know hv & you measure KE; this determines BE.**
- **Photoelectron process: Consider an ensemble of C atoms. Each C atom has 6 electrons in 1s, 2s, 2 p orbitals: C $1s^2$ $2s^2$ 2 p^2**

Introduction to X-Ray Photoelectron Spectroscopy

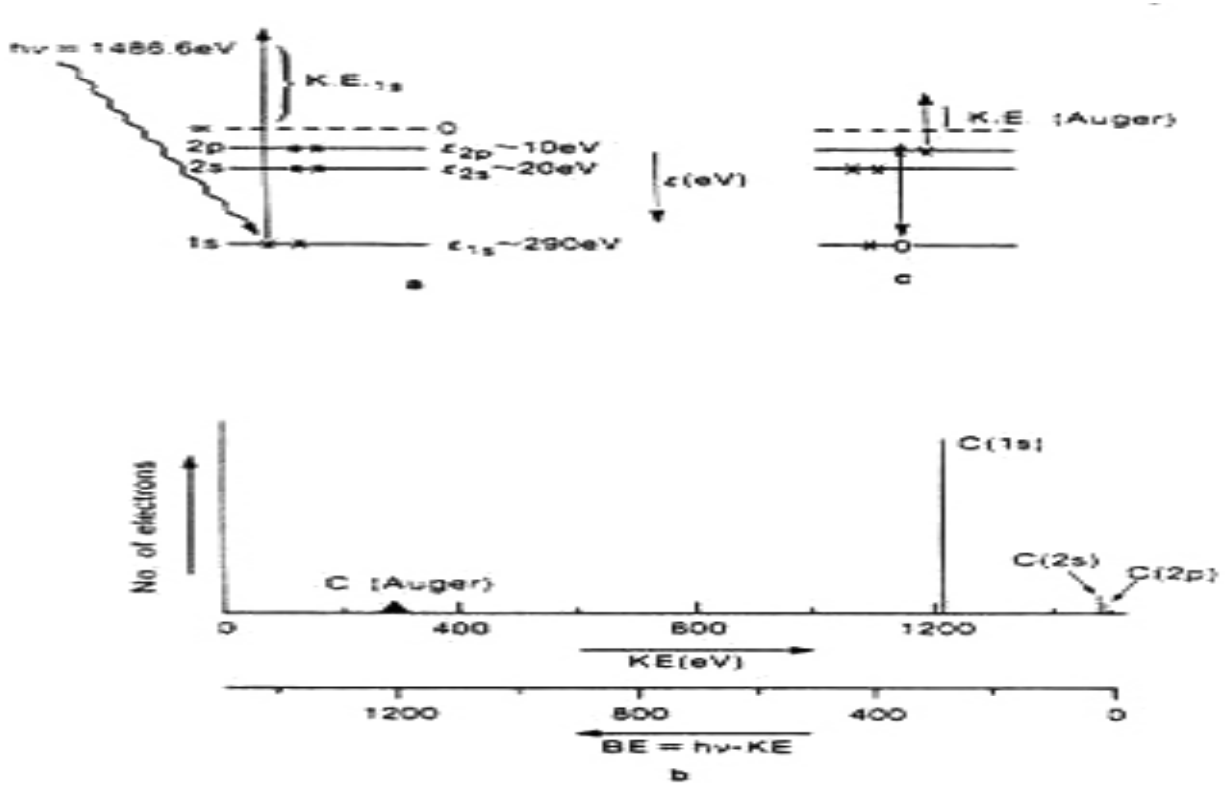

Figure 1 (a) Schematic representation of the electronic energy levels of a C atom and the photoionization of a C 1s electron. (b) Schematic of the *KE* energy distribution of photoelectrons ejected from an ensemble of C atoms subjected to 1486.6-eV X rays. (c) Auger emission relaxation process for the C 1s hole-state produced in (a).

Introduction to X-Ray Photoelectron Spectroscopy

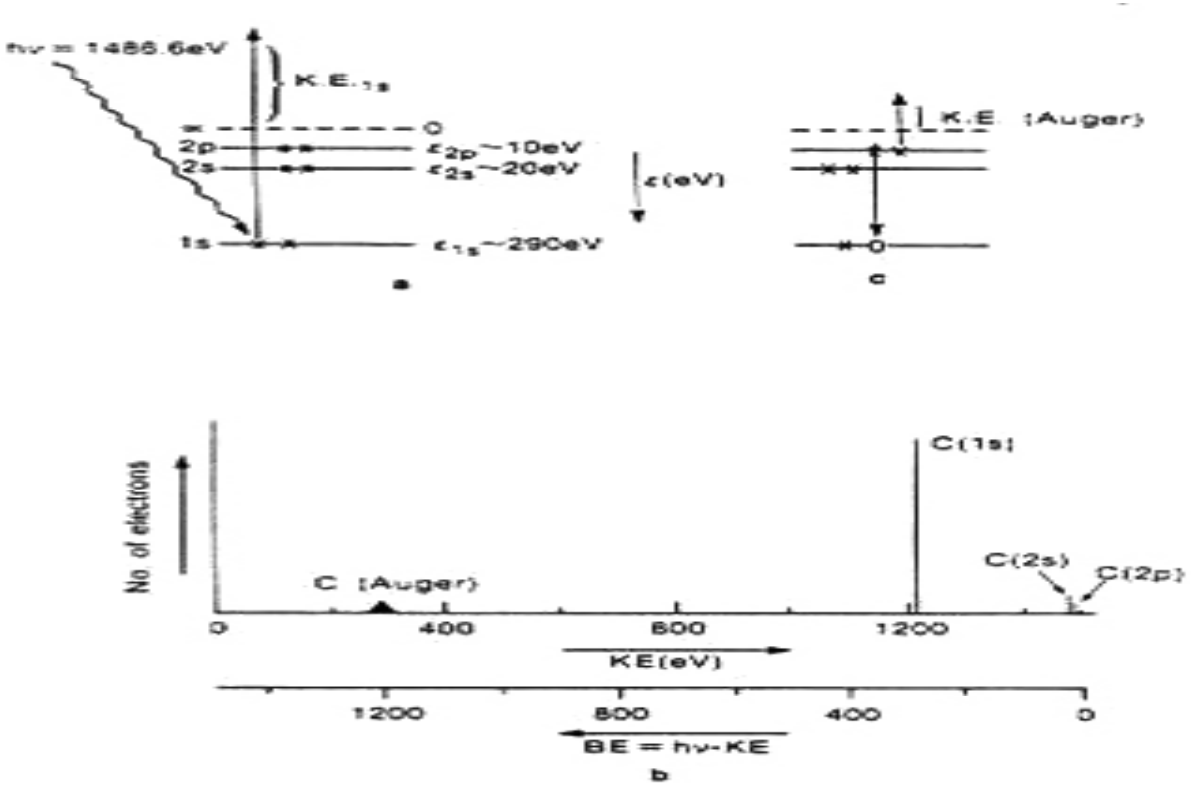

Figure 1 (a) Schematic representation of the electronic energy levels of a C atom and the photoionization of a C 1s electron. (b) Schematic of the *KE* energy distribution of photoelectrons ejected from an ensemble of C atoms subjected to 1486.6-eV X rays.(c) Auger emission relaxation process for the C 1s hole-state produced in (a).

Introduction to X-Ray Photoelectron Spectroscopy

- **Different orbitals give Different peaks in spectrum**
- **Peak intensities depend on Photoionization cross section (largest for C 1s)**
- **Extra peak: Auger emission**

Introduction to X-Ray Photoelectron Spectroscopy

- http://www.nuance.northwestern.edu/keckii/xps1.asp

Introduction to X-Ray Photoelectron Spectroscopy

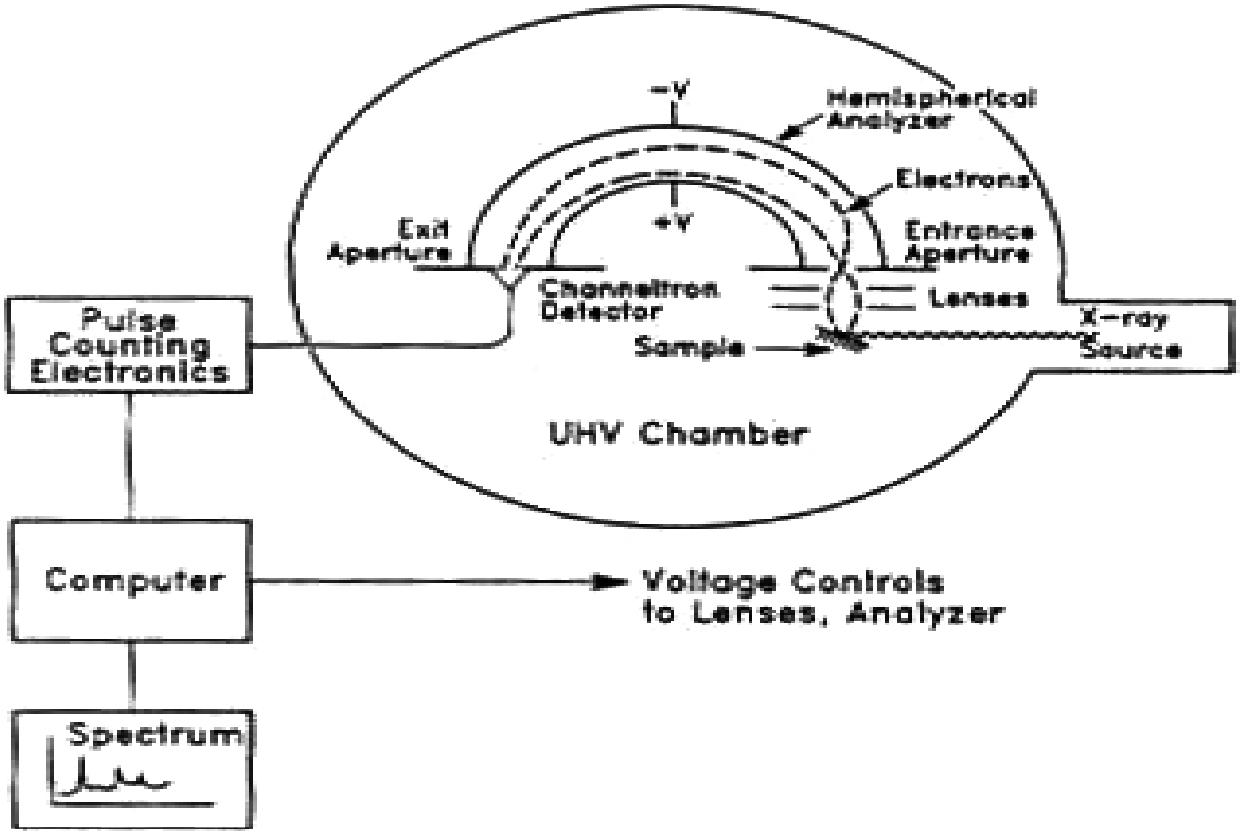

Schematic of a typical electron spectrometer showing all the necessary components. A hemispherical electrostatic electron energy analyser is depicted.

Introduction to X-Ray Photoelectron Spectroscopy

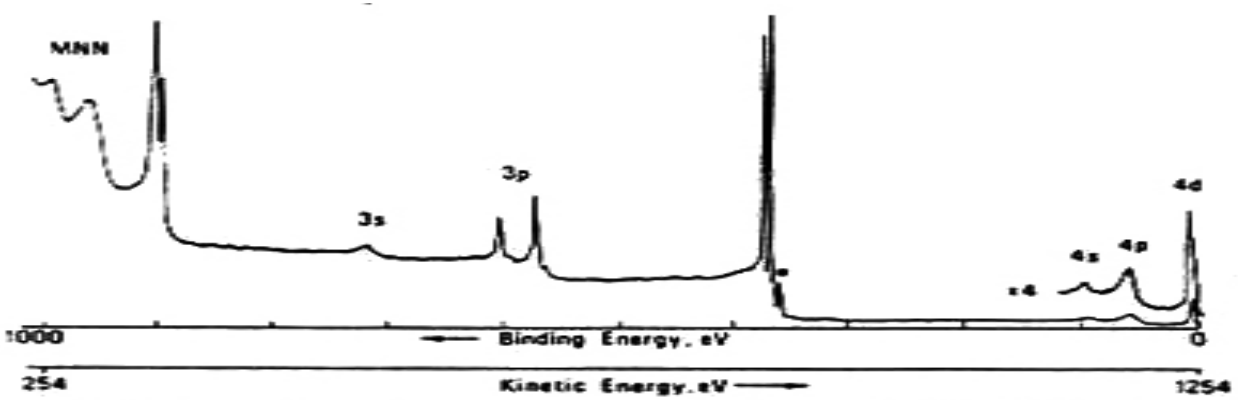

Figure 3.16 X-ray photo-electron spectrum of silver excited by Mg $K\alpha$ (essentially Mg $K\alpha_{1,2}$) and recorded with a constant analyser energy of 100 eV ("Ag 3*d* 'satellite' excited by Mg $K\alpha_{3,4}$)

"Splitting" of 3p, 3d, etc. due to spin-orbit splitting

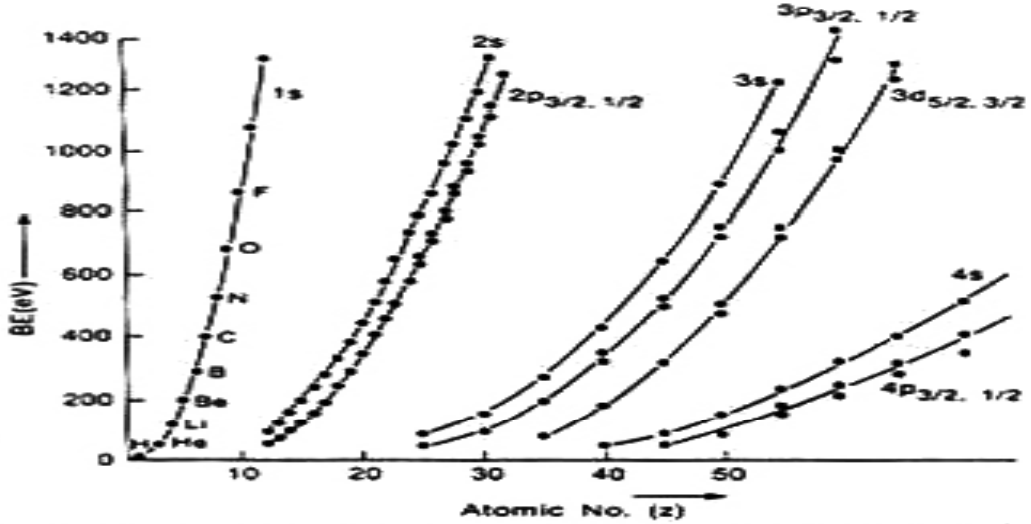

Approximate *BE*s of the different electron shells as a function of atomic number *Z* of the atom concerned, up to the 1486.6-eV limit accessible by Al Kα radiation.[2]

Electron shells

$1s^2$
$2s^2$
$2p^6$
$3s^2$
$3p^6$
$3d^{10}$
$4s^2$
$4p^2$
...

Introduction to X-Ray Photoelectron Spectroscopy

(16)

2-6

Table 2-2. *Electron binding energies, in electron volts, for the elements in their natural forms.*

Element	K 1s	L_I 2s	L_{II} $2p_{1/2}$	L_{III} $2p_{3/2}$	M_I 3s	M_{II} $3p_{1/2}$	M_{III} $3p_{3/2}$	M_{IV} $3d_{3/2}$	M_V $3d_{5/2}$	N_I 4s	N_{II} $4p_{1/2}$	N_{III} $4p_{3/2}$
1 H	16[a]											
2 He	24.6[a]											
3 Li	54.7[a]											
4 Be	111.5[a]											
5 B	188[a]											
6 C	284.2[a]											
7 N	409.9[a]	37.3[a]										
8 O	543.1[a]	41.6[a]										
9 F	696.7[a]											
10 Ne	870.2[a]	48.5[a]	21.7[a]	21.6[a]								
11 Na	1070.8[†]	63.5[†]	30.4[†]	30.5[a]								
12 Mg	1303.0[†]	88.6[a]	49.6[†]	49.2[†]								
13 Al	1558.98[a]	117.8[a]	72.9[a]	72.5[a]								
14 Si	1839	149.7[a,b]	99.8[a]	99.2[a]								
15 P	2149	189[a]	136[a]	135[a]								
16 S	2472	2309[a,b]	163.6[a]	162.5[a]								
17 Cl	2833	270[a]	202[a]	200[a]								
18 Ar	3205.9[a]	326.3[a]	250.6[a]	248.4[a]	29.3[a]	15.9[a]	15.7[a]					
19 K	3608.4[a]	378.6[a]	297.3[a]	294.6[a]	34.8[a]	18.3[a]	18.3[a]					
20 Ca	4038.5[a]	438.4[†]	349.7[†]	346.2[†]	44.3[†]	25.4[†]	25.4[†]					
21 Sc	4492	498.0[a]	403.6[a]	398.7[a]	51.1[a]	28.3[a]	28.3[a]					
22 Ti	4966	560.9[†]	461.2[†]	453.8[†]	58.7[†]	32.6[†]	32.6[†]					
23 V	5465	626.7[†]	519.8[†]	512.1[†]	66.3[†]	37.2[†]	37.2[†]					
24 Cr	5989	695.7[†]	583.8[†]	574.1[†]	74.1[†]	42.2[†]	42.2[†]					
25 Mn	6539	769.1[†]	649.9[†]	638.7[†]	82.3[†]	47.2[†]	47.2[†]					
26 Fe	7112	844.6[†]	719.9[†]	706.8[†]	91.3[†]	52.7[†]	52.7[†]					
27 Co	7709	925.1[†]	793.3[†]	778.1[†]	101.0[†]	58.9[†]	58.9[†]					
28 Ni	8333	1008.6[†]	870.0[†]	852.7[†]	110.8[†]	68.0[†]	66.2[†]					
29 Cu	8979	1096.7[†]	952.3[†]	932.5[†]	122.5[†]	77.3[†]	75.1[†]					
30 Zn	9659	1196.2[a]	1044.9[a]	1021.8[a]	139.8[a]	91.4[a]	88.6[a]	10.2[a]	10.1[a]			
31 Ga	10367	1299.0[a,b]	1143.2[†]	1116.4[†]	159.5[†]	103.5[†]	103.5[†]	18.7[†]	18.7[†]			
32 Ge	11103	1414.6[a,b]	1248.1[a,b]	1217.0[a,b]	180.1[a]	124.9[a]	120.8[a]	29.0[a]	29.0[a]			
33 As	11867	1527.0[a,b]	1359.1[a,b]	1323.6[a,b]	204.7[a]	146.2[a]	141.2[a]	41.7[a]	41.7[a]			
34 Se	12658	1652.0[a,b]	1474.3[a,b]	1433.9[a,b]	229.6[a]	166.5[a]	160.7[a]	55.5[a]	54.6[a]			
35 Br	13474	1782[a]	1596[a]	1550[a]	257[a]	189[a]	182[a]	70[a]	69[a]			
36 Kr	14326	1921	1730.9[a]	1678.4[a]	292.8[a]	222.2[a]	214.4	95.0[a]	93.8[a]	27.5[a]	14.1[a]	14.1[a]
37 Rb	15200	2065	1864	1804	326.7[a]	248.7[a]	239.1[a]	113.0[a]	112[a]	30.5[a]	16.3[a]	15.3[a]
38 Sr	16105	2216	2007	1940	358.7[†]	280.3[†]	270.0[†]	136.0[†]	134.2[†]	38.9[†]	20.3[†]	20.3[†]
39 Y	17038	2373	2156	2080	392.0[a,b]	310.6[a]	298.8[a]	157.7[†]	155.8[†]	43.8[a]	24.4[a]	23.1[a]
40 Zr	17998	2532	2307	2223	430.3[†]	343.5[†]	329.8[†]	181.1[†]	178.8[†]	50.6[†]	28.5[†]	27.7[†]
41 Nb	18986	2698	2465	2371	466.6[†]	376.1[†]	360.6[†]	205.0[†]	202.3[†]	56.4[†]	32.6[†]	30.8[†]
42 Mo	20000	2866	2625	2520	506.3[†]	410.6[†]	394.0[†]	231.1[†]	227.9[†]	63.2[†]	37.6[†]	35.5[†]
43 Tc	21044	3043	2793	2677	544[a]	447.6[a]	417.7[a]	257.6[a]	253.9[a]	69.5[a]	42.3[a]	39.9[a]
44 Ru	22117	3224	2967	2838	586.2[†]	483.3[†]	461.5[†]	284.2[†]	280.0[†]	75.0[†]	46.5[†]	43.2[†]
45 Rh	23220	3412	3146	3004	628.1[†]	521.3[†]	496.5[†]	311.9[†]	307.2[†]	81.4[a,b]	50.5[†]	47.3[†]
46 Pd	24350	3604	3330	3173	671.6[†]	559.9[†]	532.3[†]	340.5[†]	335.2[†]	87.1[a,b]	55.7[†a]	50.9[†a]
47 Ag	25514	3806	3524	3351	719.0[†]	603.8[†]	573.0[†]	374.0[†]	368.0[†]	97.0[†]	63.7[†]	58.3[†]

2.2 ELECTRON BINDING ENERGIES

Gwyn P. Williams

Table 2-2 gives the electron binding energies for the elements in their natural forms. The energies are given in electron volts relative to the vacuum level for the rare gases and for H_2, N_2, O_2, F_2, and Cl_2; relative to the Fermi level for the metals; and relative to the top of the valence bands for semiconductors. Values have been taken from Ref. 1 except as noted:

[a] Values taken from Ref. 2.
[†] Values taken from Ref. 3.
[a] One-particle approximation not valid owing to the extremely short lifetime of the core hole.
[b] Values derived from Ref. 1.

REFERENCES

1. J. A. Bearden and A. F. Burr, "Reevaluation of X-Ray Atomic Energy Levels," *Rev. Mod. Phys.* 39, 125 (1967).
2. M. Cardona and L. Ley, Eds., *Photoemission in Solids I: General Principles* (Springer-Verlag, Berlin, 1978). The present table includes several corrections to the values appearing in this reference.
3. J. C. Fuggle and N. Mårtensson, "Core-Level Binding Energies in Metals," *J. Electron Spectrosc. Relat. Phenom.* 21, 275 (1980).

Be careful: elements with similar

BEs C1s & Ru3d; Ar2p & Rb 3p

2-7

Introduction to X-Ray Photoelectron Spectroscopy

chemical shift of C 1s

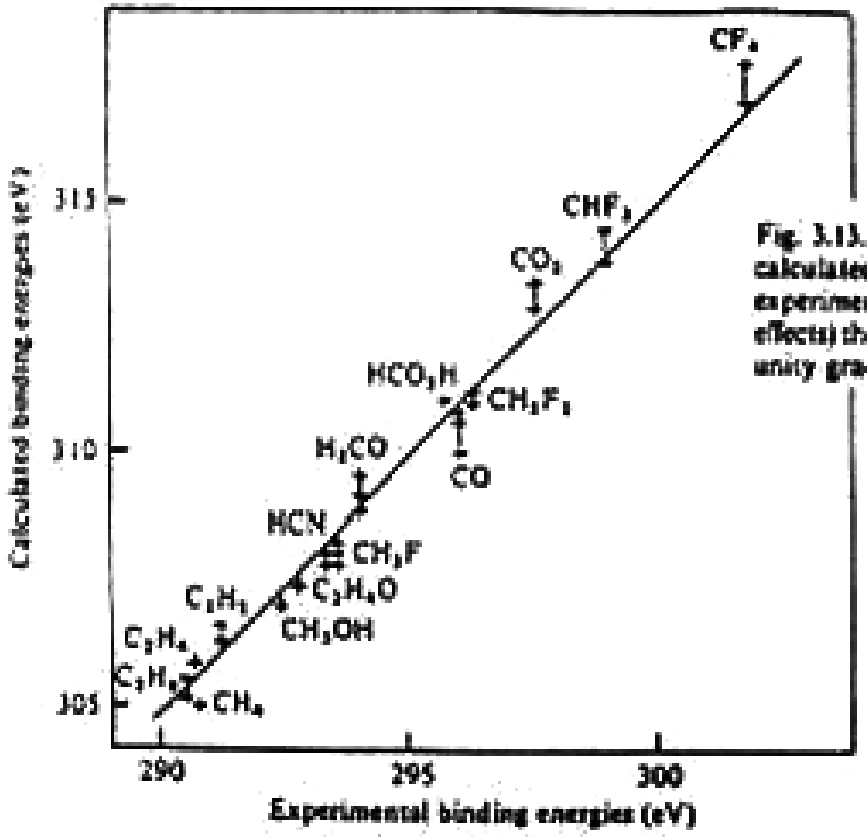

Fig. 3.13. Comparison of experimental XPS C 1s binding energies with calculated via Koopman's theorem for C in a range of molecules. Although experimental and theoretical values differ by 15 eV (associated with relaxation effects) the systematic comparison is excellent as indicated by the straight line of unity gradient (after Shirley, 1973).

Chemical shift of C 1s varies systematically with initial state calculations.

Introduction to X-Ray Photoelectron Spectroscopy

4. Surface Sensitivity

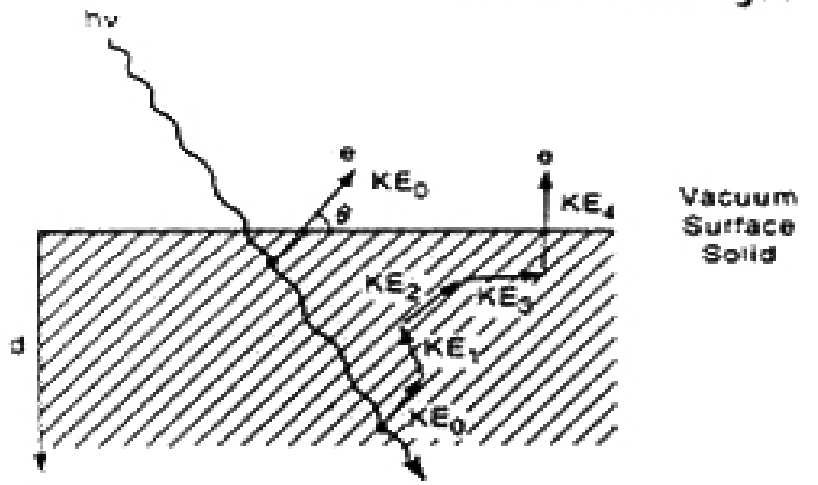

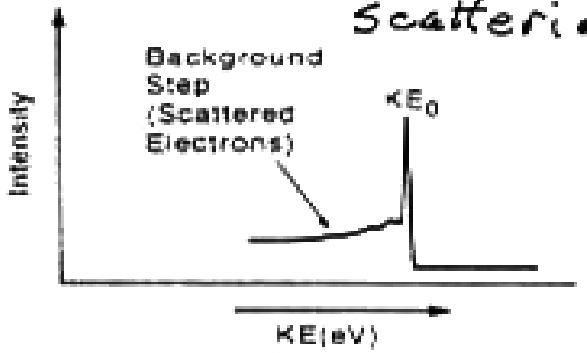

λ = mean free path
= ave. distance traveled by e⁻ before inelastic scattering

a b

Figure 5 (a) Schematic of inelastic electron scattering occurring as a photoelectron, initial energy KE_0, tries to escape the solid, starting at different depths. $KE_4 < KE_3 < KE_2 < KE_1 < KE_0$. (b) KE energy distribution (i.e., electron spectrum) obtained due to the inelastic scattering in (a). Note that the peak, at E_0, must come mainly from the surface region, and the background step, consisting of the lower energy scattered electrons, from the bulk.

Introduction to X-Ray Photoelectron Spectroscopy

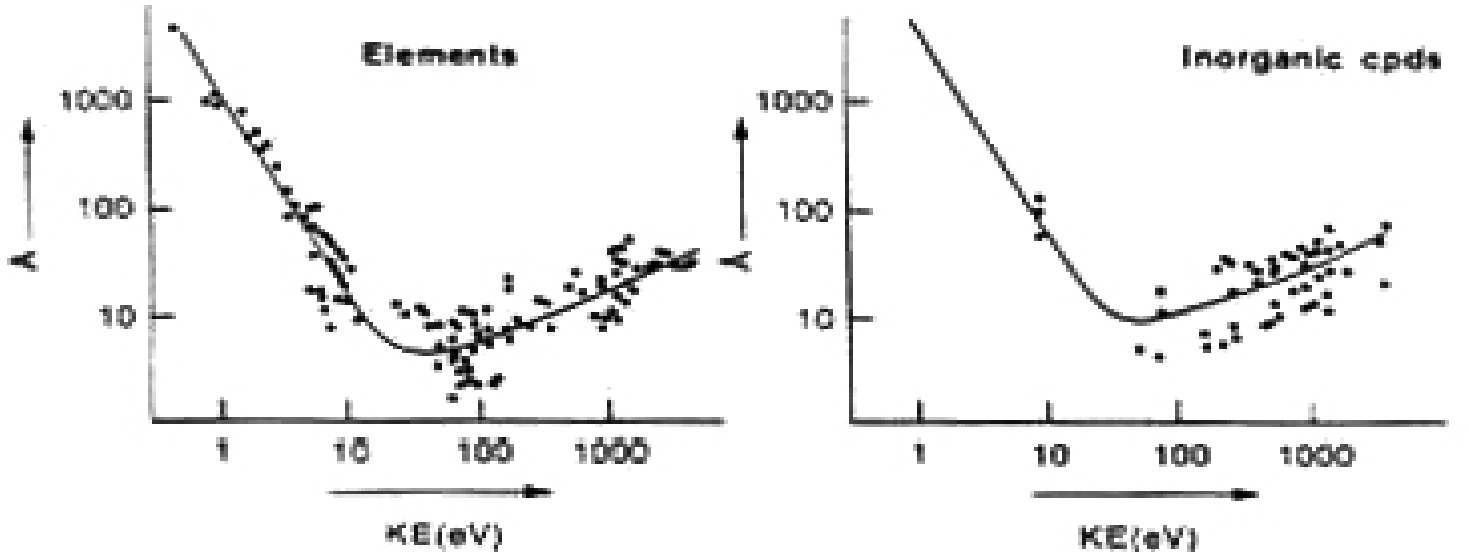

Mean free path lengths λ_e as a function of *KE*, determined for (a) metals and (b) inorganic compounds.[9]

e.g., 50 eV electrons, l~5Å, t < 15Å
1200 eV electrons, l~20Å , t< 60Å

Enhance surface sensitivity by grazing take-off.

Important factor is *surface sensitivity*; short mean free path l for Inelastic electron scattering.
95% of signal comes from top layer (t=3l)

Introduction to X-Ray Photoelectron Spectroscopy

- **Applications**

- **-- Surface contamination**
- **-- Failure analysis**
- **-- Effects of surface treatments**
- **-- Coating, films**
- **-- Tribological effects**

- **-- Depth Profiling (Ar+ sputtering**

Introduction to X-Ray Photoelectron Spectroscopy

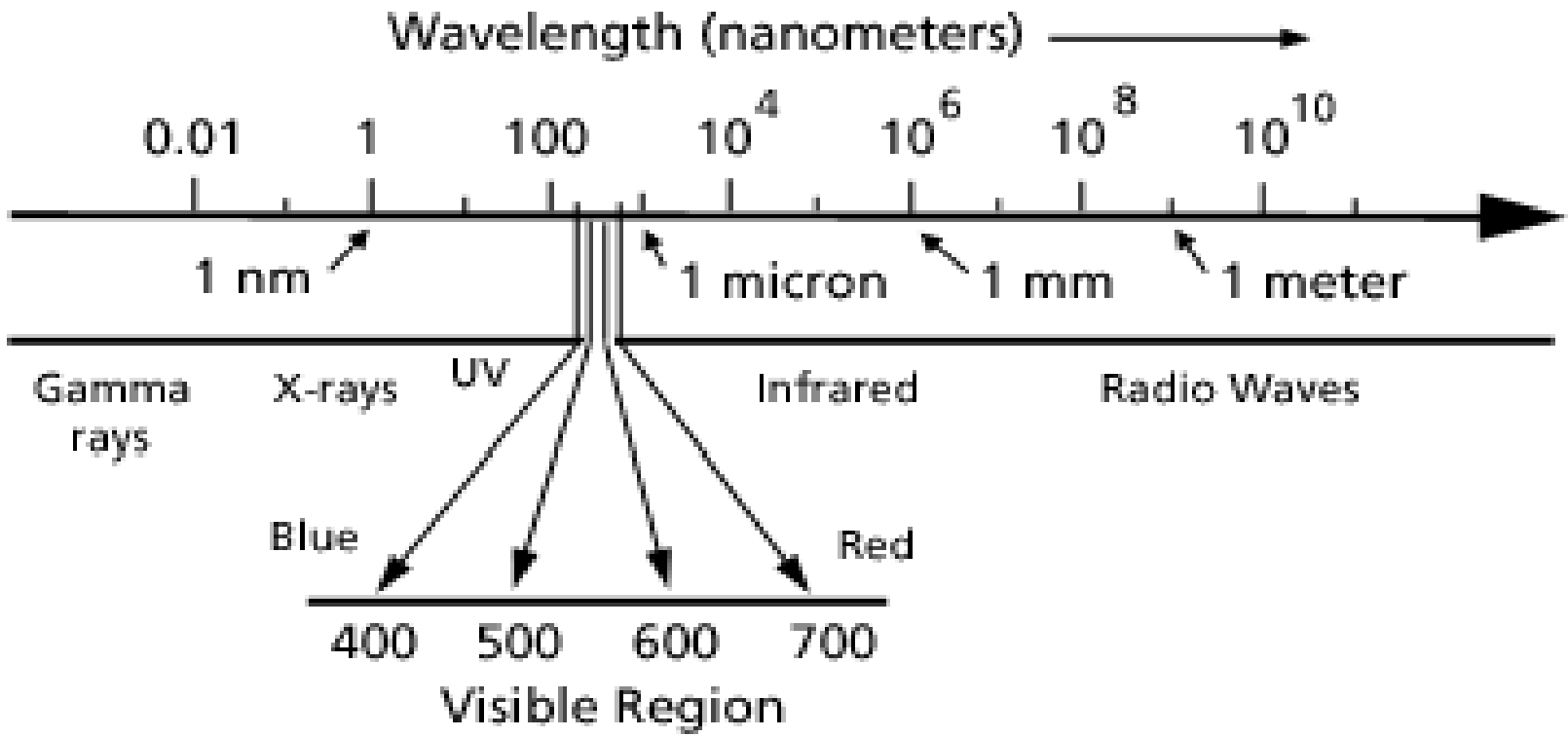

Electromagnetic Spectrum

Introduction to X-Ray Photoelectron Spectroscopy

the square of its amplitude and this is recordable by various photodetectors ('square law' detectors). The associated phase is recordable by holographic techniques.

4.3 The electromagnetic spectrum

4.3.1 The full spectral range

Radiant energy of an electromagnetic nature may conveniently be categorized by either wavelength or frequency into the *electromagnetic spectrum* (see Figure 4.2). Many of the properties of systems discussed in this book, such as light sources, image-forming systems, filters and detectors, are chiefly categorized by reference to behaviour in the appropriate region of the EM spectrum.

4.3.2 The visible spectrum

The small spectral band corresponding to the integrated wavelengths known as 'white light' is particularly narrow. The approximate wavebands corresponding to colours are given in Figure 4.2. The human visual system is poor at spectral frequency analysis: a colour is perceived as being identical whether synthesized by a minimum of three spectral lines or by bands of wavelengths. In terms of sound terminology, whereas the whole EM spectrum covers a 70-octave range with a frequency range of $2^{70}-1$, visible light occupies less than one octave from 400 to 700 nm.

4.3.3 Spectral power distribution

Light and radiation sources of thermal types emit energy over extended or discrete spectral regions to give continuous or line spectra characterizing the stimulated movements of electrons in the outer molecular shells of the materials. A graph of emitted power against wavelength gives the *spectral power distribution* (SPD). A source emitting energy (W_λ) at every wavelength is a *full radiator* (black body), and its SPD is predicted by Planck's Law. For a temperature T in kelvin (K) and constants c_1 and c_2

$$W_\lambda = \frac{c_1}{\lambda^5(\exp(c_2/\lambda t) - 1)} \tag{4.8}$$

Figure 4.3 shows full radiator SPDs for various colour temperatures (T) in kelvin. The maximum emission shifts to shorter wavelengths with increasing T, but the maximum falls inside the visible spectrum only when a temperature of 4000 K is reached. The straight line joining the maxima is given by Wien's Law:

$$\lambda_{max} = \frac{2898}{T} \quad \text{(unit: } \mu\text{m)} \tag{4.9}$$

The total emission is related to the area under the curve by Stefan–Boltzmann's Law:

$$W_T = \sigma T^4 \quad \text{(unit: W m}^{-2}\text{)} \tag{4.10}$$

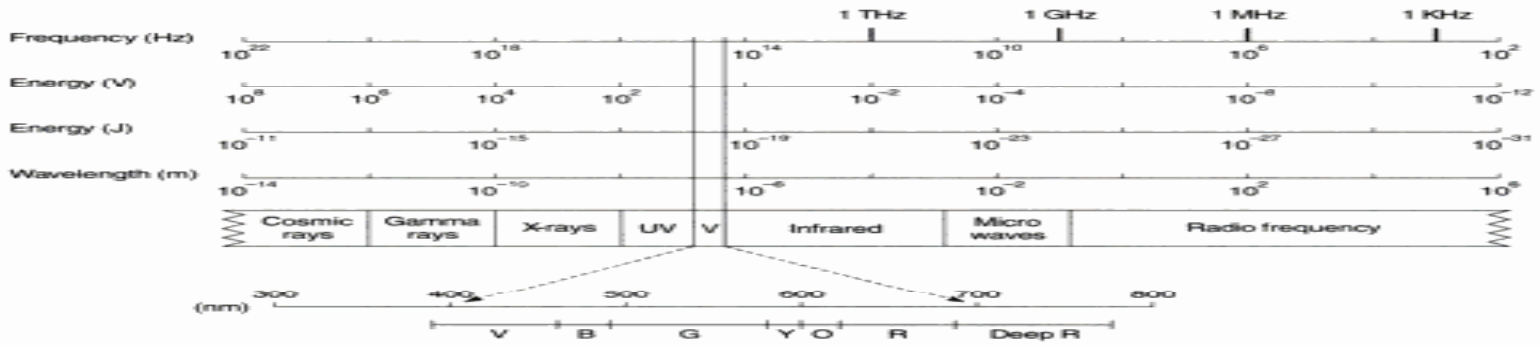

Figure 4.2 The electromagnetic spectrum
The bands of the EM spectrum together with appropriate units of measurement. The visible spectrum (V) is shown expanded into its zones of spectral colours.

Copyrighted material

The Electromagnetic Spectrum

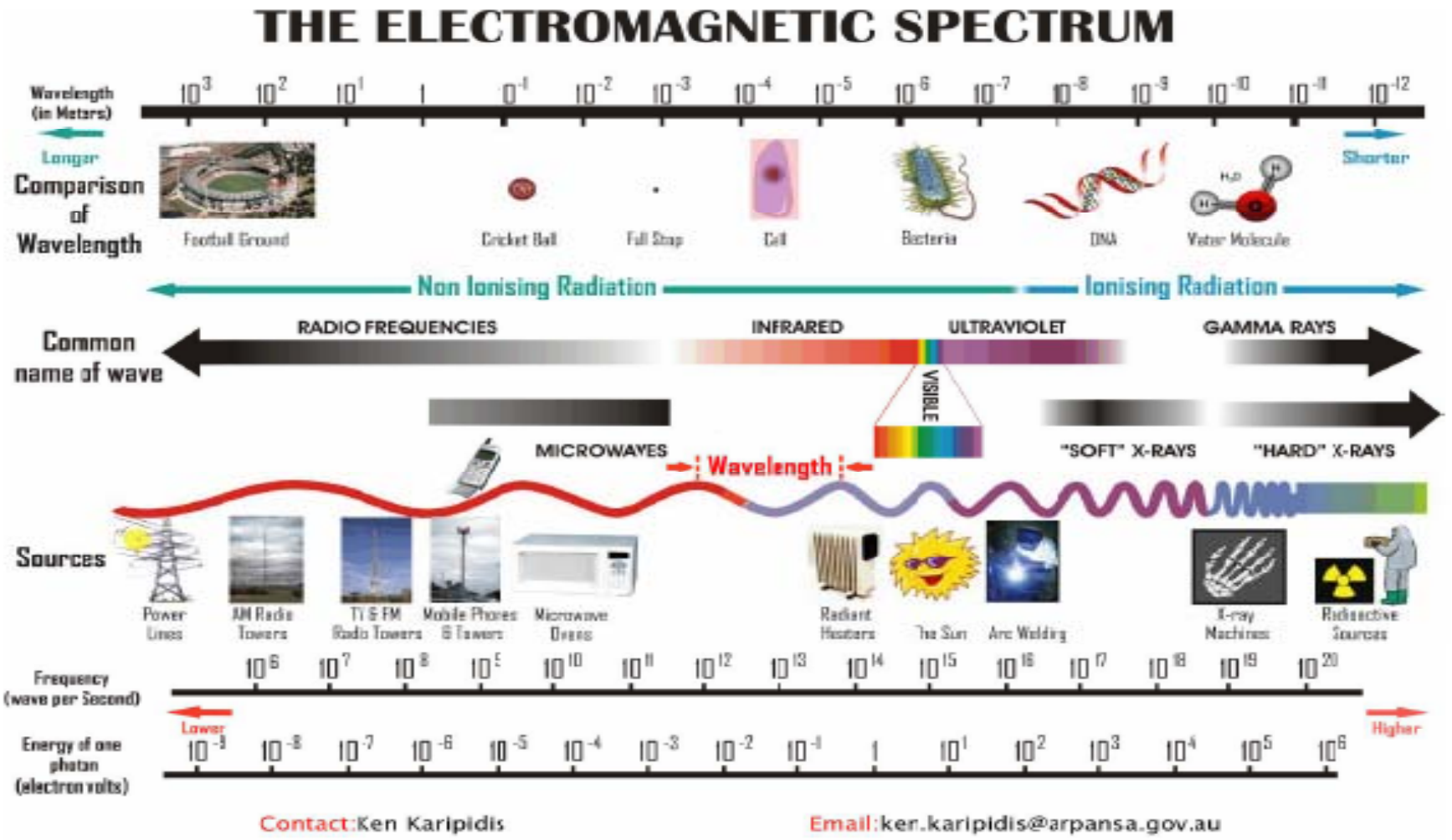

Introduction to X-Ray Photoelectron Spectroscopy

- Others
- Photon must be in resonance with transition energy
- Measure absorbance or transmittance of photons
- Can photon energies

- Photoelectron
- Photons just need enough energy to eject electron
- Measure kinetic energy of ejected electrons
- Monochromatic photon source

Introduction to X-Ray Photoelectron Spectroscopy

WHY WOULD A CHEMIST CARE ABOUT IONIZATIONS ANYWAY?

- Models for description of electronic structure are typically based on an orbital approximation
- Tjalling C Koopmans “ordering of wave functions and eigen values to the individual electrons of an atom” Physical 1,104 (1933).
- Koopman’s theorem “ **The negative of an energy of an occupied orbital from a theoretical calculation is equal to the vertical ionization energy due to the removal of an electron from that orbital”**
- $\Psi = \prod_{1}^{n} \Phi_i$ $\quad\quad$ $(I.E.)_i = -(E_i-)$

Introduction to X-Ray Photoelectron Spectroscopy

- Ionization is still a transition between states
- Initial state (neutral or ion)
- Final state (atom/molecule/ion after an electron is removed plus the ejected electron)
- $M \dashrightarrow M^{+} + e^{-}$

Introduction to X-Ray Photoelectron Spectroscopy

What took so long?

- Development of electron kinetic energy analyzers with sufficient resolution to be useful.
- Development of suitable sources of ionizing radiation, vacuum UV, soft X ray
- Development of electron detectors
- Development of UHV technology

Introduction to X-Ray Photoelectron Spectroscopy

General overview of spectroscopy

- Spectroscopy uses interaction of electromagnetic radiation with matter to learn about the matter.
- If the electromagnetic radiation is in resonance with the energy spacing between different states (electronic, vibrational, rotational, etc) of matter, radiation will be absorbed and transitions will occur.
- The radiation that is transmitted through the sample is measured and spectrum can be reported as either transmittance or absorbance of radiation
- Photoelectron spectroscopy is entirely different.

Introduction to X-Ray Photoelectron Spectroscopy

Historical Timeline

- First spectrophotometer: 1850s
- First IR:1880s
- First crystallography: 1912
- First NMR: 1938
- First EPR: 1944
- First PES: 1957

Introduction to X-Ray Photoelectron Spectroscopy

Kai Seigbahn

Development of X-ray Photoelectron Spectroscopy

- Kai Seigbahn: Development of X-ray Photoelectron Spectroscopy Nobel Prize in Physics 1981
- (His father, Manne Siegbahn, won the Nobel Prize in Physics in 1924 for the development of X-ray spectroscopy) C. Nordling E. Sokolowski and K. Siegbahn, Phys. Rev. 1957, 105, 1676.

Introduction to X-Ray Photoelectron Spectroscopy

David Turner

- Development of Ultraviolet Photoelectron Spectroscopy :
- David Turner: Development of Ultraviolet Photoelectron Spectroscopy D.W. Turner and M.I. Al Jobory, J. Chem. Phys. 1962, 37, 3007

Applications of photoelectron spectroscopy

Comparison XPS & UPS:

- XPS sources cannot be used for studying the fine structure of the valence band .

- UPS sources can excite core energy level like carbon 1s level. They can be used in applications ranging from 0 tot 60 eV .

Applications of photoelectron spectroscopy

Respective UPS and XPS applications domains

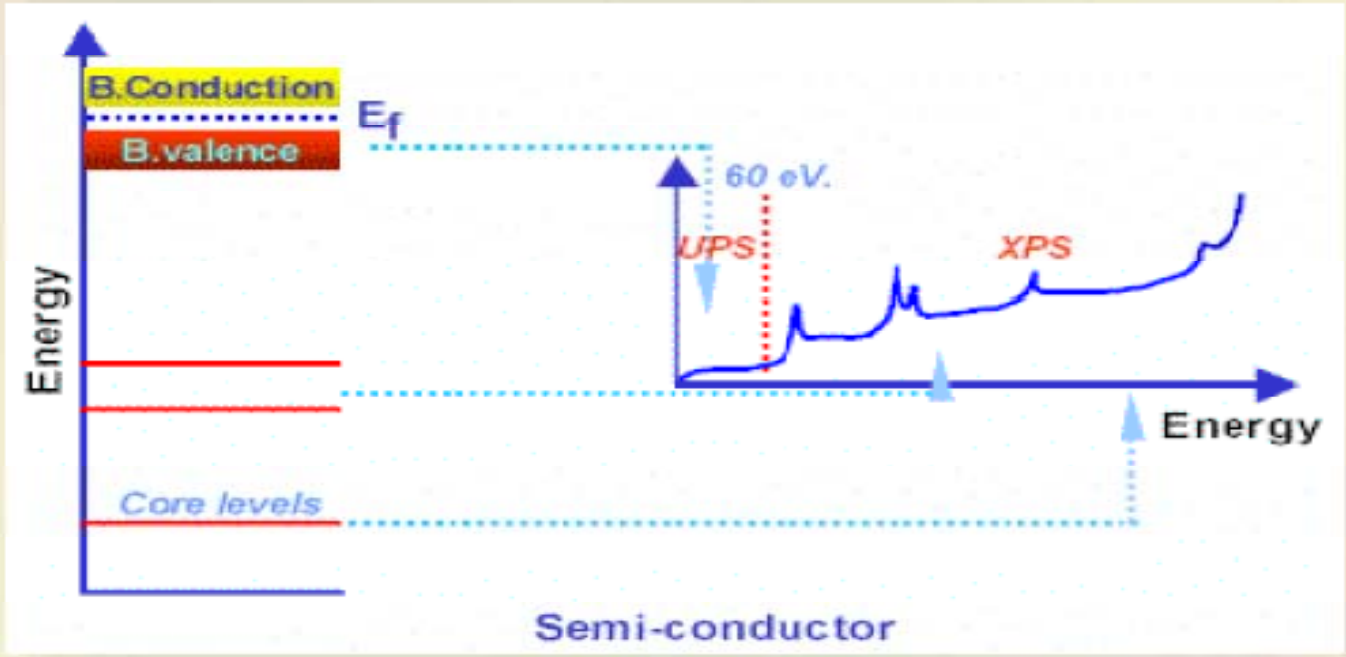

Introduction to X-Ray Photoelectron Spectroscopy

David Turner

- Development of Ultraviolet Photoelectron Spectroscopy :
- David Turner: Development of Ultraviolet Photoelectron Spectroscopy D.W. Turner and M.I. Al Jobory, J. Chem. Phys. 1962, 37, 3007

Applications of photoelectron spectroscopy

1. Rubidium-doped PPV Work function : UPS
2. Ba / Al on polymer interface : UPS/XPS
3. PEDOT+PSS , PEDOT+TSO interaction : XPS
4. PPV/ITO & MEH-PPV/ITO interface : XPS

Applications of photoelectron spectroscopy

Example 1 : UPS

Polaron to **bipolaron transition** in a **conjugated** polymer. Rubidium-doped poly (p-phenylenevinylene)

G Iucci, K Xing, M Logdlund, M Fahlman, WR ... - Chemical Physics Letters, 1995

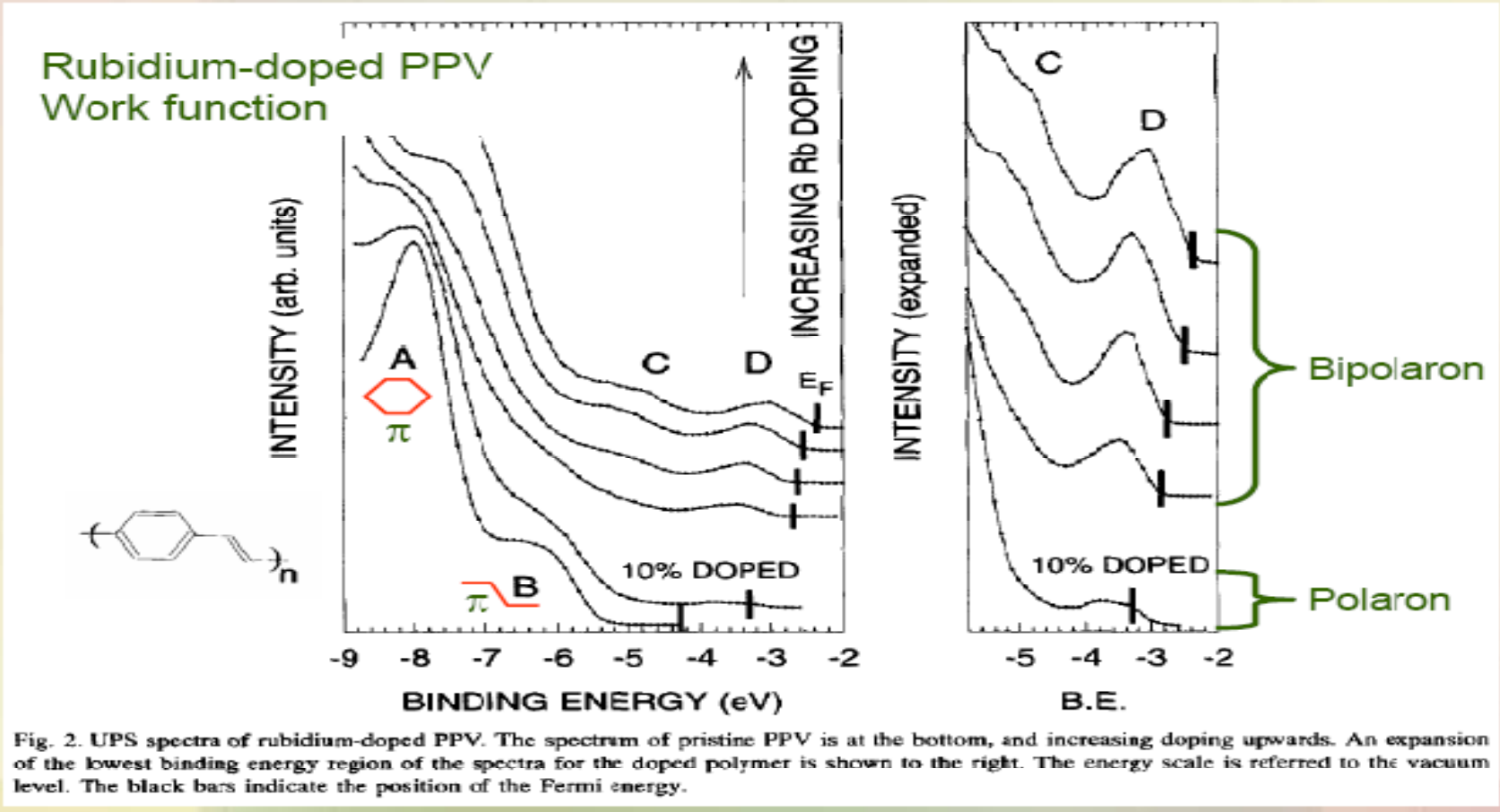

Fig. 2. UPS spectra of rubidium-doped PPV. The spectrum of pristine PPV is at the bottom, and increasing doping upwards. An expansion of the lowest binding energy region of the spectra for the doped polymer is shown to the right. The energy scale is referred to the vacuum level. The black bars indicate the position of the Fermi energy.

Applications of photoelectron spectroscopy

Example 1 : UPS

Polaron to **bipolaron transition** in a **conjugated** polymer. Rubidium-doped poly (p-phenylenevinylene)

G Iucci, K Xing, M Logdlund, M Fahlman, WR … - Chemical Physics Letters, 1995

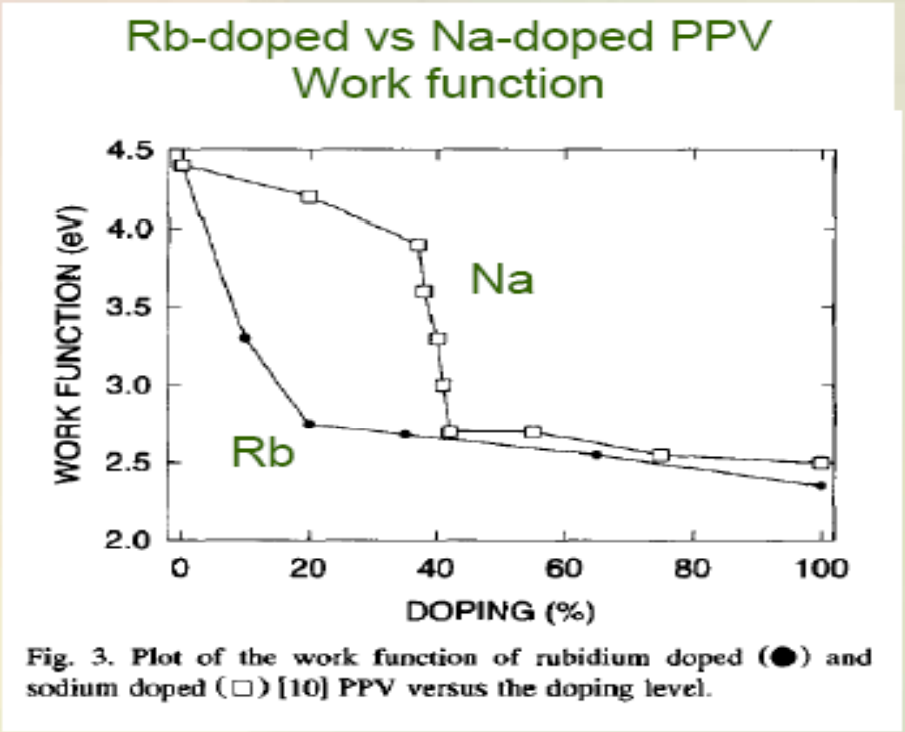

Fig. 3. Plot of the work function of rubidium doped (●) and sodium doped (□) [10] PPV versus the doping level.

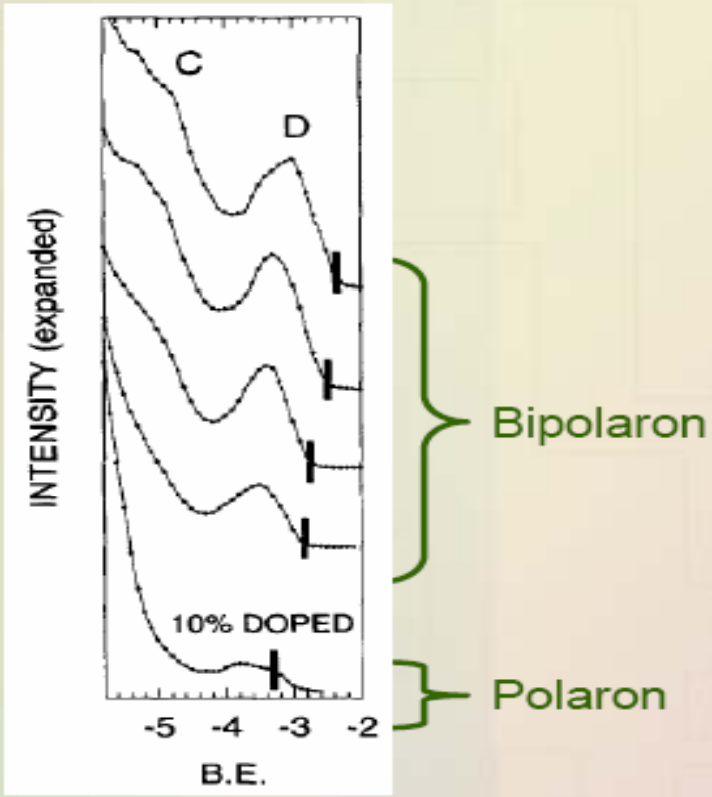

Applications of photoelectron spectroscopy

Example 2-1 : UPS/XPS

Aluminum–barium interfaces on some processable poly (p-phenylene vinylene) polymers studied by photoelectron spectroscopy

A Crispin, A Jonsson, M Fahlman, WR Salaneck - The Journal of Chemical Physics, 2001

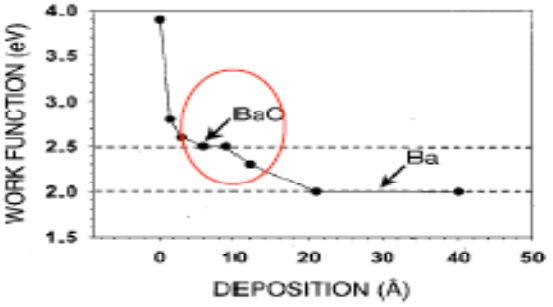

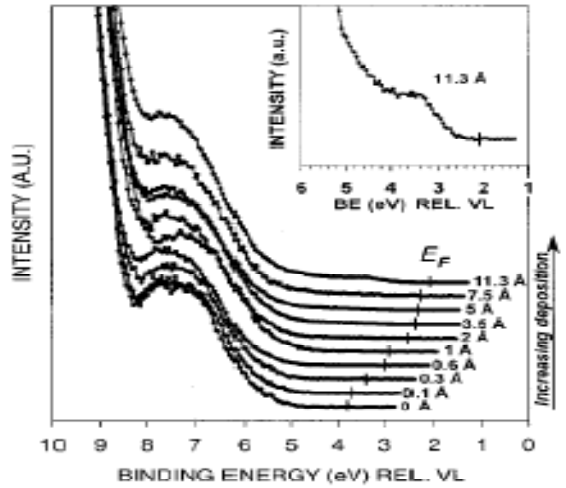

FIG. 3. Evolution of the valence band spectra upon increasing the deposition of barium onto a polymer film heated overnight in UHV at 120 °C. The lowest curve corresponds to the bare polymer. This structure is consistent with the formation of BaO_x species when Ba atoms are deposited onto the polymer surface.

Ba atoms on polymer

- **BaO : ~10Å**

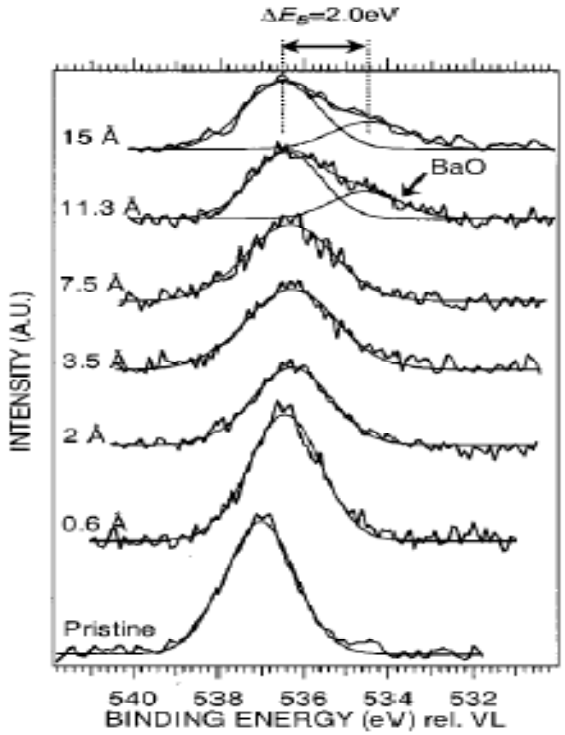

FIG. 2. The O(1*s*) signal as a function of increasing time of deposition of Ba atoms on a polymer surface. The polymer film was heated overnight in UHV at 120 °C. A new feature appears (and grows) on the lower binding energy side of the pristine polymer spectral peak. This peak corresponds to oxygen in BaO_x and is shifted 2.0 eV compared to the polymer oxygen signal.

Applications of photoelectron spectroscopy

Example 2-2 : UPS/XPS

Aluminum–barium interfaces on some processable poly (p-phenylene vinylene) polymers studied by photoelectron spectroscopy

A Crispin, A Jonsson, M Fahlman, WR Salaneck - The Journal of Chemical Physics, 2001

Al atoms on polymer

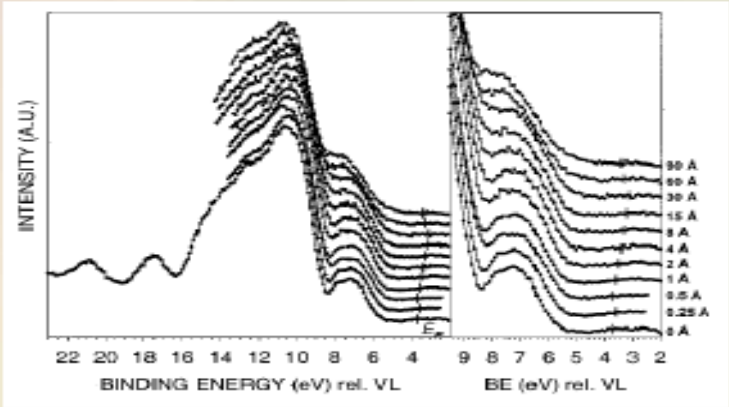

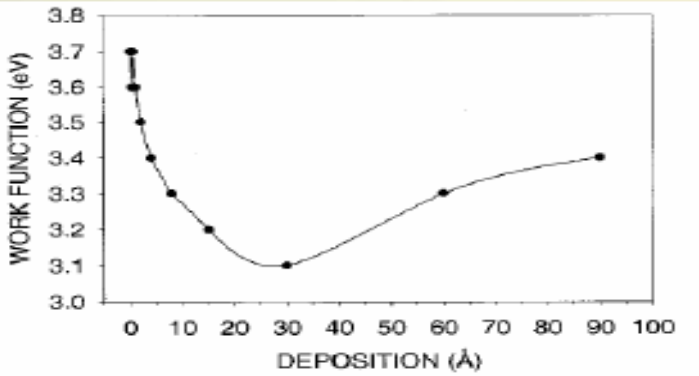

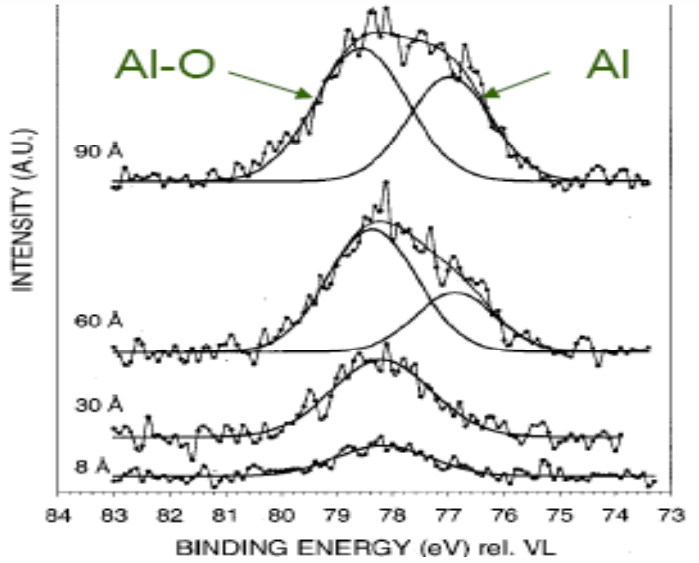

- Al 擴散進多孔性高分子的深度比 unsubstituted PPV來得深
- 0~20Å : Al 擴散進多孔性高分子
- 30~50Å : Al→Al-O

Applications of Photoelectron Spectroscopy

Example 3 : XPS

The electronic structure of poly (3, 4-ethylene-dioxythiophene): Studied by XPS and UPS

KZ Xing, M Fahlman, XW Chen, O Inganaes, WR ... - Synth. Met, 1997

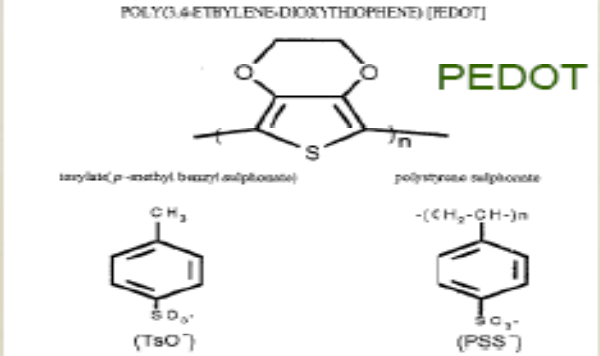

Top: PEDOT+PSS
Middle: PEDOT+TSO
Bottom: PEDOT

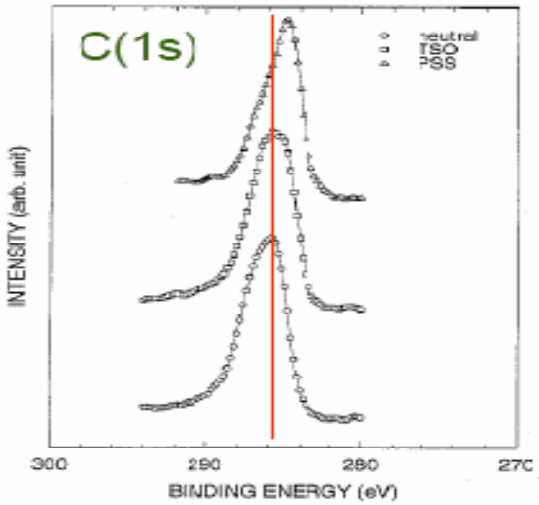

ig. 3. C(1s) XPS spectra of neutral and tosylate(p-methyl benzyl ulfonate) (TsO⁻) and polystyrene sulfonate (PSS⁻) oxidized PEDOT olymers.

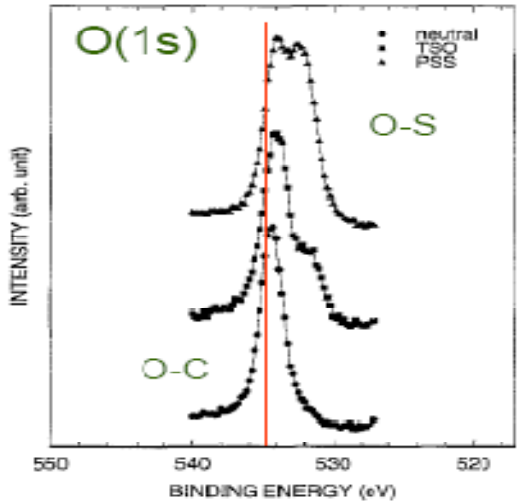

4. O(1s) XPS spectra of neutral and tosylate(p-methyl benzyl onate) (TsO⁻) and polystyrene sulfonate (PSS⁻) oxidized PEDOT /mers.

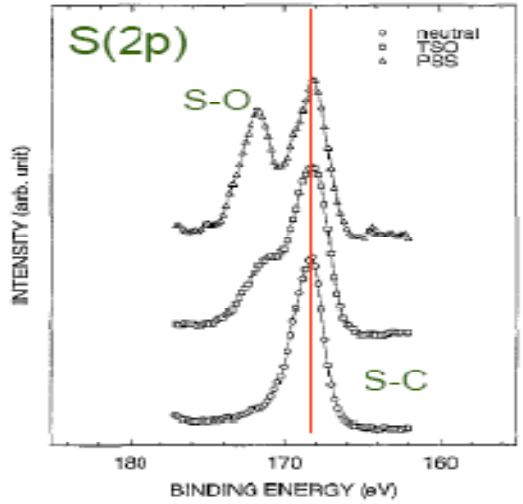

Fig. 5. S(2p) XPS spectra of neutral and tosylate(p-methyl benzyl sulfonate) (TsO⁻) and polystyrene sulfonate (PSS⁻) oxidized PEDOT polymers.

Applications of Photoelectron Spectroscopy

Example 4-1 : XPS

XPS investigation of electrode/polymer interfaces of relevance to the phenylene vinylene polymer- ...
S Li, ET Kang, ZH Ma, KL Tan - Surface and Interface Analysis, 2000

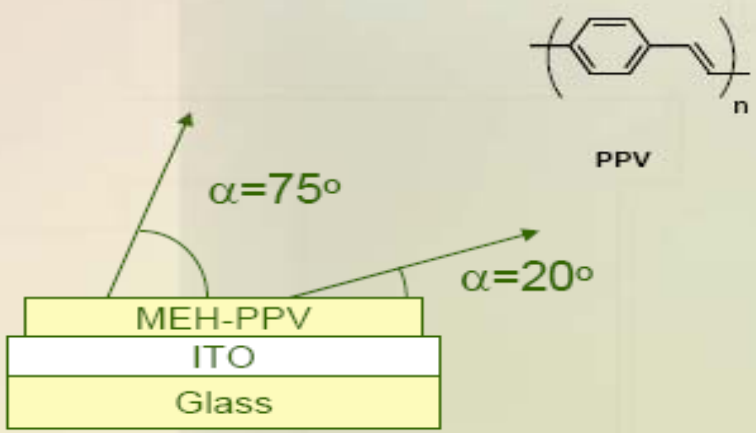

Probing depth of XPS <=7.5nm in organic

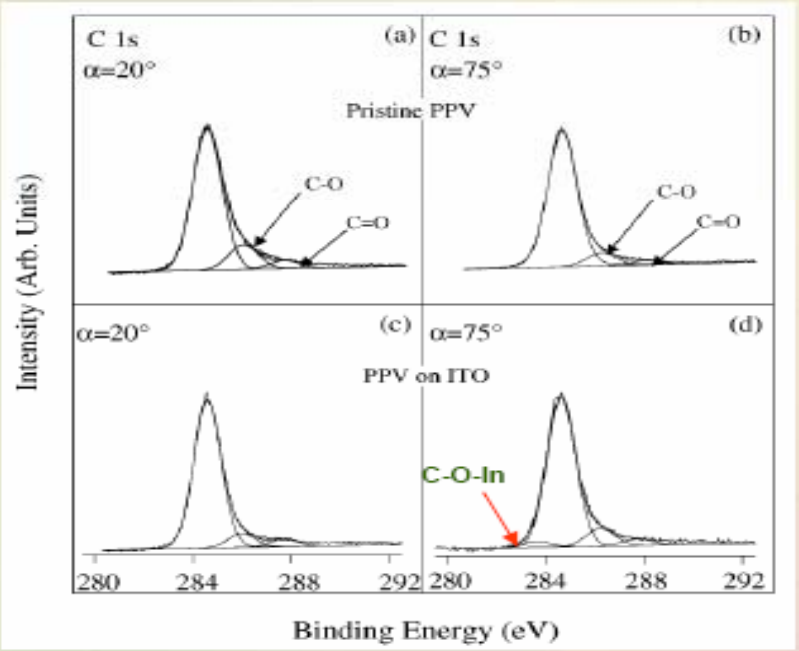

- **C-O-In : only on interface**
- **C-O & C=O : PPV not oxidize by O (from ITO)**

Applications of Photoelectron Spectroscopy

Introduction

- Materials are either conductors or semiconductors or insulators.
- Metals are conductors which have electrons in valence band and conduction band.
- Semiconductors have a energy gap which is about 1 eV.
- Insulators have energy gap greater than 6 eV.
- Materials can be made to conduct or insulate by various electronic transitions which would change the relative populations of the valence and core levels.

Applications of Photoelectron Spectroscopy

Band Structure of metals and insulators

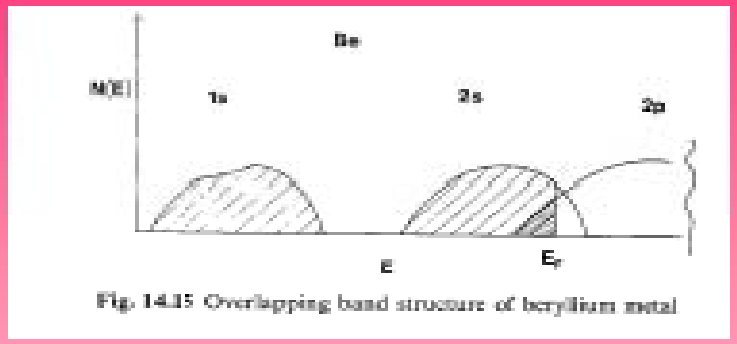

Fig. 14.15 Overlapping band structure of beryllium metal

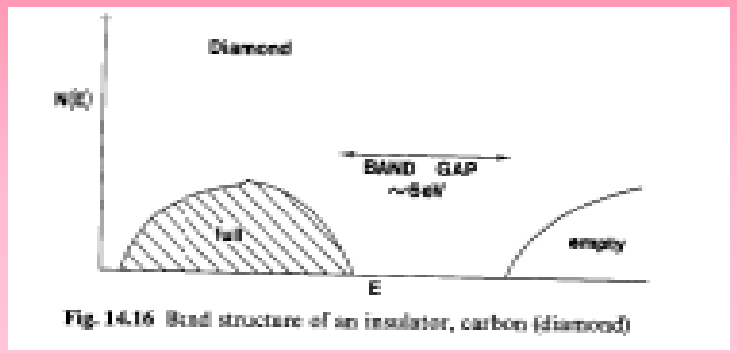

Fig. 14.16 Band structure of an insulator, carbon (diamond)

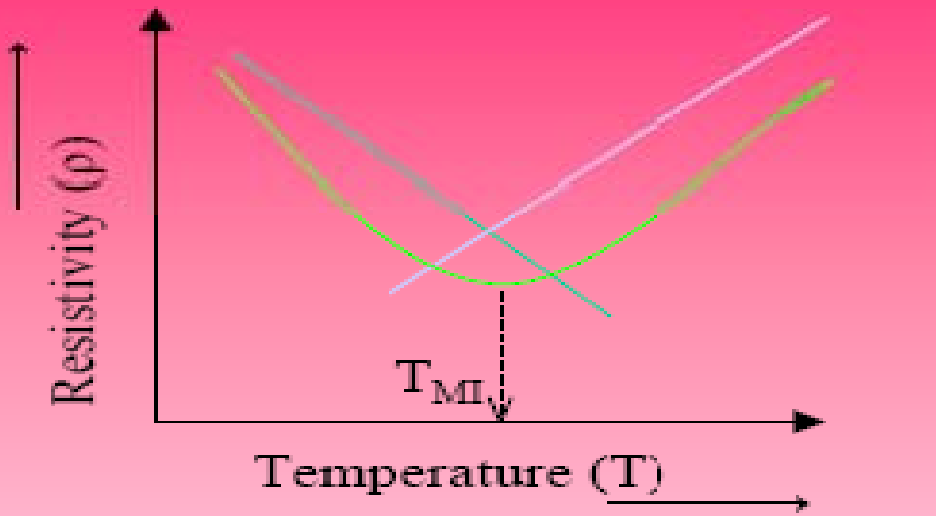

Insulator

Metal

Materials which show MI Transition

Applications of Photoelectron Spectroscopy

Materials

- Various oxides of transition metals like Ni, Cu, V, Fe etc…
- Transition metal compounds.e.g., $(NbSe_4)_3I$
- Rare earth bimetallic oxides e.g., $RNiO_3$
- Some metallic mono layers on specific surfaces. e.g., Ba

Applications of Photoelectron Spectroscopy

NiO

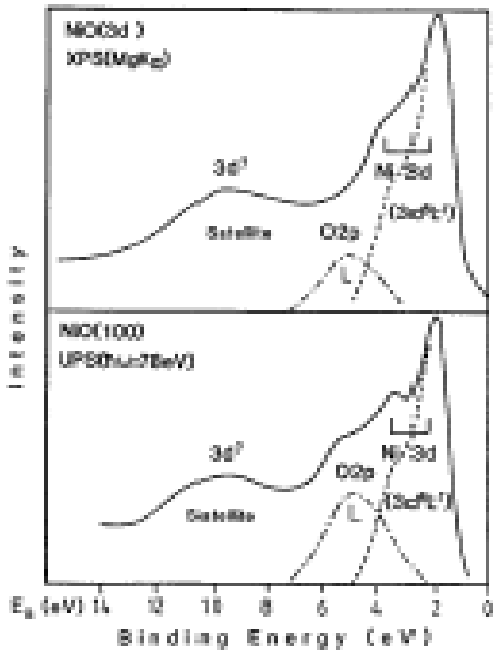

Fig.5.34. Comparison of XPS and UPS spectra of NiO [5.65]. In the XPS spectrum the O 2p contribution was estimated from a comparison of XPS spectra with those of other transition-metal oxides (see also Fig.5.25); in the UPS spectrum the O 2p band is visible. In both cases a distinct satellite is evident. Its assignment to a $3d^7$ final state (NiO has a $3d^8$ initial state) is discussed in the text [5.65]. The zero in the experimental Fermi energy, which is close to the top of the valence band

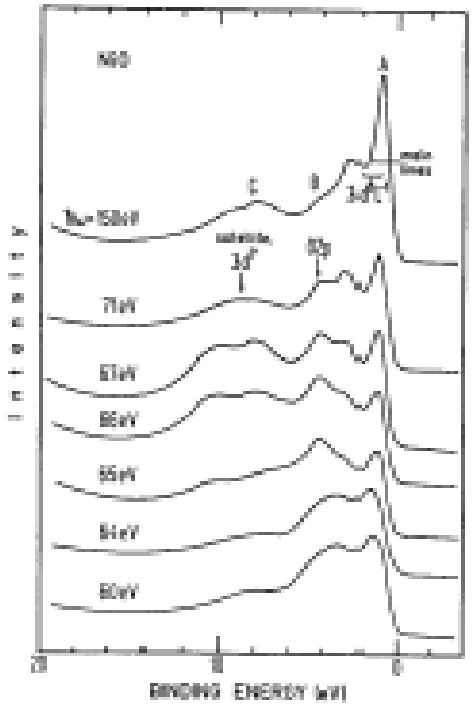

Fig.5.35. Resonance PE spectra of NiO [5.68,67]. A is the "main 3d structure", B the O 2p valence band and C the satellite. Resonance enhancement of the satellite occurs via the reaction: $3p^63d^8+h\nu \rightarrow 3p^53d^9 \rightarrow 3p^63d^7$, indicating that the satellite is a $3d^7$ final state

Applications of Photoelectron Spectroscopy

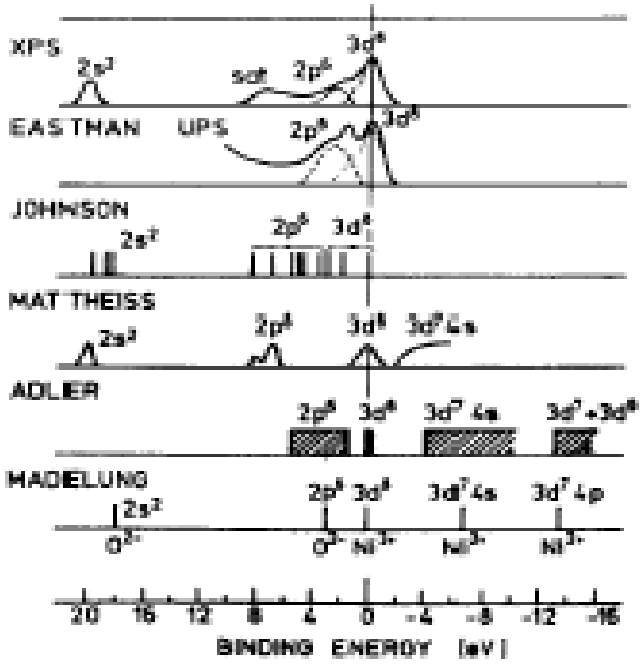

Fig. 3.11. Experimental and theoretical results for the valence band structure of NiO. In every case the zero of energy has been made to coincide with the center of the 3d band

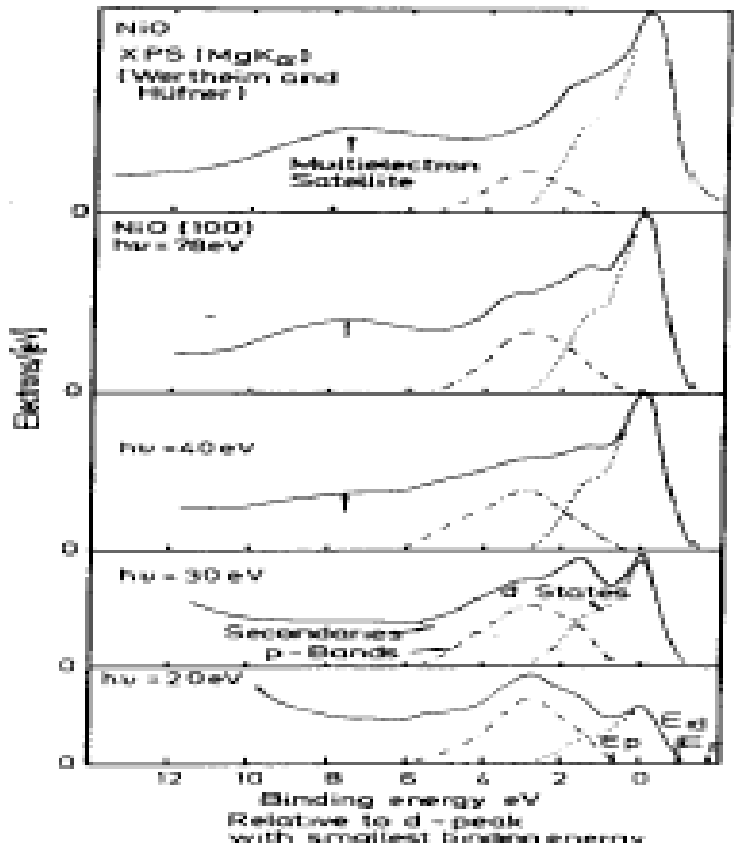

Fig. 3.10. Photoelectron spectra for NiO taken with various photon energies between 20 and 78 eV and with Mg K_α radiation. The zero of energy is placed at the d-state peak and E_v, E_d, and E_F are the Fermi energy, d-state edge, and p-band edge. Partial d-state emission intensities (dashed lines) and p-band intensities (broken lines) are shown (see text) [3.44]

Applications of Photoelectron Spectroscopy

NiO Structure

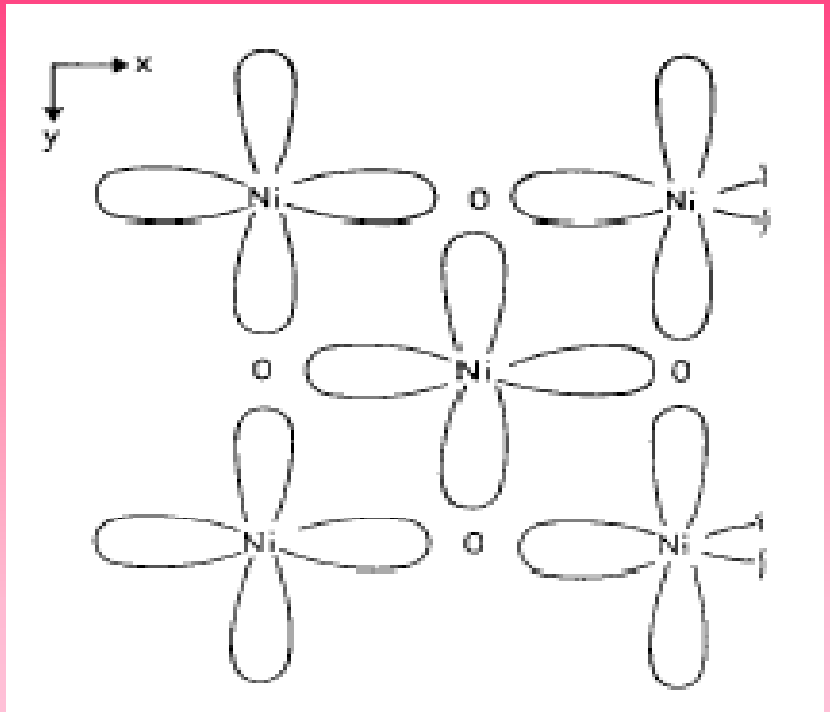

Applications of Photoelectron Spectroscopy

$MNiO_3$ (M = Pr, Sm, Eu, Nd)

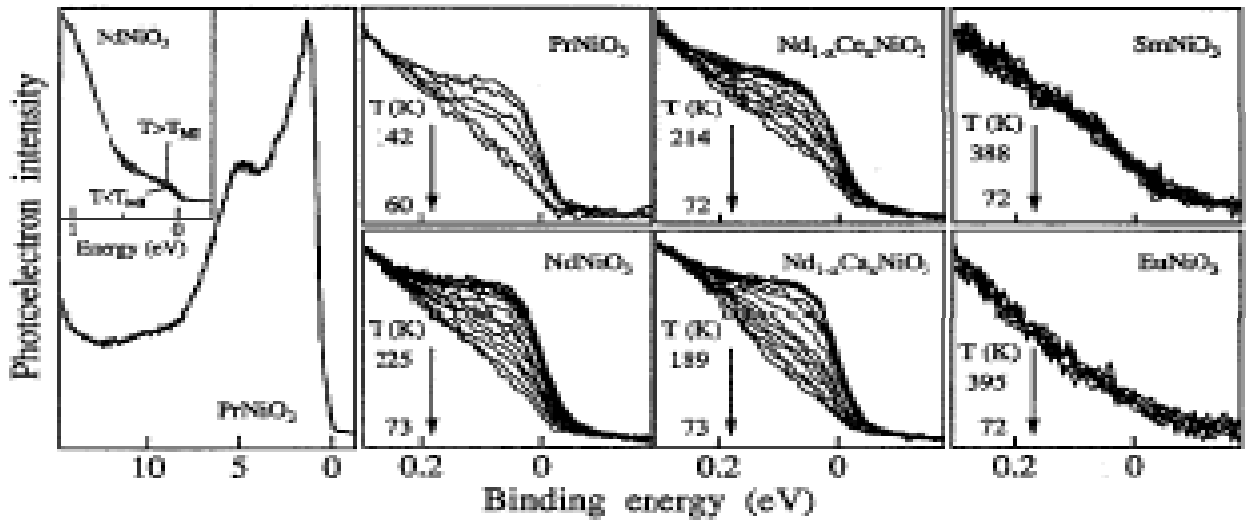

FIG. 1. First panel: Valence band of $PrNiO_3$ ($h\nu = 1486.6$ eV); Inset: The zoom-in into the energy interval of ~1 eV of E_F ($NdNiO_3$ with $h\nu = 21.2$ eV) showing the spectral weight transfer to higher binding energies below T_{MI}; Remaining panels: spectra recorded at different temperatures for $PrNiO_3$, $NdNiO_3$, electron doped $Nd_{0.98}Ce_{0.02}NiO_3$, hole doped $Nd_{0.99}Ca_{0.01}NiO_3$, $SmNiO_3$, and $EuNiO_3$ ($h\nu = 21.2$ eV).

Applications of Photoelectron Spectroscopy

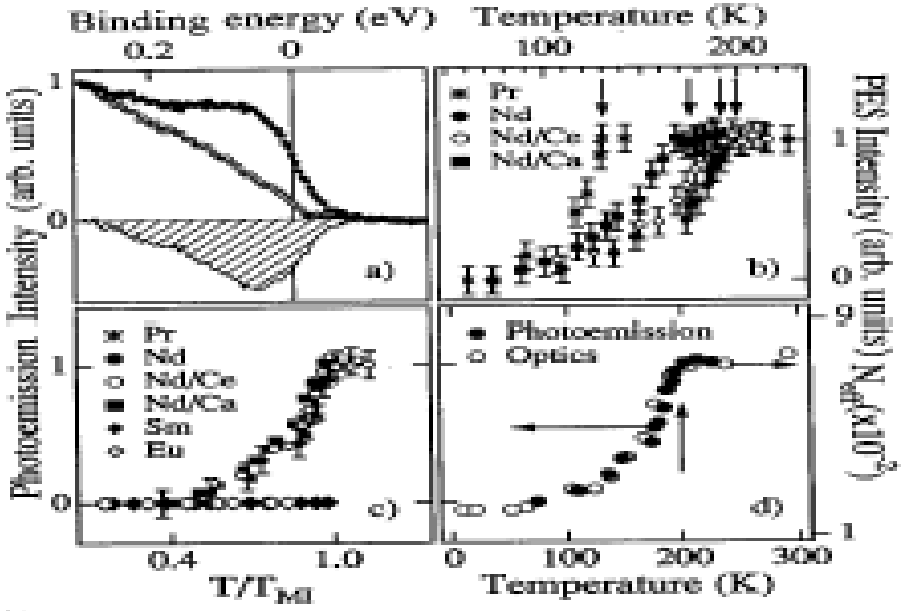

FIG. 2. (a) PES spectra of $NdNiO_3$ at 200 K (full symbols) and 73 K (open symbols) together with their difference. (b) Temperature dependence of the integrated area of the difference curves for $PrNiO_3$, $NdNiO_3$, $Nd_{0.98}Ce_{0.02}NiO_3$, $Nd_{0.99}Ca_{0.01}NiO_3$, normalized to the maximum value. (c) The same as (b) versus the reduced temperature (T/T_{MI}) and together with the results for $SmNiO_3$ and $EuNiO_3$. (d) The optics result from Katsufuji *et al.* (open symbols; right axis) together with our result from (b) for $NdNiO_3$ (closed symbols; left axis). The vertical arrows mark the MI transition temperatures.

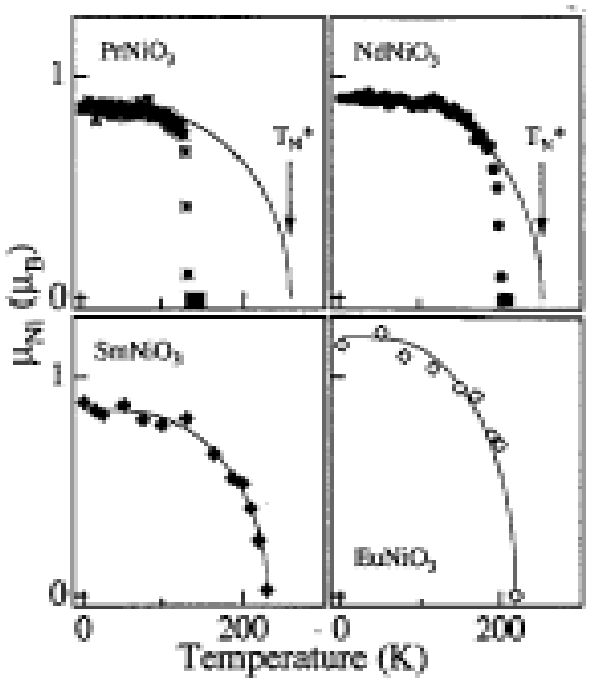

FIG. 3. The evolution of the Ni magnetic moments with temperature for $PrNiO_3$, $NdNiO_3$, $SmNiO_3$, and $EuNiO_3$. The lines are an attempt to fit the data with Brillouin function. The arrows mark the virtual Néel temperatures (T_N^*) for $PrNiO_3$ and $NdNiO_3$.

Applications of Photoelectron Spectroscopy

Example 4-2 : XPS

XPS investigation of electrode/polymer interfaces of relevance to the phenylene vinylene polymer- ...

S Li, ET Kang, ZH Ma, KL Tan - Surface and Interface Analysis, 2000

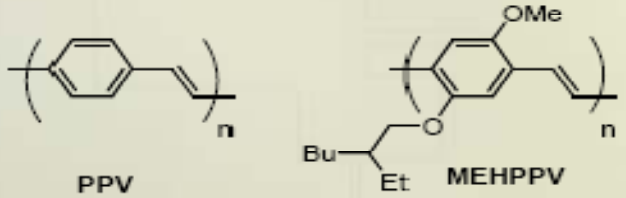

PPV MEHPPV

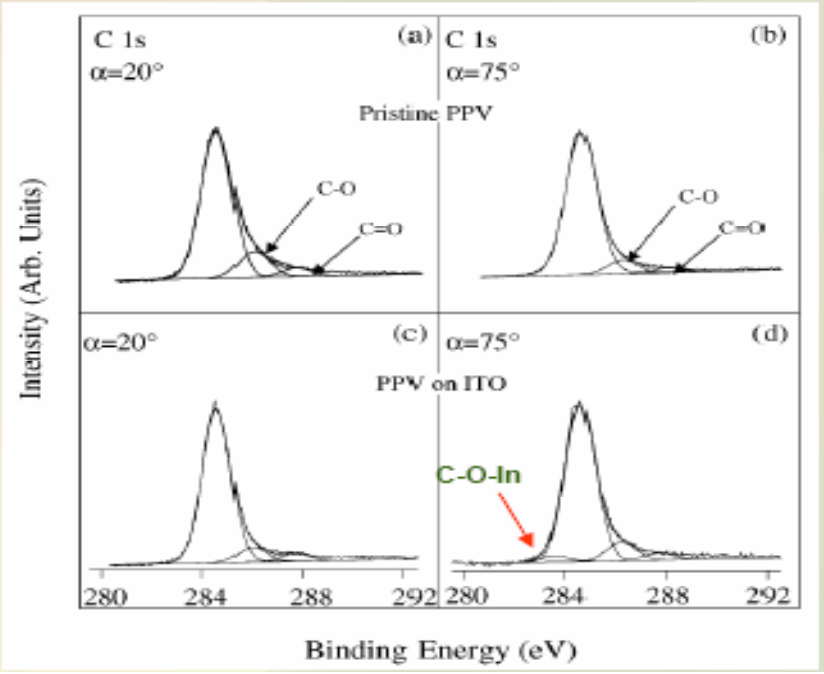

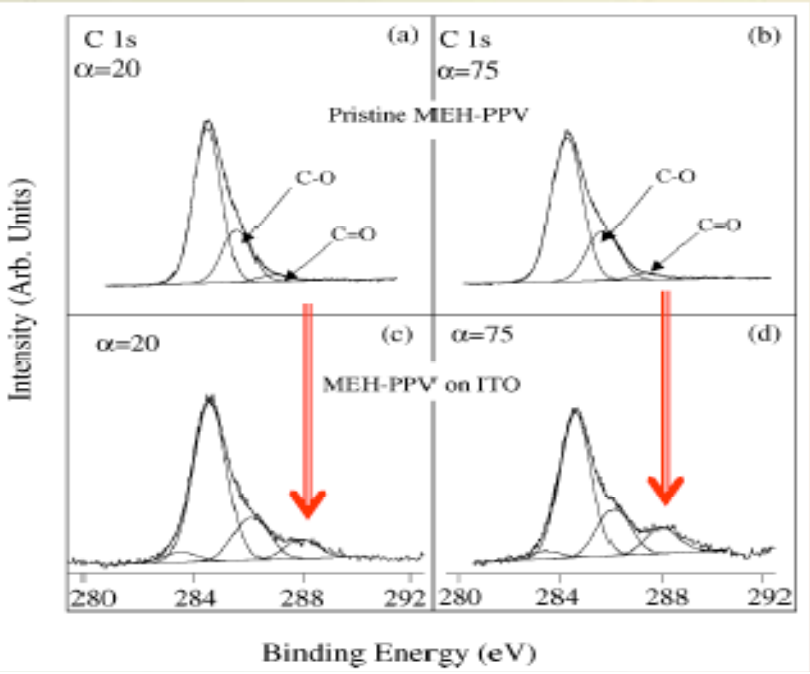

Applications of Photoelectron Spectroscopy

Ba (3x1) on Si(111)

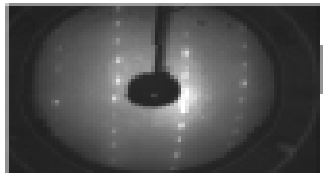

Figure 2:
LEED image of the single-domain (3×1) reconstruction, recorded at 84 eV.

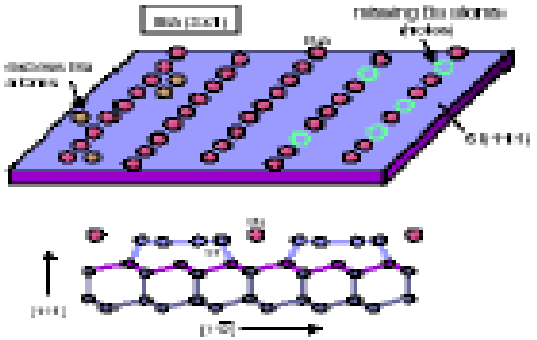

Figure 1:
Schematic of the Ba(3×1)/Si(111) reconstruction. It is possible to prepare the system with excess or missing Ba atoms (top). The channel-tunnel model as currently discussed in the literature as the most likely one. Removal of Ba atoms does not involve bond breaking and leaves a hole-doped one-dimensional chain (bottom).

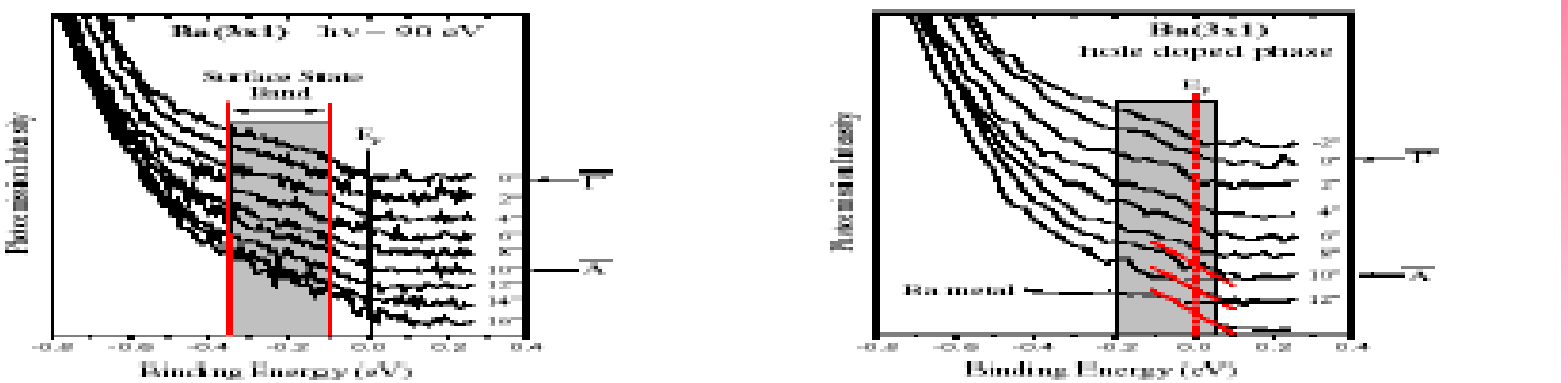

Figure 3:
The left panel shows the surface state band of the Ba(3×1) reconstruction under typical preparation conditions. A weakly dispersing band is identified around ~0.3 eV below E_F. Upon sufficient Ba desorption (right panel), the band is shifted upward by about 0.2 eV such that the band crosses E_F.

Applications of Photoelectron Spectroscopy

$(NbSe_4)_3I$

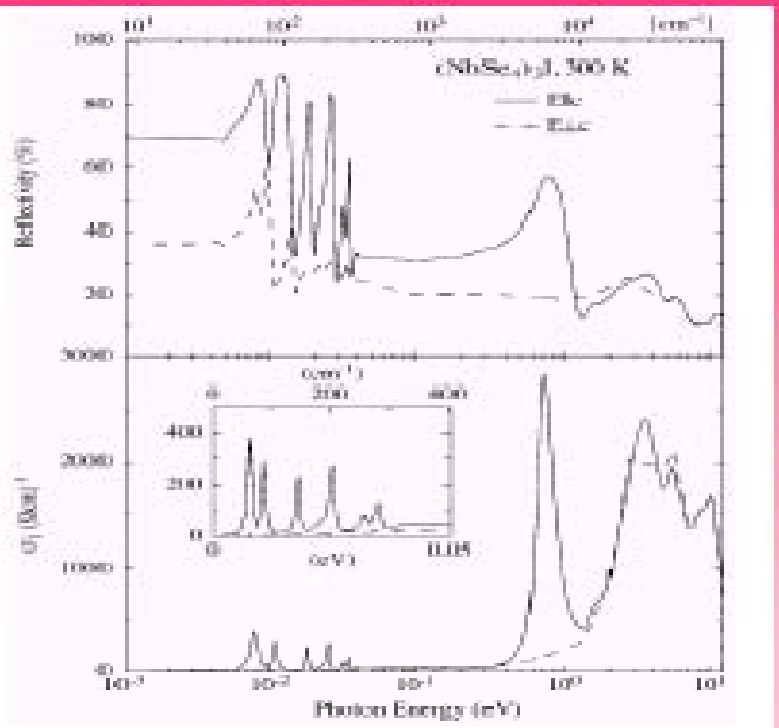

FIG. 1. Reflectivity and real part of the optical conductivity of $(NbSe_4)_3I$ at 300 K and for light polarized along and perpendicular to the c axis. The inset is an enlargement of the far-infrared spectral range, showing the phonon modes.

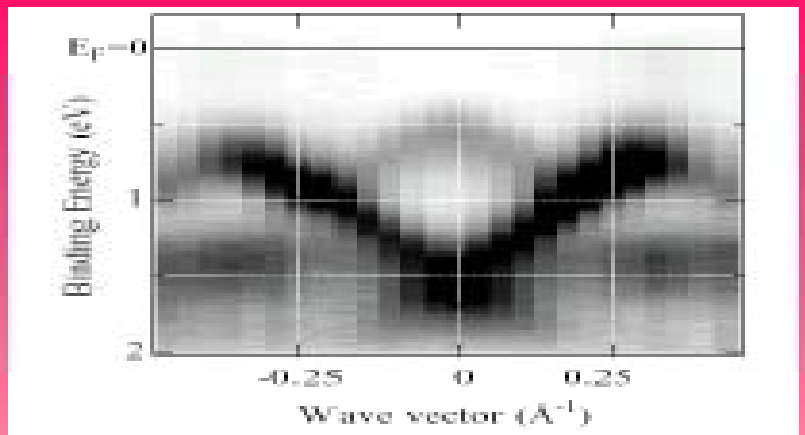

FIG. 2. ARPES intensity map ($\hbar\nu = 21.2$ eV; $T = 300$ K) of $(NbSe_4)_3I$. Each column represents the intensity of an ARPES spectrum collected at the indicated wave vector along the 1D (ΓZ) chain direction.

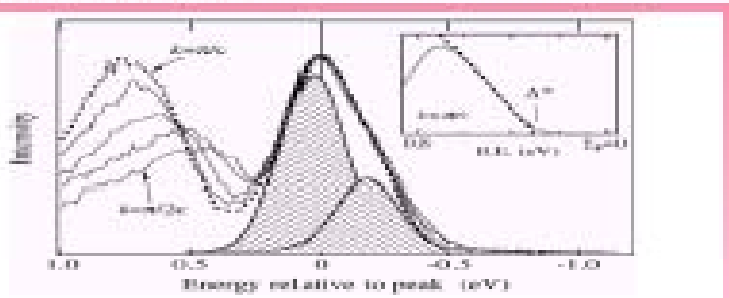

FIG. 4. ARPES spectra of $(NbSe_4)_3I$ for wave vectors $\pi/2c < k < \pi/c$. The peak intensities and energy positions have been normalized to those of the $k = \pi/c$ spectrum to illustrate the k-independent line shape. A satisfactory fit is tentatively obtained by two Gaussian peaks of equal width (FWHM = 0.29 eV) and 5:2 intensity ratio, separated by 0.20 eV. Inset: a linear extrapolation of the $k = \pi/c$ spectrum identifies a baseline intersection $\Delta^* = 0.3$ eV.

Applications of Photoelectron Spectroscopy

Magnetic transitions

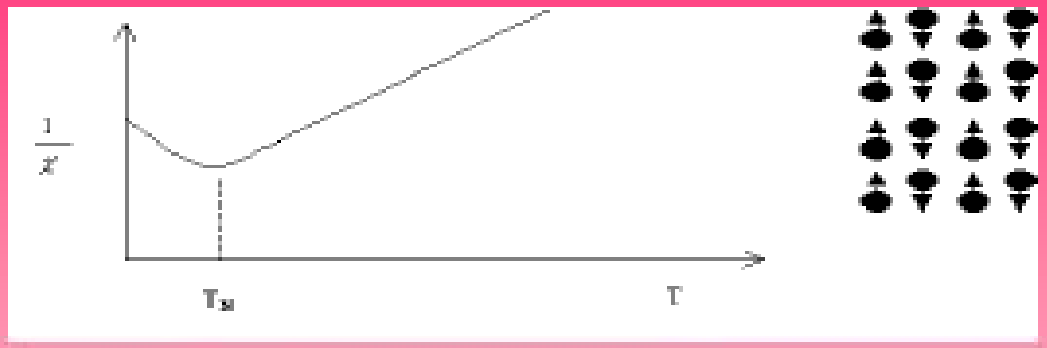

T_N Néel Temperature

Louis Néel

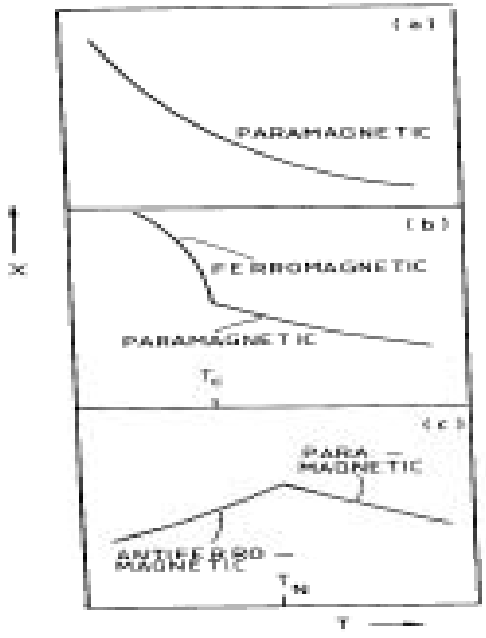

Fig. 16.3 Temperature dependence of the magnetic susceptibility for (a) paramagnetic, (b) ferromagnetic and (c) antiferromagnetic materials

Applications of Photoelectron Spectroscopy

VO_2

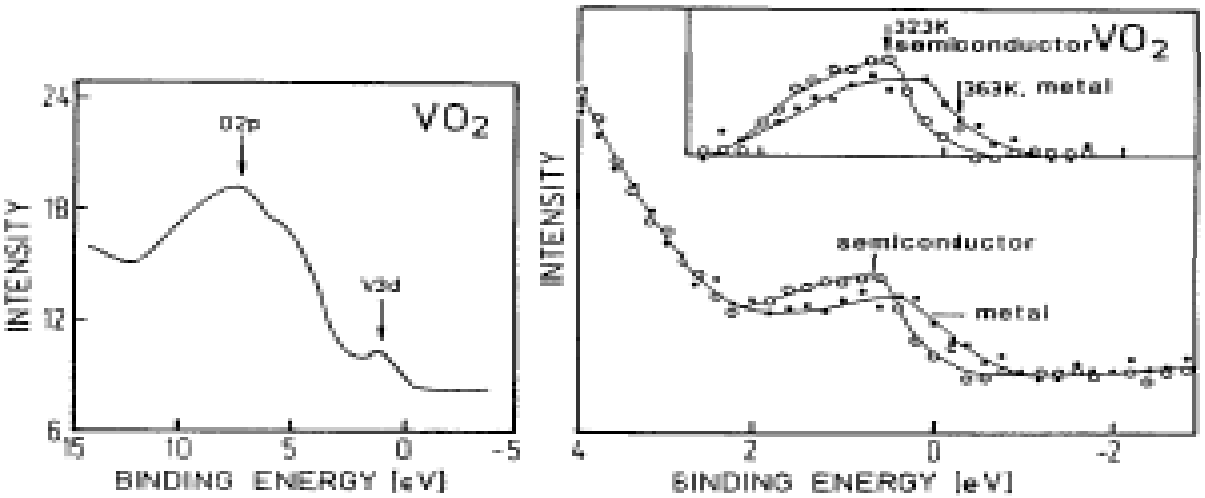

Fig.5.51. XPS valence band spectra of the metal–nonmetal transition in VO_2 [5.107, 108]. The left panel gives the complete valence band. The right panel gives the 3d structure above (363K), and below (323K) the metal–nonmetal transition (T_N = 340K). In going through the transition the 3d band moves towards the Fermi energy to intersect it

Applications of Photoelectron Spectroscopy

- The metal insulator transitions are studied using PES
- XPS, UPS, AES, ARPES are all tools which help in studying the transitions.
- As the molecule gets bigger the electronic structure gets more complicated and is tough to study.

Principle of X-ray Photoelectron spectroscopy

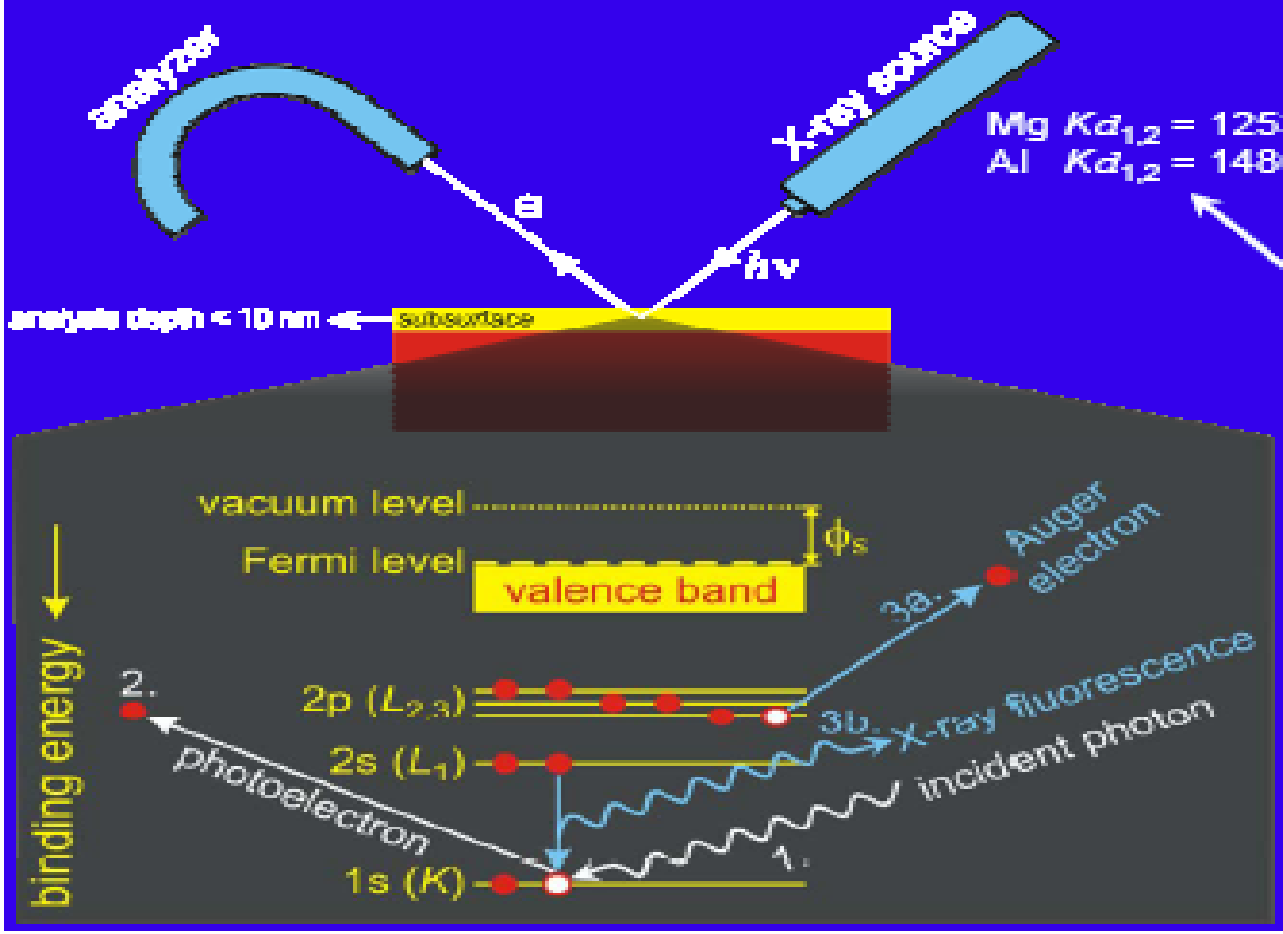

Mg $K\alpha_{1,2}$ = 1253.6 eV
Al $K\alpha_{1,2}$ = 1486.6 eV

source	energy (eV)	width (eV)
Y Mz	132.3	0.5
Ti La	395.3	3.0
Cu La	929.7	3.8
Mg Ka	1253.6	0.7
Al Ka	1486.6	0.9
Y La	1922.6	1.5
Ti Ka	4510.0	2.0
Cu Ka	8048.0	2.6

Principle of X-ray Photoelectron spectroscopy

Conservation of energy: $E_{\text{initial}}^{N} + h\nu \equiv E_{\text{final}}^{(N-1)} + E_{\text{k}}$

$$E_{\text{B}}^{\text{vac}} = E_{\text{final}}^{(N-1)} - E_{\text{initial}}^{N}$$

The measured binding energy incorporates the relaxation of the (N-1) electron system upon photoemission (i.e. no 'frozen' orbitals)

Electrical contact between sample and spectrometer

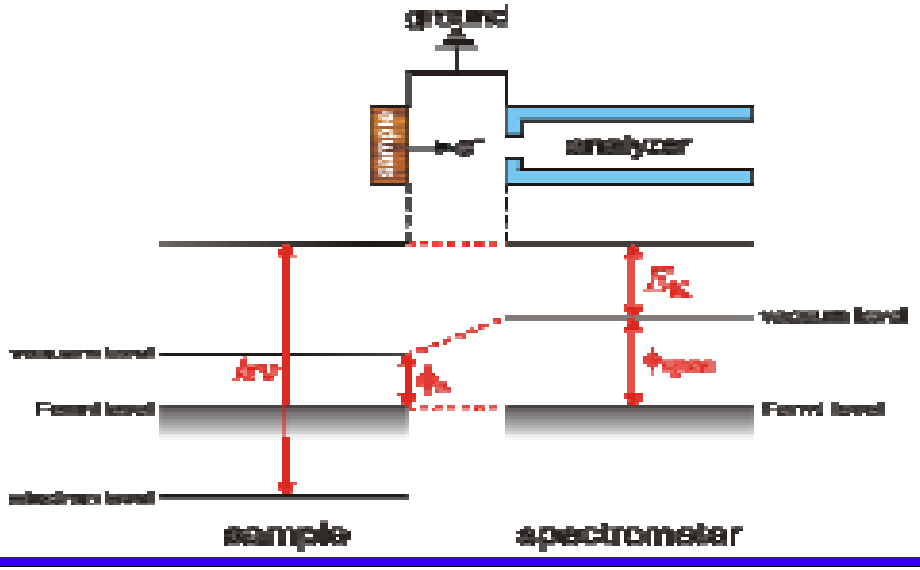

Principle XPS equation:

$$E_{\text{B}}^{\text{Fermi}} = h\nu - E_{\text{k}}^{\text{measured}} - \phi_{\text{spec}}$$

Principle of X-ray Photoelectron spectroscopy

Recorded X-ray photoelectron spectra of α-Al_2O_3

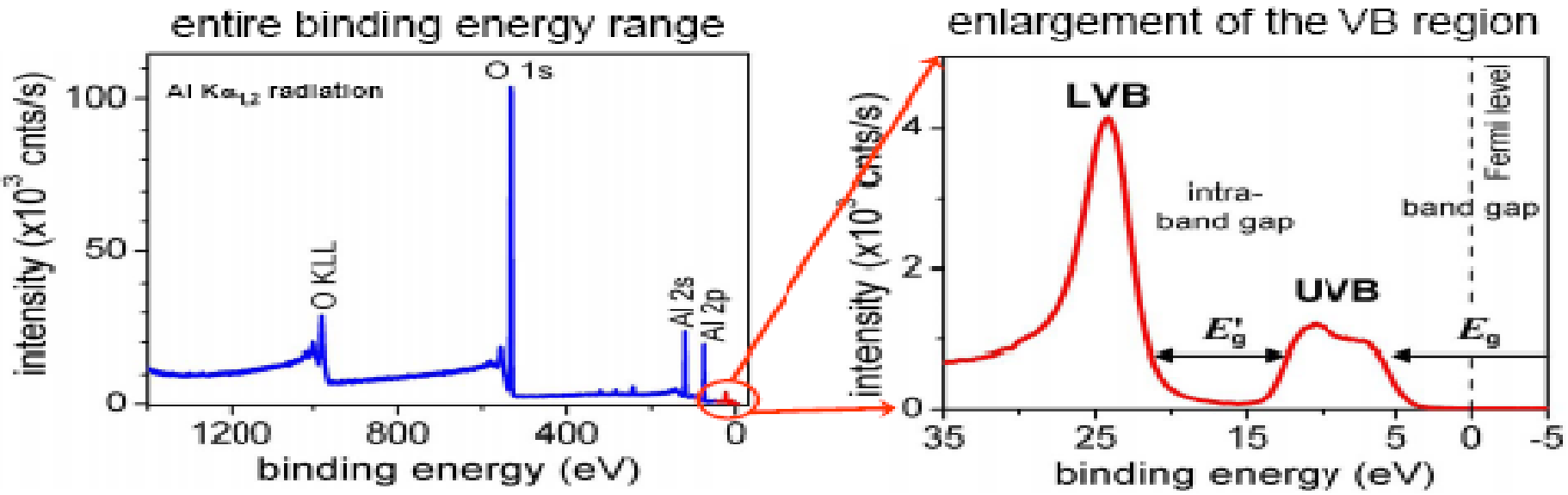

core levels/valence levels

Al (Z = 13): $1s^2 2s^2 2p^6 3s^2 3p^1$

O (Z = 8): $1s^2 2s^2 2p^4$

Principle of X-ray Photoelectron spectroscopy

Angle definitions

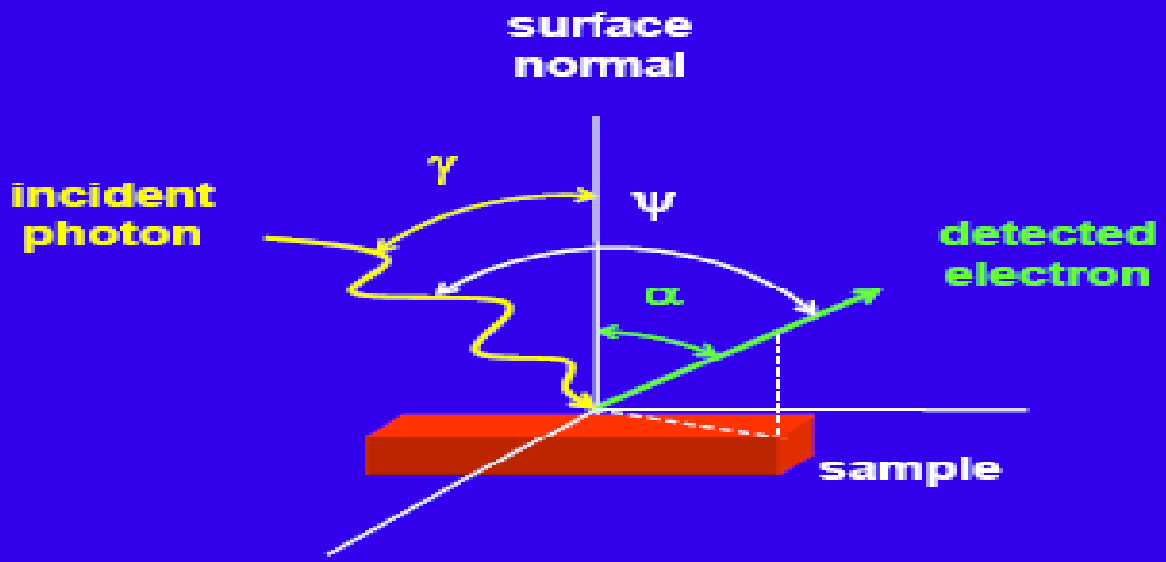

Quantitative AR-XPS analysis

The recorded photoelectron intensity

The observed zero-loss photoelectron intensity of element A in a solid

$$I^{\infty}_{AX_n} = K \cdot \sigma_{AX_n} \cdot W(\psi) \cdot \int_{z=0}^{\infty} C_A(z) \cdot \exp\left[-\int_{z'=0}^{z} \frac{dz'}{\lambda_{AX_n}(z') \cdot \cos\alpha} \right] dz$$

- instrumental factors
- total photoionization cross section
- anisotropy of the photoionization cross section
- concentration of element A as a function of depth z below surface
- depth dependence of the IMFP

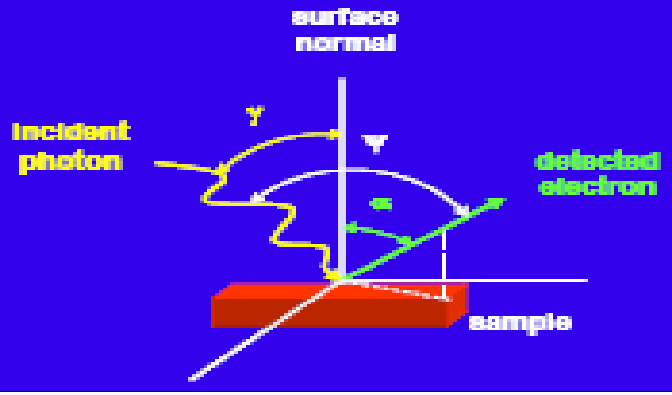

Principle of X-ray Photoelectron spectroscopy

The inelastic mean free path

Inelastic Mean Free Path (IMFP, symbol λ):

Average distance that an electron with a given kinetic energy travels between successive inelastic collisions in the solid

TPP-2M equation for IMFP (Tanuma, Powell & Penn, Surf. Interf. Anal. 21 (1994), 165)

$$\lambda = E_k \cdot \left(\left[28.8 \sqrt{\frac{N_v \rho}{M}} \right]^2 \left\{ \beta \ln(\gamma E_k) - C \cdot E_k^{-1} + D \cdot E_k^{-2} \right\} \right)^{-1}$$

E_k : kinetic energy of concerned electron

N_v : number of valence electrons per atom/molecule of solid

ρ : density of solid

M : atomic/molecular weight

β, γ, C, D : material dependent parameters (depend e.g. on band gap)

→ **IMFP dependent on both electron energy and material !**

Principle of X-ray Photoelectron spectroscopy

The inelastic mean free path and information depth

Inelastic Mean Free Path (IMFP) vs. electron energy

from: S. Tanuma, in: "Surface Analysis by Auger and X-ray Photoelectron Spectroscopy" (2003, eds. D. Briggs & J.T. Grant)

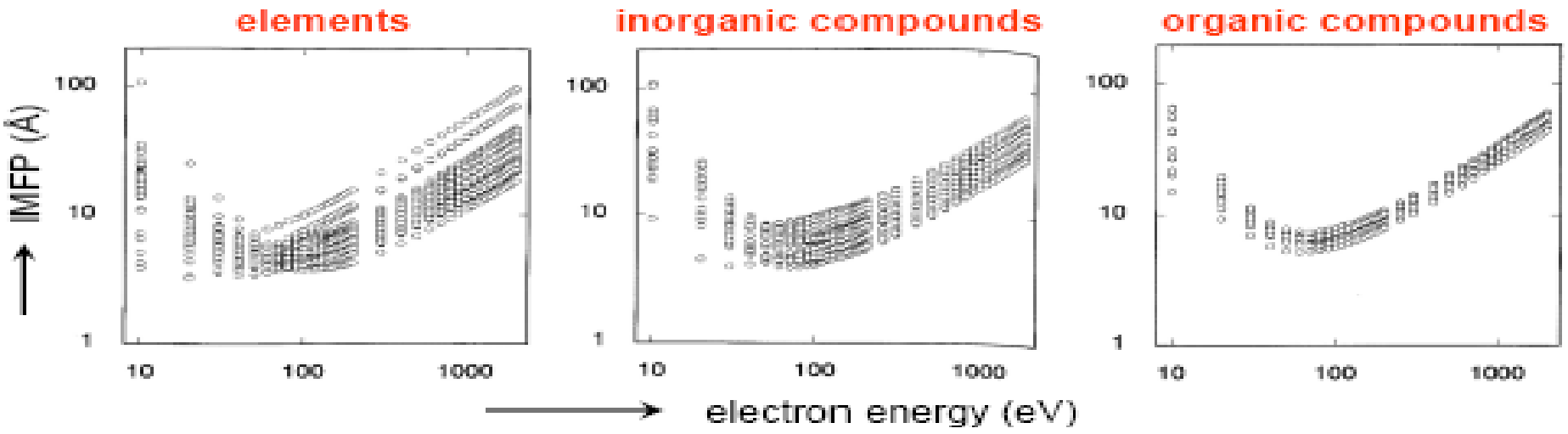

Information depth:

Maximum depth (normal to the surface) from which useful information is obtained
i.e. 95% of the detected signal originates from 3λ (neglecting elastic scattering effects)

→ **information depth for XPS analysis < 10 nm !**

Quantitative AR-XPS analysis

The recorded photoelectron intensity

The observed zero-loss photoelectron intensity of element A in a solid

$$I^{\infty}_{AX_n} = K \cdot \sigma_{AX_n} \cdot W(\psi) \cdot \int_{z=0}^{\infty} C_A(z) \cdot \exp\left[-\int_{z'=0}^{z} \frac{dz'}{\lambda_{AX_n}(z') \cdot \cos\alpha} \right] dz$$

- K: instrumental factors
- σ_{AX_n}: total photoionization cross section
- $W(\psi)$: anisotropy of the photoionization cross section
- $C_A(z)$: concentration of element A as a function of depth z below surface
- $\exp\left[-\int_{z'=0}^{z} \frac{dz'}{\lambda_{AX_n}(z') \cdot \cos\alpha} \right]$: depth dependence of the IMFP

e.g. the change in IMFP when going from the metal substrate to the oxide overlayer !

Principle of angle-resolved XPS (AR-XPS)

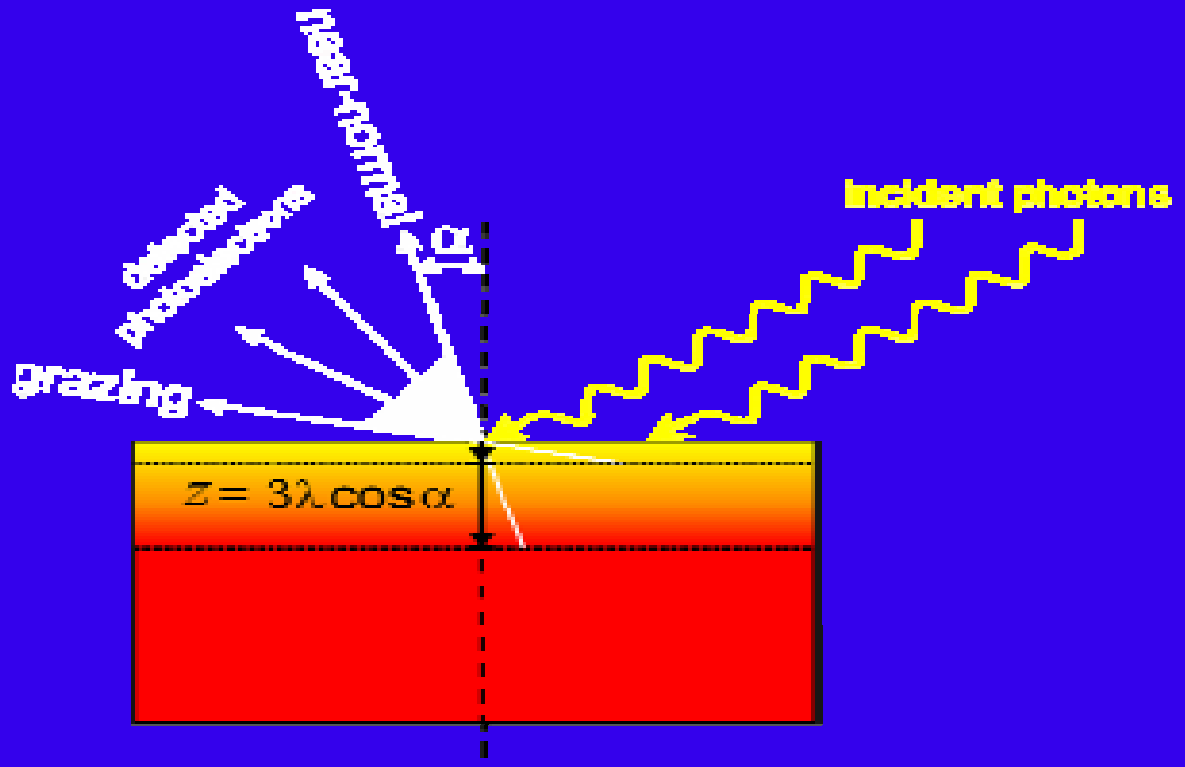

Information depth z varies with the photoelectron detection angle α !

grazing → more surface sensitive

Principle of angle-resolved XPS (AR-XPS)

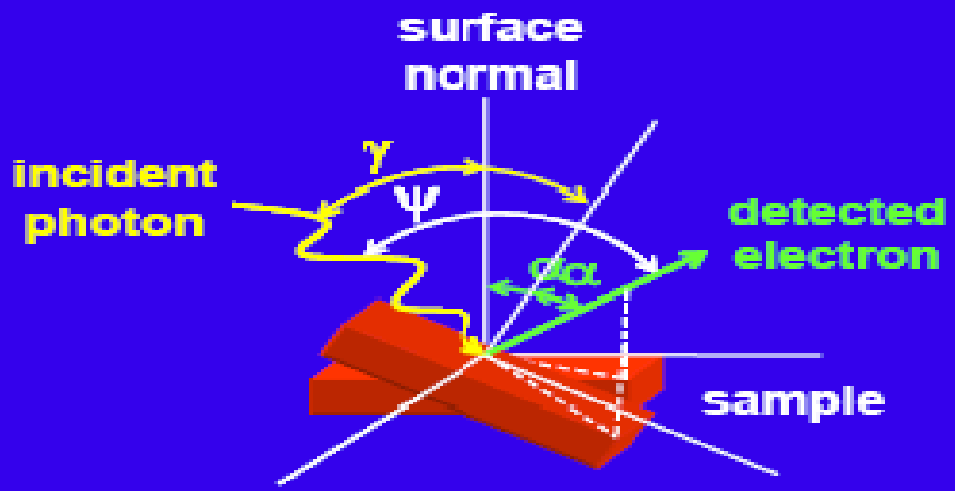

Conventional AR-XPS

Tilting of the sample

→ ψ fixed, γ and α vary

advantage: - anisotropy of photoemission constant

disadvantages: - long measurement times
- analyzed area and position vary

Principle of angle-resolved XPS (AR-XPS)

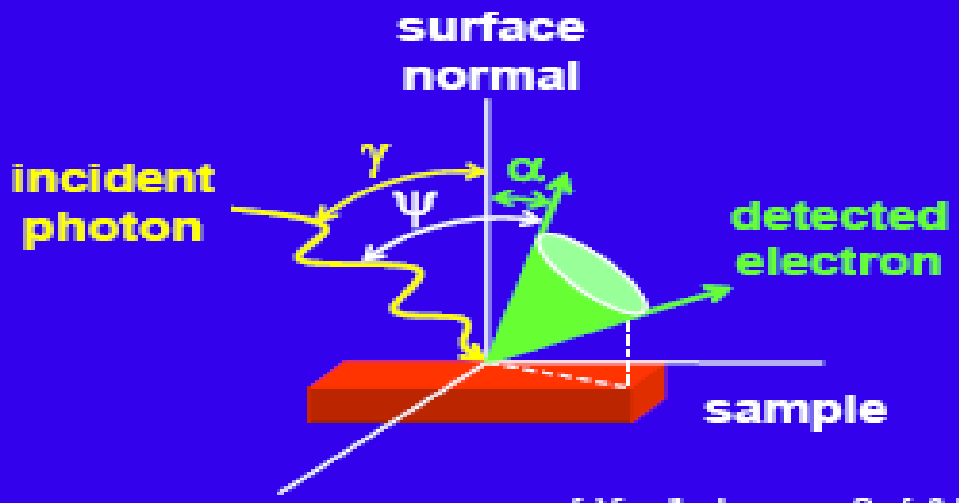

cf. Vinodh, Jeurgens, Surf. & Interf. Anal. 36 (2004) 1629.

Conventional AR-XPS

Tilting of the sample

→ ψ fixed, γ and α vary

advantage: - anisotropy of photoemission constant

disadvantages: - long measurement times
- analyzed area and position vary

AR-XPS by parallel data acquisition

No tilting of the sample required

→ γ fixed, ψ and α vary

advantages: - fast (up to 96 intervals over range α = 23°–83° measured simultaneously)
- analyzed position and area constant

disadvantage: - anisotropy of photoemission varies

Oxide-film constitution from AR-XPS

Example: The initial, low-*T* oxidation of Mg-based MgAl alloys

Measured and reconstructed AR-XPS spectra of an oxidized $MgAl_{2.6}$ alloy
(oxidized for 1h at 301K and pO_2=10^{-4} Pa)

Mg 2p – Al 2p spectra

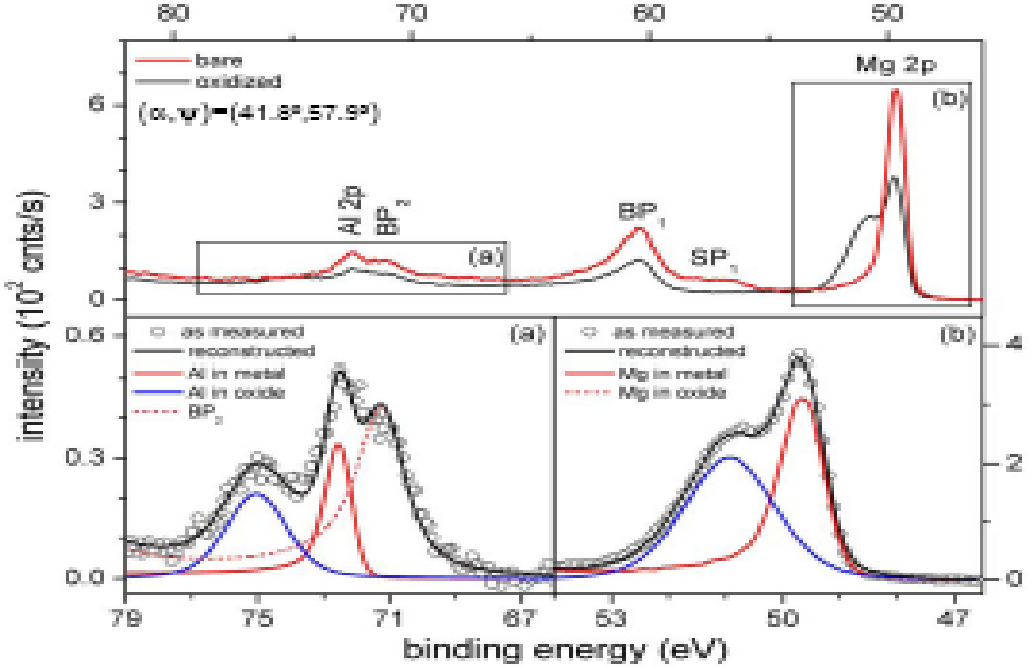

O 1s spectra

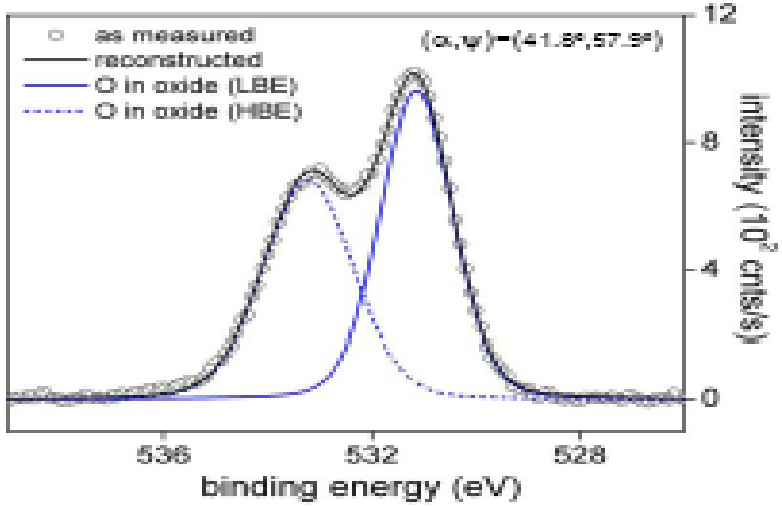

6 different species identified !

Auger Electron Spectroscopy

Auger Electron Spectroscopy (*Auger spectroscopy* or AES) was developed in the late 1960's , deriving its name from the effect first observed by **Pierre Auger**, a French Physicist, in the mid-1920's. It is a surface specific technique utilizing the **emission of low energy electrons** in the *Auger process* and is one of the most commonly employed surface analytical techniques for determining the composition of the surface layers of a sample.

Electronic Structure - Isolated Atoms

The diagram below schematically illustrates the energies of the various electron energy levels in an isolated, multi-electron atom, with the conventional chemical nomenclature for these orbitals given on the right hand side. It is convenient to expand the part of the energy scale close to the vacuum level in order to more clearly distinguish between the higher levels ....

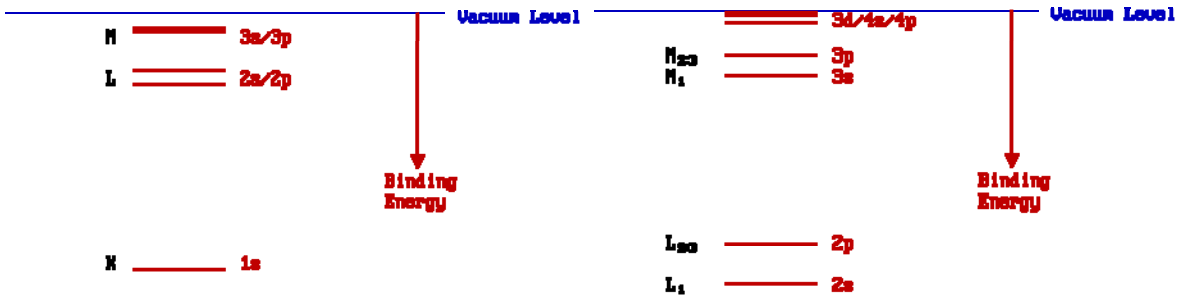

For more details, see http://www.chem.qmw.ac.uk/surfaces/scc/scat5_1.htm

Electronic Structure - Solid State

In the solid state the core levels of atoms are little perturbed and essentially remain as discrete, localized (i.e. atomic-like) levels. The valence orbitals, however, overlap significantly with those of neighboring atoms generating bands of spatially-delocalized energy levels

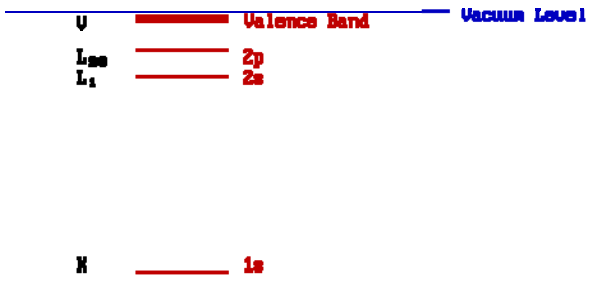

electronic structure of Na metal :

Physics basis

I. Ionization

The Auger process is initiated by creation of a core hole – this is typically carried out by exposing the sample to a beam of high energy electrons (typically having a primary energy in the range 2 - 10 keV). Such electrons have sufficient energy to ionize all levels of the lighter elements, and higher core levels of the heavier elements.

In the diagram below, ionization is shown to occur by removal of a K-shell electron, but in practice such a crude method of ionization will lead to ions with holes in a variety of inner shell levels.

In some studies, the initial ionization process is instead carried out using **soft x-rays (hν = 1000-2000 eV).** In this case, the acronym **XAES** is sometimes used. As we shall see, however, this change in the method of ionization has no significant effect on the final Auger spectrum

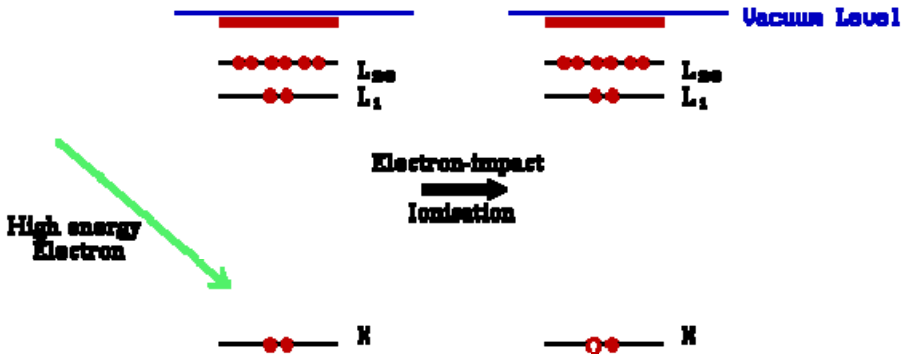

II. Relaxation & Auger Emission

The ionized atom that remains after the removal of the core hole electron is, of course, in a highly excited state and will rapidly relax back to a lower energy state by one of two routes :

X-ray fluorescence , or
Auger emission

We will only consider the latter mechanism, an example of which is illustrated schematically below ....

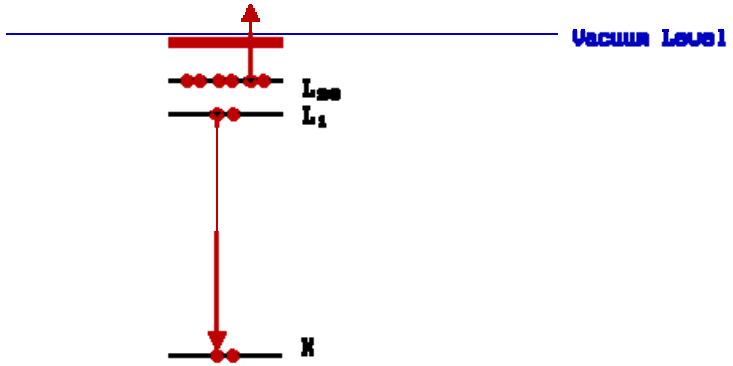

a rough estimate of the KE of the Auger electron from the binding energies of the various levels involved.
In this particular example,
KE = (E_K - E_{L1}) - E_{L23} = E_K - (E_{L1} + E_{L23})

Note : the KE of the Auger electron is independent of the mechanism of initial core hole formation.

Physics basis

An Auger transition is therefore characterized primarily by :-

1. the location of the initial hole
2. the location of the final two holes

although the existence of different electronic states (terms) of the final doubly-ionized atom may lead to fine structure in high resolution spectra.
When describing the transition, the initial hole location is given first, followed by the locations of the final two holes in order of decreasing binding energy. i.e. the transition illustrated is a $KL_1L_{2,3}$ transition .

In general, since the initial ionisation is non-selective and the initial hole may therefore be in various shells, there will be many possible Auger transitions for a given element - some weak, some strong in intensity. AUGER SPECTROSCOPY is based upon the measurement of the kinetic energies of the emitted electrons. Each element in a sample being studied will give rise to a characteristic spectrum of peaks at various kinetic energies.

This is an Auger spectrum of Pd metal - generated using a 2.5 keV electron beam to produce the initial core vacancies and hence to stimulate the Auger emission process. The main peaks for palladium occur between 220 & 340 eV. The peaks are situated on a high background which arises from the vast number of so-called *secondary electrons* generated by a multitude of inelastic scattering processes.
Auger spectra are also often shown in a differentiated form : the reasons for this are partly historical, partly because it is possible to actually measure spectra directly in this form and by doing so get a better sensitivity for detection. The plot below shows the same spectrum in such a differentiated form.

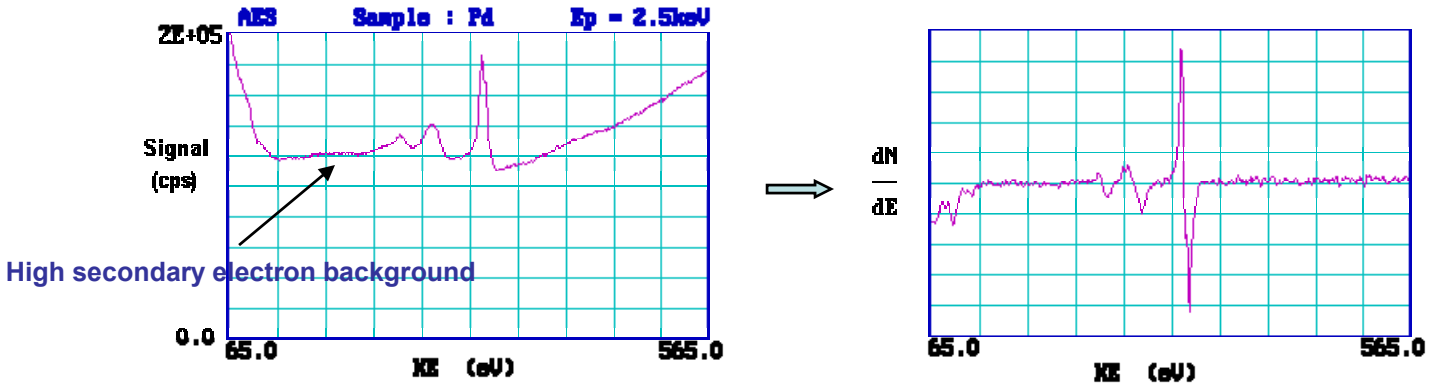

Photoelectron Spectroscopy

Photoelectron spectroscopy utilizes photo-ionization and energy-dispersive analysis of the emitted photoelectrons to study the composition and electronic state of the surface region of a sample.

Traditionally, when the technique has been used for surface studies it has been subdivided according to the source of exciting radiation into :

X-ray Photoelectron Spectroscopy (XPS)	**- using soft x-ray (*200-2000 eV*) radiation to examine core-levels.**
Ultraviolet Photoelectron Spectroscopy (UPS)	**- using vacuum UV (*10-45 eV*) radiation to examine valence levels.**

The development of synchrotron radiation sources has enabled high resolution studies to be carried out with radiation spanning a much wider and more complete energy range (5 - 5000+ eV) but such work is, and will remain, a very small minority of all photoelectron studies due to the expense, complexity and limited availability of such sources.

For more details, see http://www.chem.qmw.ac.uk/surfaces/scc/scat5_1.htm

Physics Basis

- Photoelectron spectroscopy is based upon a single photon in/electron out process and from many viewpoints this underlying process is a much simpler phenomenon than the Auger process.
- Photoelectron spectroscopy uses monochromatic sources of radiation (i.e. photons of fixed energy).

- In XPS the photon $h\nu$ is absorbed by an atom in a molecule or solid, leading to ionization and the emission of a core (inner shell) electron. By contrast, in UPS the photon interacts with valence levels of the molecule or solid, leading to ionization by removal of one of these valence electrons.

- The kinetic energy distribution of the emitted photoelectrons (i.e. the number of emitted photoelectrons as a function of their kinetic energy) can be measured using any appropriate electron energy analyser and a photoelectron spectrum can thus be recorded.

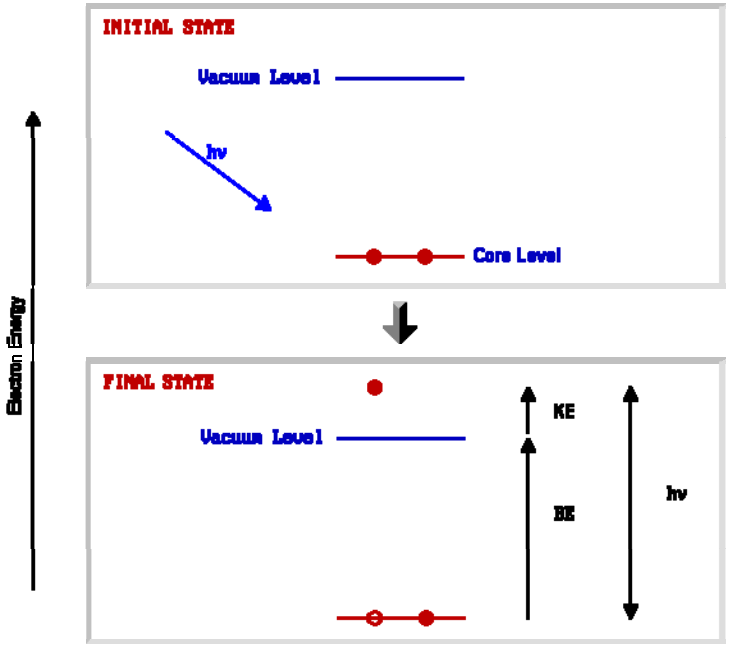

KE: photoelectron's kinetic energy
BE: the *binding energy* of the electron

KE = $h\nu$ - BE

NOTE - the binding energies (BE) of energy levels in solids are conventionally measured with respect to the Fermi-level of the solid, rather than the vacuum level. This involves a small correction to the equation given above in order to account for the *work function* (F) of the solid, but for the purposes of the discussion below this correction will be neglected.

Experimental Details

The basic requirements for a photoemission experiment (XPS or UPS) are:
1. a source of fixed-energy radiation (an x-ray source for XPS or, typically, a He discharge lamp for UPS)

2. an electron energy analyzer (which can disperse the emitted electrons according to their kinetic energy, and thereby measure the flux of emitted electrons of a particular energy)

3. a high vacuum environment (to enable the emitted photoelectrons to be analyzed without interference from gas phase collisions)

Such a system is illustrated schematically below:

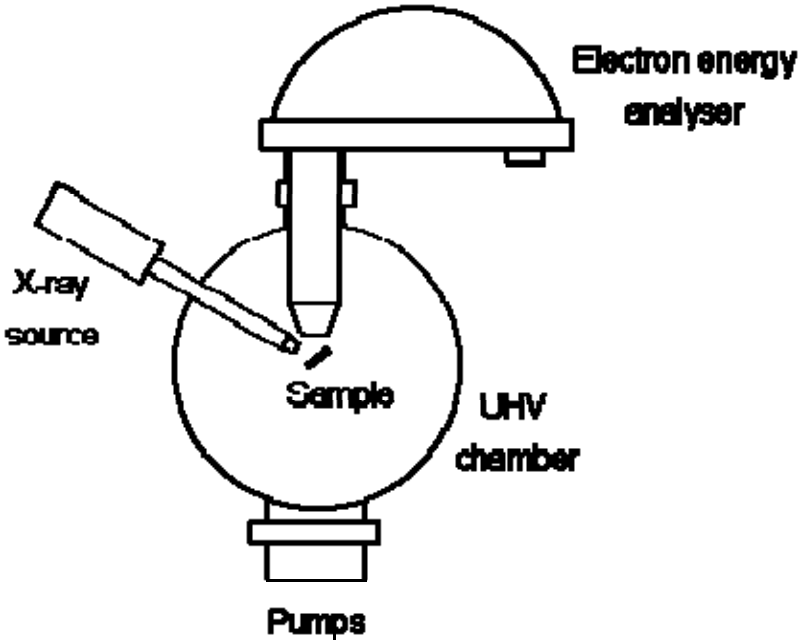

Note: There are many different designs of electron energy analyzer but the preferred option for photoemission experiments is a concentric hemispherical analyzer (CHA) which uses an electric field between two hemispherical surfaces to disperse the electrons according to their kinetic energy.

X-ray Photoelectron Spectroscopy (XPS)

- For each and every element, there will be a characteristic binding energy associated with each core atomic orbital i.e. each element will give rise to a characteristic set of peaks in the photoelectron spectrum at kinetic energies determined by the photon energy and the respective binding energies.
- The presence of peaks at particular energies therefore indicates the presence of a specific element in the sample under study - furthermore, the intensity of the peaks is related to the concentration of the element within the sampled region. Thus, the technique provides a *quantitative analysis of the surface composition and is sometimes known by the alternative acronym , ESCA (Electron Spectroscopy for Chemical Analysis).*
The most commonly employed x-ray sources are those giving rise to :

Mg K $_{\alpha}$ ***radiation : h*** ν ***= 1253.6 eV***

Al K $_{\alpha}$ ***radiation : h*** ν ***= 1486.6 eV***

- The emitted photoelectrons will therefore have kinetic energies in the range of ca. 0 - 1250 eV or 0 - 1480 eV . Since such electrons have very short inelastic mean free paths (IMFPs) in solids, the technique is necessarily surface sensitive.

- The diagram shows a real XPS spectrum obtained from a Pd metal sample using Mg K_{α} radiation

the main peaks occur at kinetic energies of ca. 330, 690, 720, 910 and 920 eV.

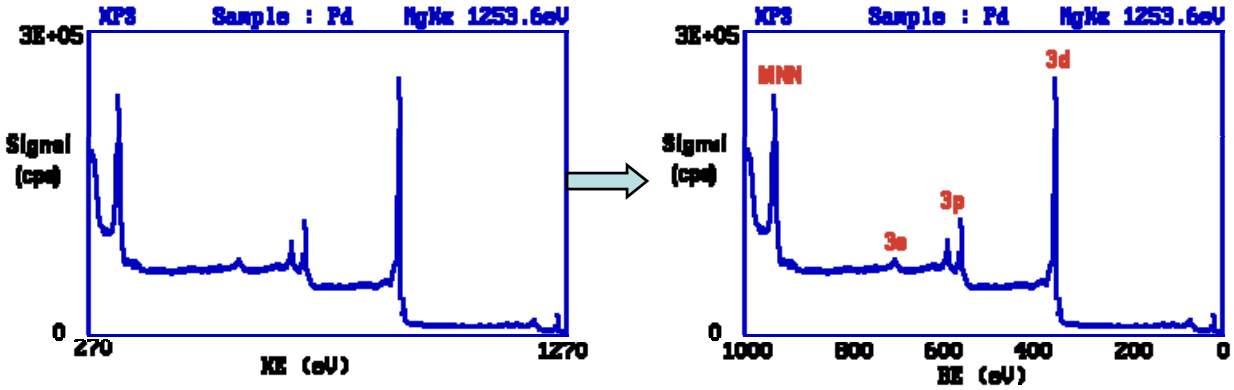

Chemical Shifts

The exact binding energy of an electron depends not only upon the level from which photoemission is occurring, but also upon :
- the formal oxidation state of the atom
- the local chemical and physical environment

Changes in either (1) or (2) give rise to small shifts in the peak positions in the spectrum - so-called ***chemical shifts*** .
Such shifts are readily observable and interpretable in XP spectra (unlike in Auger spectra) because the technique :
- is of high intrinsic resolution (as core levels are discrete and generally of a well-defined energy)
- is a one electron process (thus simplifying the interpretation)

Atoms of a higher positive oxidation state exhibit **a higher binding energy** due to the extra coulombic interaction between the photo-emitted electron and the ion core. *This ability to discriminate between different oxidation states and chemical environments is one of the major strengths of the XPS technique.*

Note: In practice, the ability to resolve between atoms exhibiting slightly different chemical shifts is limited by the peak widths which are governed by a combination of factors ; especially
- the intrinsic width of the initial level and the lifetime of the final state
- the line-width of the incident radiation - which for traditional x-ray sources can only be improved by using x-ray monochromators
- the resolving power of the electron-energy analyzer

In most cases, the second factor is the major contribution to the overall line width.

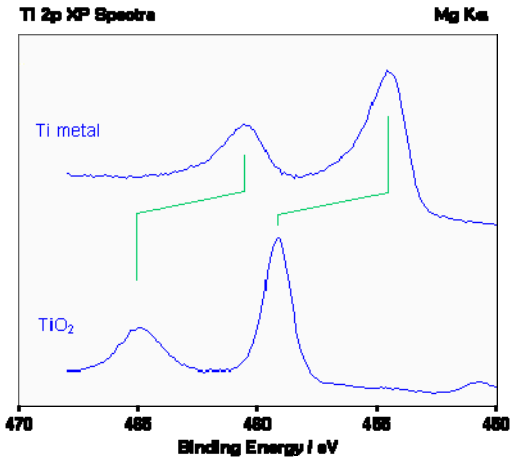

Example: Oxidation States of Titanium. Titanium exhibits very large chemical shifts between different oxidation states of the metal; in the diagram below a Ti 2p spectrum from the pure metal (Ti^{o}) is compared with a spectrum of titanium dioxide (Ti^{4+}).

Various ways to estimate Auger electron kinetic energy

$$E_{KL1\,L23} = E_k^{(z)} - E_{L1}^{(z)} - E_{L23}\,(z + \Delta) - \phi_A$$
$$= E_k^{(z)} - E_{L1}^{(z)} - E_{L23}^{(z)} - \Delta[E_{L2,3}\,(z+1) - E_{L2,3}^{(z)}]$$

$$E_{xyz} = E_x - \tfrac{1}{2}\,(E_x(z) + E_y(z+1)) - \tfrac{1}{2}\,(E_2(z) + E_2(z+1)) - \phi_A$$

Δ has been found to vary from 0.5 + 1.5.

Relaxation more important than ESCA.

Auger energy is independent of sample work function. Electron loses energy equal to the work function of the sample during emission but gains or loses energy equal to the difference in the work function of the sample and the analyser. Thus the energy is dependent only on the work function of the analyser.

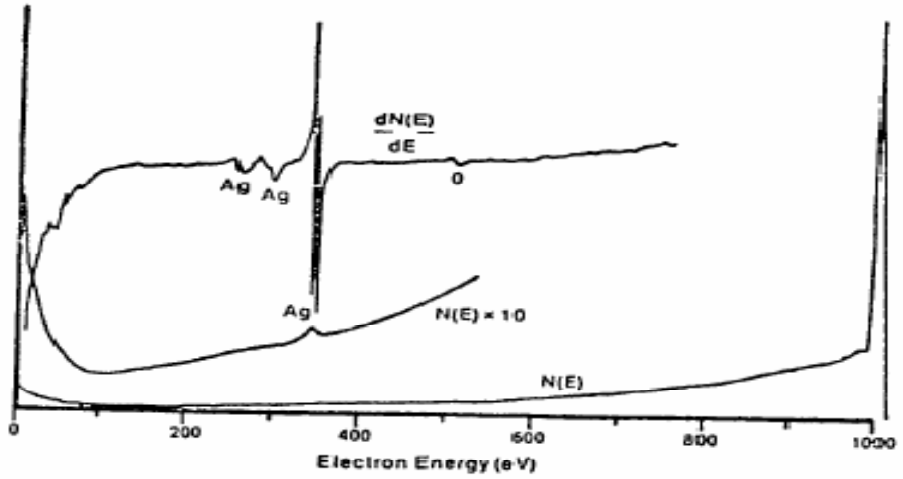

Fig. 1. Energy distribution and derivative of the energy distribution of secondary electrons from a silver target with an incident beam of 1000 eV electrons.

Use of dN(E)/dE plot

Instrumentation

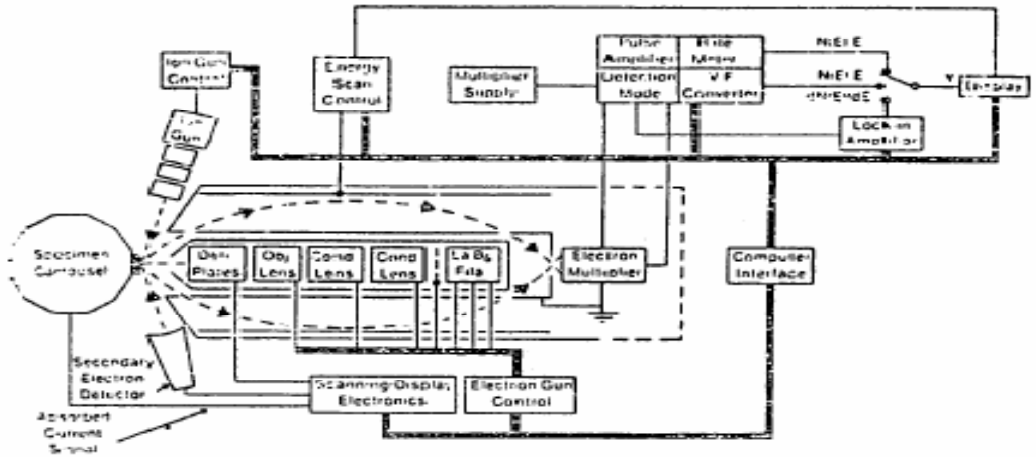

Fig. 4. Schematic layout of electron optics and electronics for a scanning Auger spectrometer.

Early analysers

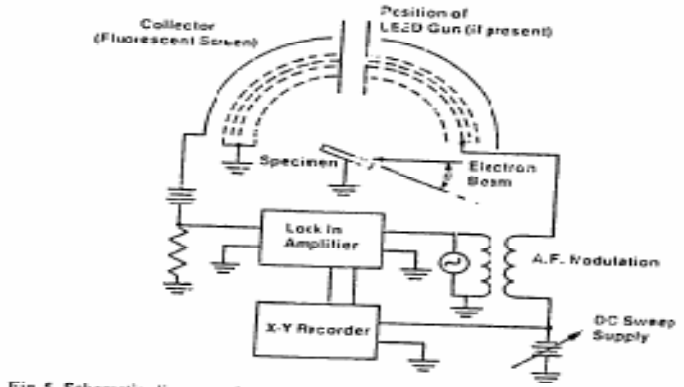

Fig 5. Schematic diagram of a retarding field analyzer.

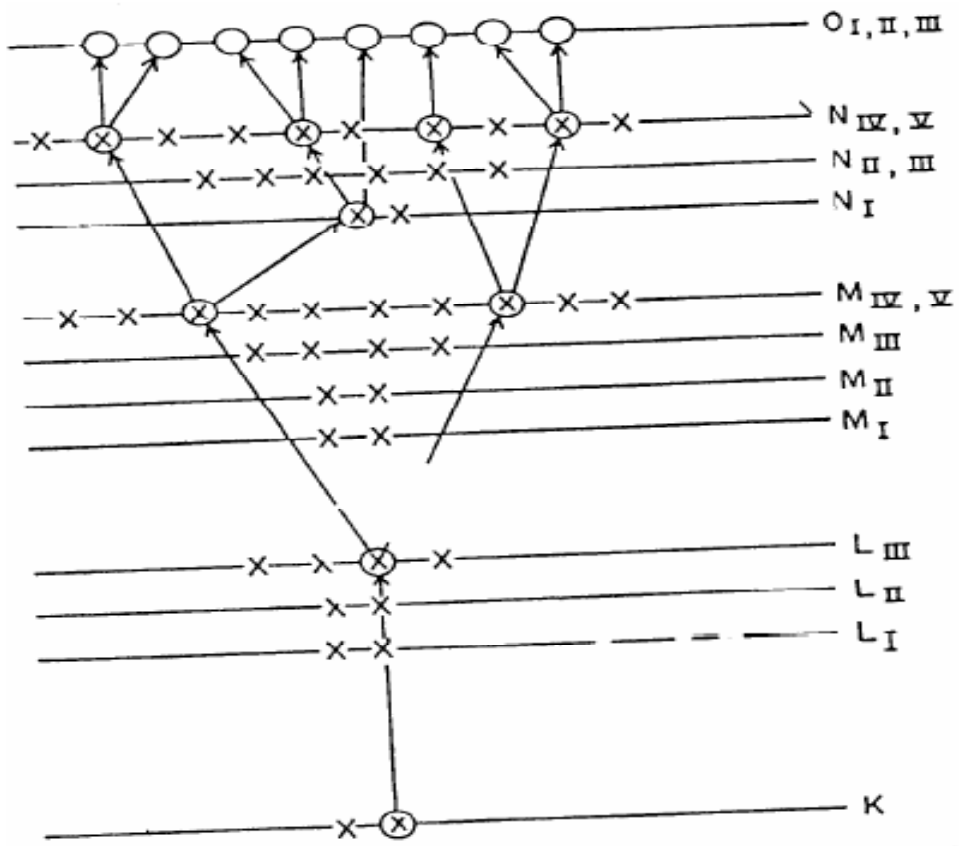

FIGURE 6.2. Schematic representation of a vacancy cascade in Xe. ×, Electrons; ○, vacancies; ⊗, vacancies that were subsequently filled by electrons.

What happens to the system after Auger emission

Chemical differences

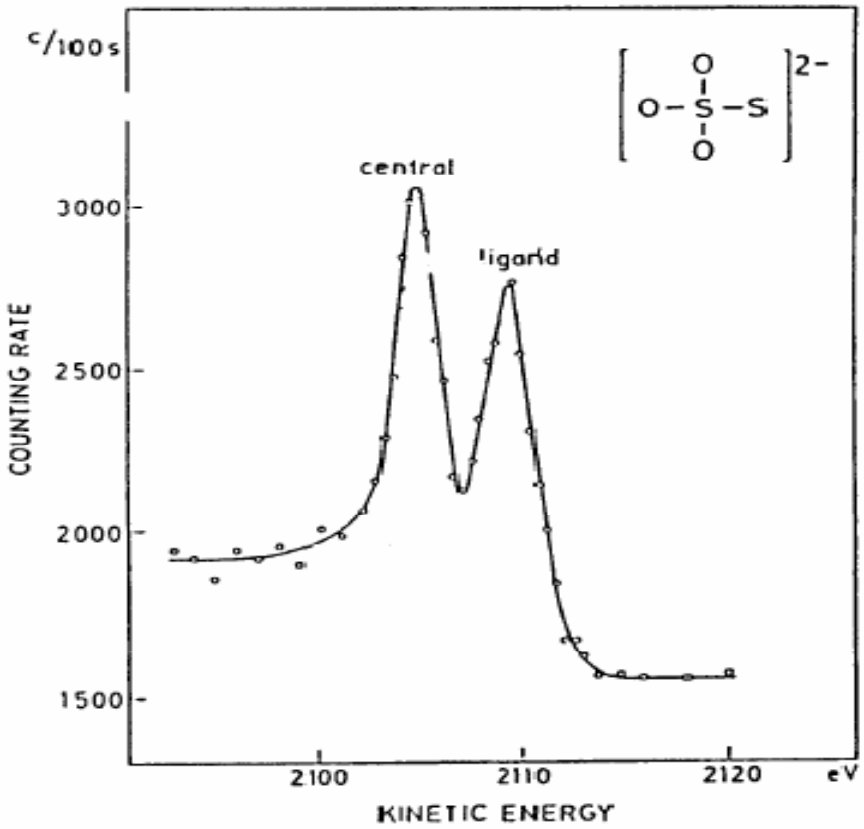

FIGURE 6.6. The $K-LL$ [$2s^22p^4$ ($^1D_2$)] Auger spectrum of sulfur for $Na_2S_2O_3$, showing two peaks corresponding to differences in chemical environment. [Reproduced from Fahlman *et al.*[32]]

When core electrons are involved in Auger, the chemical shifts are similar to XPS.

For $S_2O_3^-$, the chemical shifts between +6 and –2 oxidation states are 7eV for k shell and 6 eV for α_p. The chemical shift for Auger is given as $\Delta E = \Delta E_1 - 2\Delta E\ (L_{II,III}) = 5$ eV

The experimental value is 4.7 eV

Chemical sifts of core levels - change in relaxation energy.

Characteristics

Electron and photon excitation (XAES). Auger emission is possible for elements z >3. Lithium is a special case.
No Auger in the gas phase but shows in the solid state.

Auger emission from outer shells is constant with z. Thus KLL, LMM, MNN series etc can be used for elemental analysis.
Detection limits are 0.1 % atomic.

Spatial resolution ~ 50nm.

Depth resolution is better normal to the surface than in the plane.
Mean free path.

Complications

Plasmons, doubly ionized initial electron states, multiplet splitting, Multiple excitations, Coster-Kronig transitions. Super coster-Kronig transitions.

Volume and surface plasmons. Inter and intra band transitions or shake up

Coster – Kronig $L_1L_3\,X \quad X \neq L$
Super Coster Kronig $L_1L_3\,X \quad X = L$
Cross over transitions. Eg. MgO. Hole in O may be filled by electron from Mg - Non isotropic Auger emission from single crystals.
Diffraction.
Isotropic from polycrystalline samples.

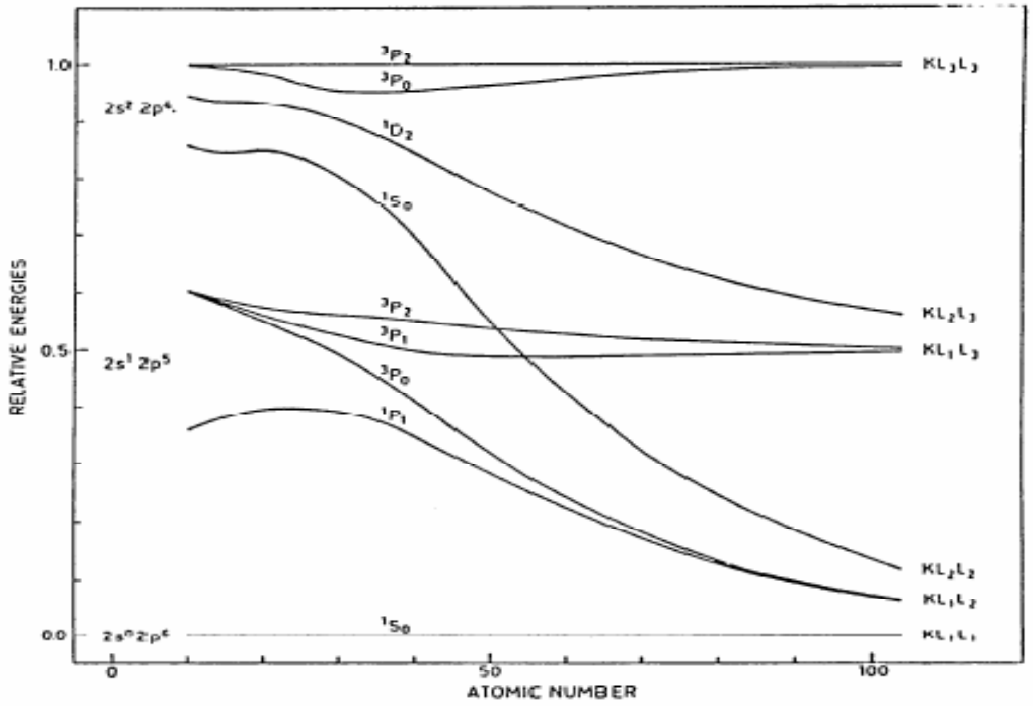

FIGURE 6.1. Relative line positions in K–LL Auger transitions as a function of Z. At low Z one has nearly pure L–S coupling and six lines. However, the $2s^22p^4\ ^3P$ is strongly forbidden in the nonrelativistic region. At high Z one has nearly pure jj coupling and six lines; nine lines are possible in the intermediate coupling region. [Reproduced from Siegbahn *et al.*[6.3] Figure 4.1.]

Chemical effects

Relaxation is larger than in XPS. Chemical effects in XPS will not directly correspond with those of Auger. The difference between XPS and Auger energies is called Auger parameter, used to characterise the chemical state. More changes for transitions involving valence states.

Applications in:

Corrosion
Adhesion
Catalysis
Chemical characterization
Surface reaction
Electronic materials

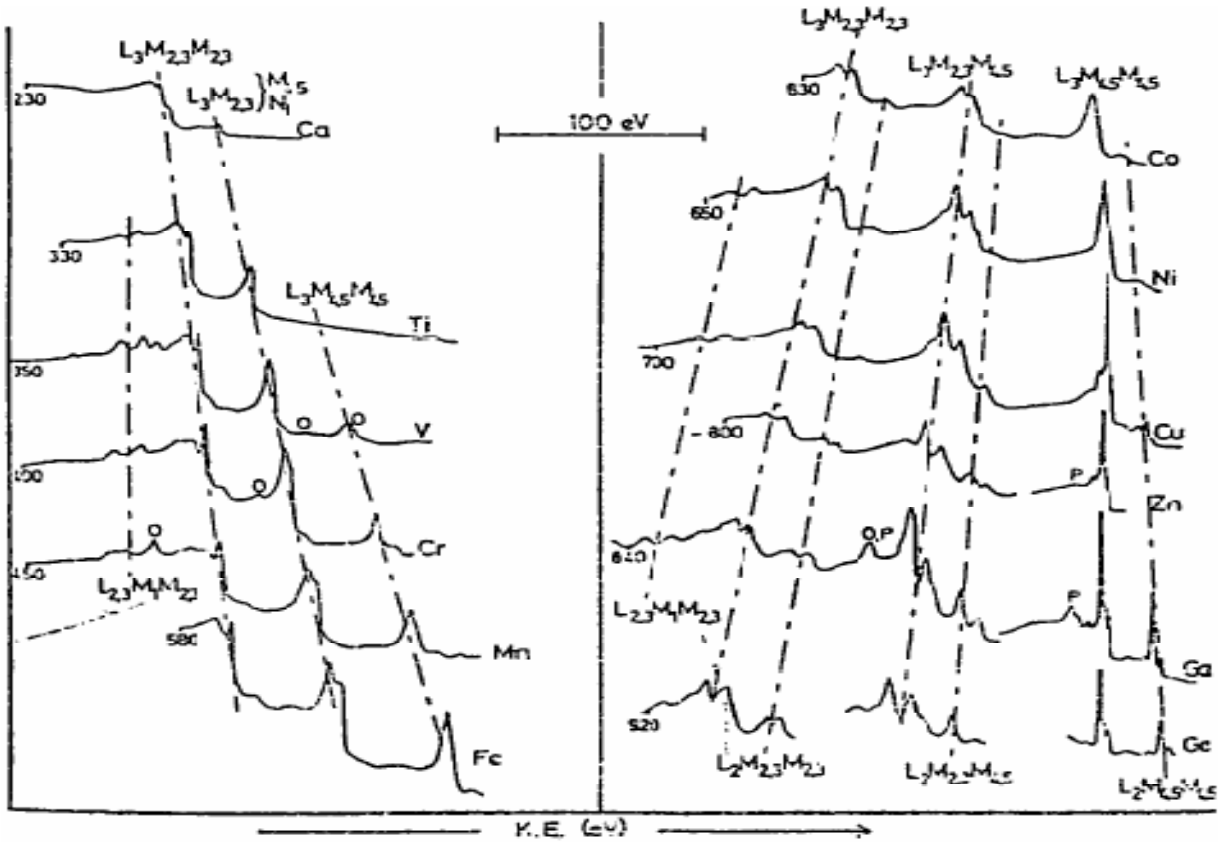

Fig. 18. LMM Auger spectra of elements Ca to Ge. Spectra of samples with low contamination levels have been chosen but some of the peak labelled O may contain contributions from oxygen KPS and Auger peaks. Peaks labelled P are due to plasmon-like energy losses. All spectra, except that of Ge, were recorded with instruments retarding the electrons to a constant analyser pass energy (increased sensitivity at low K.E.) Sources of spectra: Ca, Ti, Cr, Mn, Co, Cu (ref. 82); V (refs 82, 189, 218); Fe (ref. 189); Ni (refs 82, 218); Zn (refs 53, 123, 219, 220); Ga, Ge (refs 82, 53).

High resolution AES using photons

Beam effects
Electron stimulated desorption
Core hole lifetimes are smaller than vibrational time scale and dissociation is not important. But the core hole will lead to electron cascade and multiply charged ion many result which will have a large dissociation probability.

Photon induced desorption is also important but photon fluxes are much lower. Beam effect are important.

Excitation cross sections in XAES and EAES are different.

Threshold effects in Auger

Decay of the core hole leading to double ionization post collision effects changing peak energies.

$L_{2,3}$ spectra of Mg with Mg K_α and Al K_α.

Double ionization satellite in Al K_α not in Mg K_α.

By electrons it is found that the threshold for double ionization is ~120 eV, but the satellite was not sharp as with X-ray excitation.

When KE of outgoing electron is low, Auger emission can happen in the field of receding electron. Energy available can be re-partitioned. If threshold electron is used, Auger emission happens in the field of The receding electron. These interaction are called post collision interactions.

Plasmon gains and losses

Plasmon gain occurs by intrinsic mechanism. For it to occur, plasmon excited should be at the site of ionization, therefore it cannot be extrinsic.

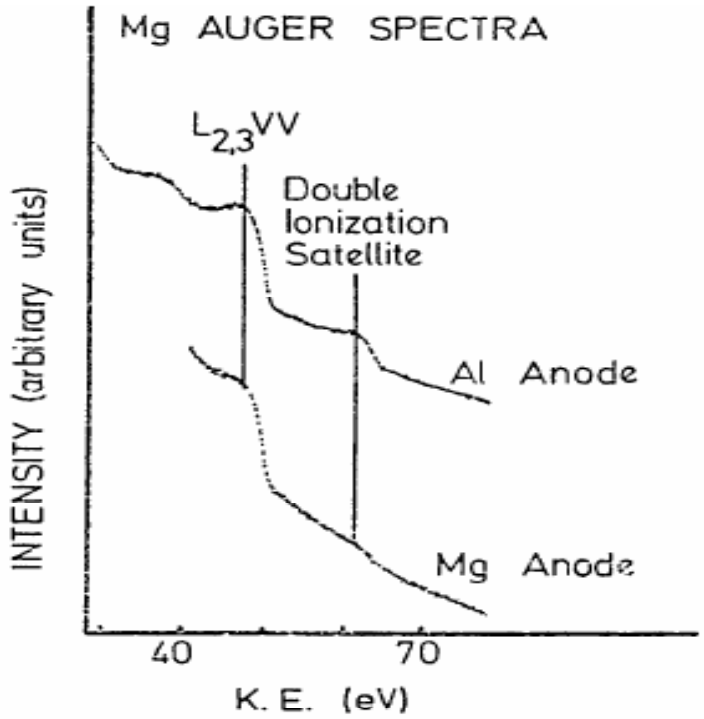

Fig. 13. Increase of the Mg LVV double ionization satellite intensity in XAES as the exciting X ray energy is increased above the Mg K ionization threshold.[175]

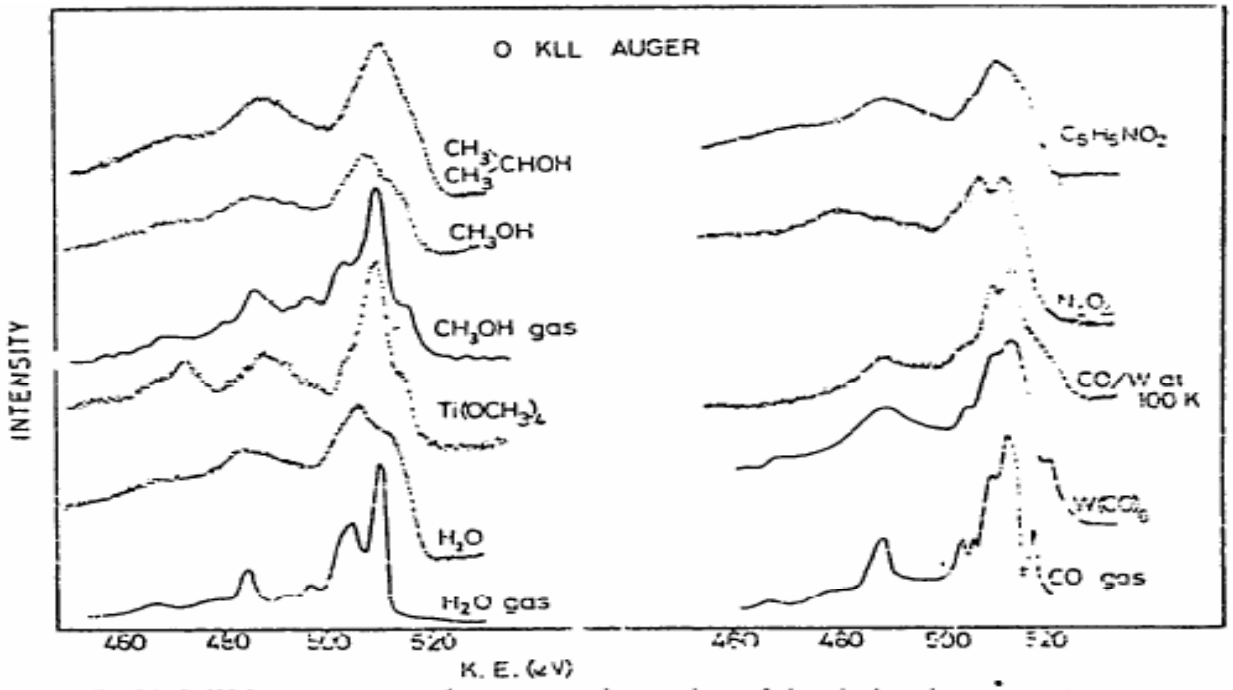

Fig. 26. O KLL Auger spectra from oxygen in a variety of chemical environments. All [illegible] are from condensed layers unless otherwise stated. The spectra of H_2O gas, CH_3OH [illegible] and CO gas have been shifted by respectively approximately 12, 11, and 16 eV to higher K.E. to allow for the different reference levels and relaxation effects (Section III.F) and to line up the characteristic features as well as possible. Differences in the low K.E. background are not significant as different instruments have been used to record the spectra. References: H_2O gas (79, 253, 256); H_2O, $Ti(OCH_3)_4$, CH_3OH, $(CH_3)_2CHOH$, $W(CO)_6$, N_2O_2, and $C_5H_5NO_2$ (234); CH_3CH_2OH [illegible] (241, 242); CO gas (241, 255).

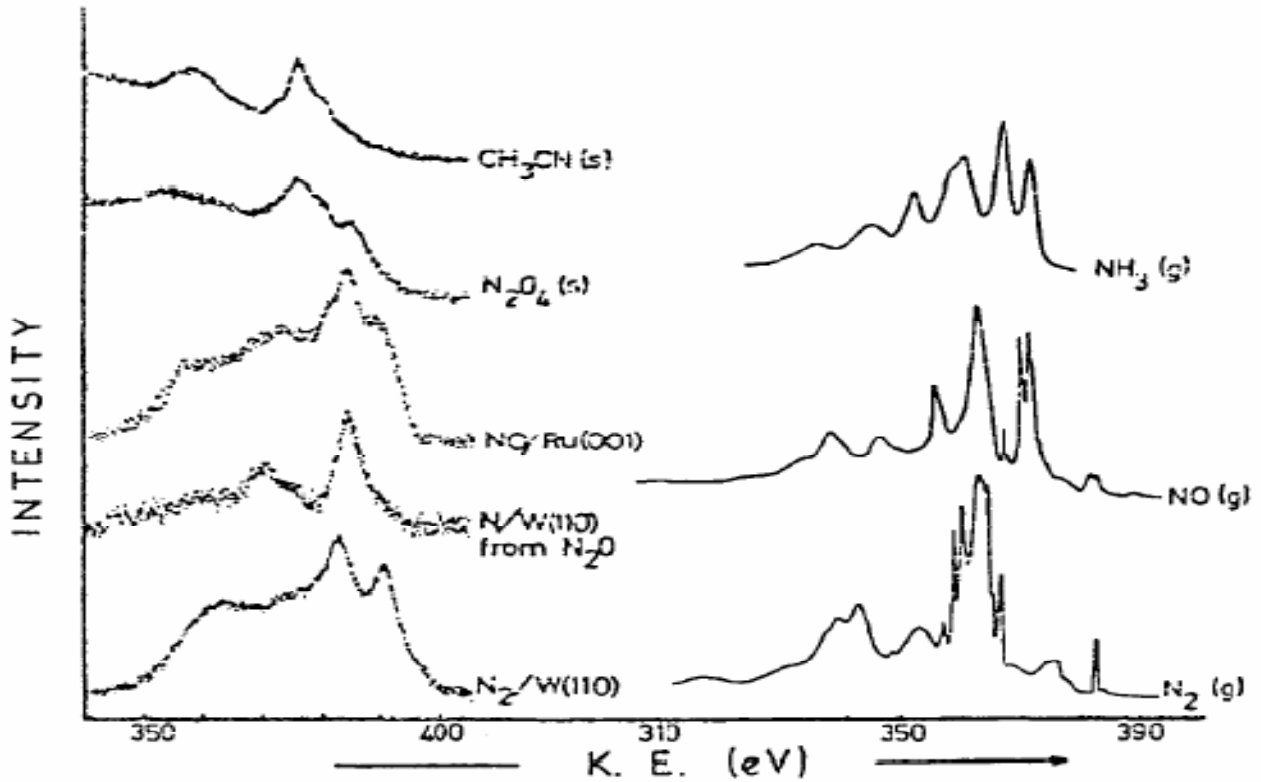

Fig. 27. N KLL Auger spectra from nitrogen in a variety of chemical environments. References NH_3 gas [259]; NO and N_2 gas [258]; CH_3CN and N_2O_4 [234]; NO Ru(001) [252]; N/W(110) [249] N_2/W(110) [249, 260].

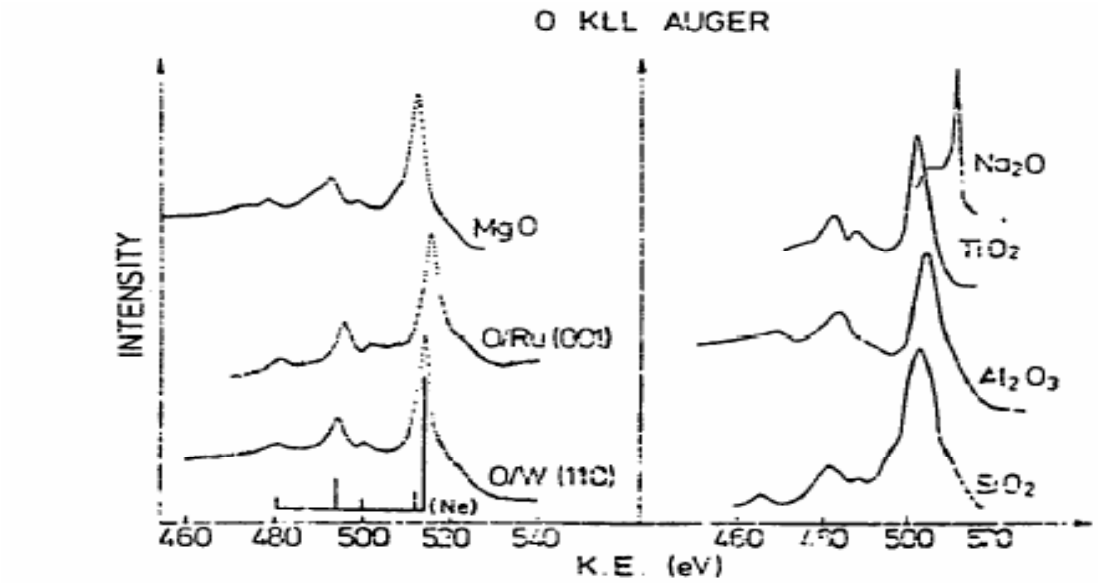

Fig. 23. Oxygen KLL Auger spectra from MgO,[231, 232] oxygen chemisorbed on Ru(001)[234, 245] and W(110),[248] Na_2O,[84] TiO_2,[97] Al_2O_3,[82] and SiO_2.[235] The *relative* spacings and intensities of Ne KLL lines[170] are also shown.

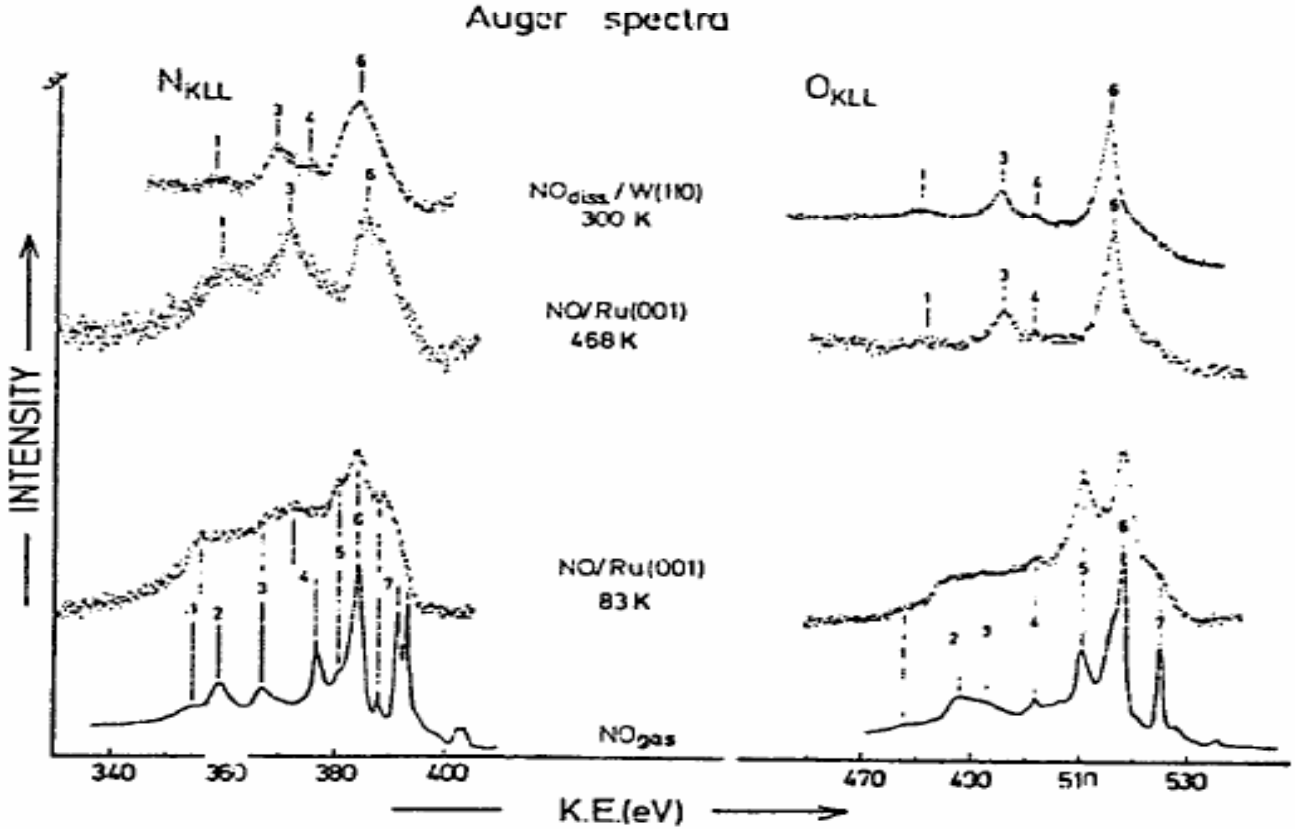

Fig. 22. Comparison of O KLL and N KLL Auger spectra from NO gas[238] and NO adsorbed on Ru(0001) at low temperatures and then warmed to 468 K. On warming the NO is seen to dissociate as shown by the similarity of O KLL spectra to those of chemisorbed oxygen shown in Fig. 23. The dissociated NO spectra are similar to those of NO on W(110) where dissociative adsorption is found at both 100 K and 300 K.[249] (From ref. 252).